CITY OF HOMER RESERVOIR PROJECT: GROUNDWATER STUDY

2023

PREPARED FOR

City of Homer,
Public Works Department

City of Homer Reservoir Project: Groundwater Study

ERG Report # 2023-01/Final Report Agreement # 069687242

Prepared for

The City of Homer, Public Works Department

by

Tyelyn Brigino, Kai Rains, Edgar Guerron-Orejuela, Syverine Bentz, and Mark Rains

on behalf of

The Ecohydrology Research Group, University of South Florida

and

The Kachemak Bay National Estuarine Research Reserve, University of Alaska Anchorage

September 2023

Table of Contents

Suggested Citation: Brigino, T., Rains, K., Guerrón-Orejuela, E., Bentz, S., & Rains, M. (2023). City of Homer Reservoir Project: Groundwater Study. Ecohydrology Research Group Report # 2023-01/Final Report Agreement # 069687242. University of South Florida, Tampa, FL.

Corresponding Author: Mark Rains, mrains@usf.edu

Introduction

Globally, groundwater is used for agriculture (70.1%), public water supply (21.2%), and industrial activities (8.7%), thus playing a vital role in food security and human health (de Graaf et al., 2019; Forslund et al., 2009; Margat & van der Gun, 2013; United Nations, 2022). In the United States groundwater discharge comprises 14-90% of streamflow (Winter et al., 1998), which implies that groundwater discharge also plays an important role in the provision of surface water resources, including reservoirs. Therefore, it's crucial to understand the dynamics between these competing needs. Afterall, groundwater is a renewable resource only if managed properly, and the sustained availability of this resource depends on maintaining the balance between groundwater recharge, use, and discharge (Baldwin & McGuinness, 1963; Famiglietti, 2014).

The University of South Florida Ecohydrology Research Group (USF ERG) and the Kachemak Bay National Estuarine Research Reserve (KBNERR) have been investigating groundwater dynamics in the Lower Kenai Peninsula for over two decades (e.g., Callahan et al., 2015, 2017; Dekar et al., 2012; Gerlach et al., 2022; Guerrón-Orejuela et al., 2023; Shaftel et al., 2011, 2012; Walker et al., 2012; Whigham et al., 2017). In 2022, the City of Homer contracted with USF ERG and KBNERR to conduct a focused investigation on the groundwater dynamics in the Bridge Creek Reservoir (BCR) which supplies water for city residents and serves as the headwaters for the South Fork Anchor River. The City of Homer is growing at a rate of 10%, which is higher than both the Kenai Peninsula (6%) and the national (7%) rates (US Census). As regional population grows, consumptive use of groundwater is expected to increase, stressing this limited shared resource.

Specifically, the City of Homer contracted us, the USF ERG and KBNERR, to validate regional maps of groundwater discharge (Gerlach et al., 2022) and recharge (Guerrón-Orejuela et al., 2023) for use in the BCR Watershed. At the time of contracting, we had recently completed the regional map of groundwater discharge (Gerlach et al., 2022) and were working on the regional map of groundwater recharge (Guerrón-Orejuela et al., 2023). However, those maps had few field validation points in the BCR Watershed. The validation of these map products in the BCR Watershed constituted the extent of the contracted work (Appendix 1). However, because of the opportunity provided to us by this contract to spend time in the BCR Watershed, we integrated these waters into our ongoing regional geochemical studies in which we address questions such as: What is the relative contribution of groundwater to streamflow? Does this relative contribution change seasonally? These regional studies are still in progress, but we recognize the significance these issues have on water management of the BCR Watershed and have included some of our preliminary results in this report. As an additional out-of-scope product, we have included the results of our investigation of the feasibility of calculating a water budget for the BCR Watershed.

Study Area

This study took place in the BCR Watershed, located in the headwaters of the Anchor River on the Kenai Peninsula Lowlands in south-central Alaska (Figure 1). The climate, geology, and topography are typical of the Kenai Peninsula Lowlands.

The climate is driven by intersecting continental and maritime patterns and consists of short, cool summers and long, cold winters. Mean annual temperature and precipitation are 2.9 °C and 755 mm, respectively (HOMER 8 NW, AK US USC00503672, 1991–2020). Seasonal precipitation is influenced by the strength and position of the Aleutian Low, with most of the precipitation occurring between November and March and with orographic effects enhancing precipitation at the highest elevations (Broadman et al., 2020).

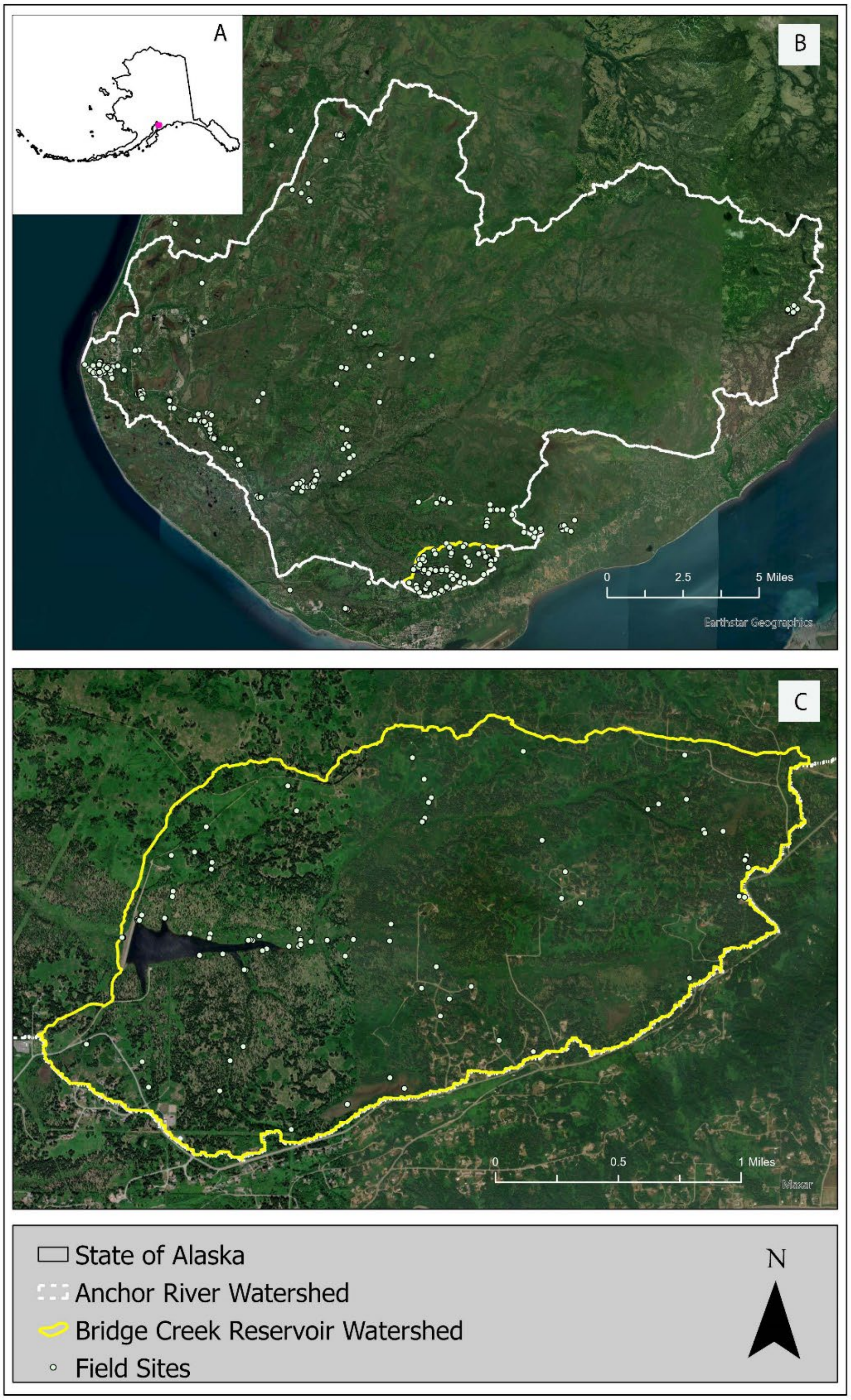

Figure 1. A. General location of the study site within the State of Alaska. B. The boundaries of the Anchor River Watershed (white line) and the BCR Watershed (yellow line) along with locations within both watersheds where we collected water samples and/or field validated our maps of groundwater discharge and recharge. C. The boundary of the BCR Watershed (yellow line) and the locations within the BCR Watershed where we collected water samples and/or field validated our maps of groundwater discharge and recharge. Water samples were not collected at all point locations.

The Kenai Peninsula Lowlands has experienced at least five major Pleistocene glaciations and two minor post-Pleistocene glacial advances in the last 125,000 years (Karlstrom, 1964). Glacier dynamics are extremely variable and uniquely coupled with mass movement and fluvial processes. As continental glaciers advance, continental landmasses in front of the advancing glaciers subside under the weight of the glaciers. This creates accommodation space in front of the glaciers which is filled by sediments, including proglacial channel, floodplain, and lakebed deposits. Channel deposits are formed as outwash streams transport and deposit coarse-grained material, such as sand and gravel. When cut off as oxbows, they may also accumulate organic matter and fine-grained material, such as silt and clay. Floodplain deposits are formed as overbank flows and winds transport and deposit fine-grained materials, such as silt and clay. These may be overlain by moraines and other sub- and periglacial deposits. As continental glaciers recede, continental landmasses in front of the receding glaciers rebound, and rivers down cut into the complex deposits, creating new valleys. As continental glaciers once again advance, continental landmasses under and in front of the advancing glaciers once again subside, and the recently cut valleys are filled and this sequence repeats. This repeated sequence left complex deposits of variable permeability throughout the Kenai Peninsula Lowlands, including thin, meandering coarse-grained buried channel deposits, which serve as the primary water-bearing formations (i.e., aquifers). Modern rivers have downcut into these complex deposits, creating steep sided valleys and exposing outcrops, including outcrops of the buried channel deposits.

This complex setting creates two types of groundwater discharge: hillslope groundwater discharge and aquifer-outcrop groundwater discharge (Gerlach et al., 2022). Hillslope groundwater discharge is annual precipitation that mixes with antecedent soil moisture, which then moves downslope and discharges from diffuse seeps at toeslopes (Figure 2). Aquifer-outcrop groundwater discharge is groundwater that has infiltrated more deeply and recharged aquifers, which then moves laterally and discharges from aquifer outcrops (Figure 2). These groundwater dynamics are very localized, with groundwater recharge and discharge typically being near one another, typically within the same watershed.

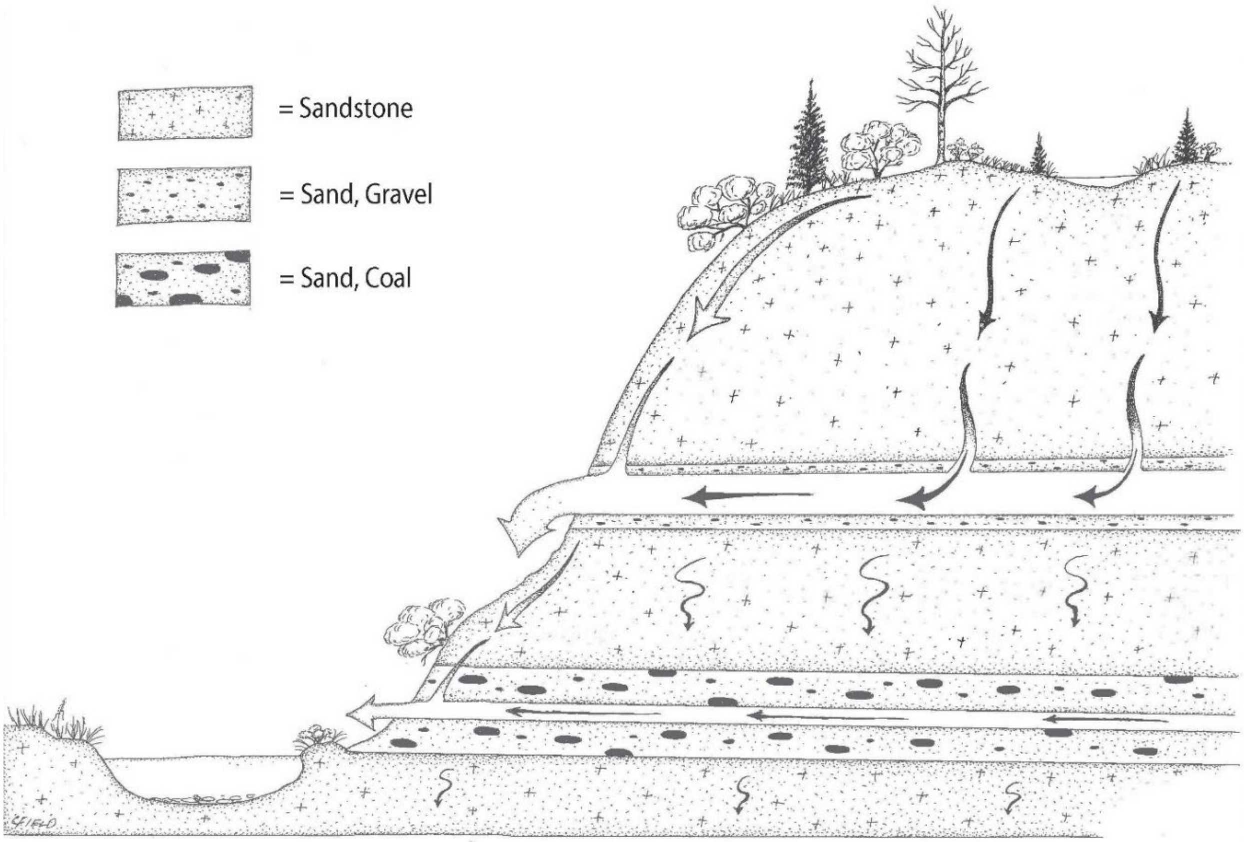

Figure 2. Cross section showing the two types of groundwater discharge: hillslope groundwater discharge moves along the shallow subsurface and discharges from diffuse seeps and aquifer-outcrop groundwater discharge moves through deeper aquifers and discharges from springs. Illustration by Conrad Field (KBNERR) based on field sketches and notes prepared by the USF ERG.

Methods

Overall Approach

At the foundation of this current study were the insights and datasets from four prior investigations we have conducted in the broader Kenai Peninsula Lowlands: two investigations of the role of groundwater discharge in augmenting streamflow (Callahan et al., 2015; Brigino et al., unpublished data) and geospatial analyses resulting in maps of high probability locations of groundwater discharge (Gerlach et al., 2022) and recharge (Guerrón-Orejuela et al., 2023). We have built upon this work in the BCR Watershed, including data collection at 84 field sites, several of which were sampled repeatedly for a total of 145 data collection events (Figure 1 and Figure 3). Data collection included groundwater discharge validation (presence/absence of water or other indicators of flow), groundwater recharge validation (presence/absence of features consistent with high recharge potential in the Kenai Peninsula Lowlands), and/or water sample collection (for geochemical analyses and used to investigate the role of groundwater discharge in augmenting streamflow). Data collection is explained in more detail below.

Figure 3. Representative photographs of field data collection by USF ERG and KBNERR in the BCR Watershed.

Groundwater Contribution to the Bridge Creek Reservoir

Though not included in the contracted scope of this project, we first determined the relative contribution of groundwater discharge to the BCR and to the tributaries of the BCR using methods and insights developed as part of our research program in the broader Kenai Peninsula Lowlands.

Our groundwater discharge to the BCR dataset consisted of 93 water samples: *Outflow,* 55 samples collected at weekly intervals from the BCR outflow between June 2022 and July 2023; *Groundwater,* 24 samples collected at wells, seeps, or springs in the BCR Watershed; *Precipitation,* 14 direct precipitation and runoff samples collected in the South Fork Anchor Watershed. This dataset does not include data from the single well sampled whose depth was lower than the elevation of the BCR outflow.

Our groundwater discharge to the tributaries dataset consisted of 42 water samples: *Tributary,* 1-2 samples (5 total) collected at the outlets of the streams entering from the north, east, and southwest shores of the BCR in 2022; *Groundwater,* 24 samples collected at wells, seeps, or springs in the BCR Watershed; *Precipitation,* 14 direct precipitation and runoff samples collected in the South Fork Anchor Watershed.

At each water sample site, we measured pH and temperature in the field with an Oakton pH 300 (Environmental Express, Charleston, SC) or the equivalent and specific conductance with a YSI Model 30 (YSI, Yellow Springs, OH) or the equivalent. We additionally collected samples for dissolved ion analyses using the following methods. We filtered approximately 80 mL of water with a 0.45 µm nylon filter and stored samples in polypropylene tubes. Samples were stored in a cooler with ice packs in the field and then immediately frozen upon returning to the KBNERR lab in Homer, AK. We transported frozen water samples to the USF Center for Geochemical Analysis where they were analyzed for cations (i.e., Ca and Mg) with a PerkinElmer Avio 200 ICP-OES with ESI FAST SC-DX-2 Autosampler (PerkinElmer, Waltham, MA) by T. Brigino.

We used a two-end member mass balance mixing model to calculate the relative contribution of precipitation and groundwater to the BCR outflow and to each of the three tributaries to the BCR. The Ca and Mg in the water samples served as conservative, natural tracers. The concentrations of these constituents in water are the result of the dissolution of Ca- and Mg-rich siliciclastic deposits by groundwater, and our work throughout the broader Kenai Peninsula Lowlands suggests they are suitable natural tracers for determining the relative contribution of groundwater to a given sample of water (Callahan et al., 2015; Intveld et al., 2022; Brigino et al., unpublished data). We calculated the relative contribution of groundwater to the BCR and to the three tributaries as described in Equation 1:

$$f_{gw} = (C_{sf} - C_{pr})/(C_{gw} - C_{pr}) \quad \text{Equation 1}$$

where f_{gw} is the fraction of streamflow (i.e., BCR outflow or tributary) attributable to groundwater, C_{sf} is the concentration of the natural tracer in streamflow, C_{pr} is the average concentration of the natural tracer in precipitation, C_{gw} is the average concentration of the natural tracer in groundwater. The final reported fraction of streamflow attributed to groundwater reported is the average of the values calculated based on the concentrations of Ca and of Mg.

Development and Validation of Groundwater Discharge and Recharge Maps

We constructed a map of high probability locations of groundwater discharge in the broader Kenai Peninsula Lowlands using geospatial data and machine learning (Gerlach et al., 2022). In that study, we identified two types of groundwater discharge: hillslope groundwater discharge, commonly manifested as diffuse seeps, and aquifer-outcrop groundwater discharge, commonly manifested as springs. We developed multistep manual procedures that allowed us to accurately predict the locations of both types of groundwater discharge, though only where geologic data were available. To extend our analyses beyond the areas where geologic data was available, we applied maximum entropy modeling, a machine learning technique, to predict the prevalence of both types of groundwater discharge throughout the entire Kenai Peninsula Lowlands. Additional details can be found in Gerlach et al. (2022), which is included in Appendix 2.

We constructed a map depicting the variation in groundwater recharge potential (GWRP) in the Anchor River Watershed (Guerrón-Orejuela et al., 2023). GWRP was mapped using geospatial data and Analytic Hierarchy Process (AHP) (Arulbalaji et al., 2019; Guerrón-Orejuela et al., 2023; Saaty, 1990). AHP is a multicriteria decision analysis method that provides a systematic methodology to classify and prioritize among heterogenous spatial datasets. GIS-AHP techniques can be used to address complex, multidimensional problems, such as delineating GWRP. The coupling of GIS and AHP has made them a powerful tool for regional hydrogeologic research and decision-making. Additional details can be found in Guerrón-Orejuela et al. (2023), which is included in Appendix 3.

Both the groundwater discharge and recharge maps were validated for the original study areas. However, given the large size of those original study areas, it is unsurprising that few of the original validation points fell within the BCR Watershed. In this study, we assessed the accuracy of the groundwater discharge and recharge maps as they apply to the BCR Watershed through field work conducted at 84 field sites, several of which were visited twice, once following an extended dry period (June 10-July 29, 2022) and another following a series of rainfall events (Sept 21-30, 2022). At each field site, we recorded the GPS coordinates using a handheld Garmin GPS unit, photographed the location, and recorded the presence/absence of water or indicators of water, i.e., gullies, iron floc, or directionally bent vegetation. At four sites, we additionally identified the dominant soil texture, as this was an important variable in the development of the groundwater recharge map (Guerrón-Orejuela et al., 2023). We had completed the map of groundwater discharge prior to the start of this project. Therefore, we used it to identify the locations of the groundwater discharge validation sites in the BCR Watershed. We expected to observe evidence of groundwater discharge where the predicted probability of groundwater discharge was high. However, the map of GWRP was not available until Spring 2023, i.e., after field work had been completed. We overlaid our 2022 field points on the GWRP map and identified seven that had been sampled in zones mapped as "high" GWPR. We reviewed the associated field notes and photos to assess whether our field observations were consistent with traits characteristic of high GWRP as per Guerron-Orejuela et al. 2023 (e.g., areas with flat terrain, coarse-grained surficial deposits, low drainage density, and low-density development).

Results and Discussion

Groundwater Contribution to the Bridge Creek Reservoir

In a scatterplot plot of Ca vs Mg, the BCR outflow samples plot between the precipitation and groundwater samples, indicating that the BCR water is a mix of precipitation and groundwater (Figure 4). Furthermore, the isotopic signature of the groundwater we have analyzed in the broader Kenai Peninsula Lowlands is well within the range of the modern isotopic signature of precipitation (Brigino et al., unpublished data). This indicates that there is no Pleistocene groundwater expressed within this area, which includes the BCR Watershed, and we can infer that the residence time of groundwater within the BCR Watershed is relatively short (i.e., years to decades).

Precipitation samples have consistently low Ca and Mg concentrations while groundwater samples have widely varying Ca and Mg concentrations (Figure 4), reflecting differing residence times. This is typical of the Kenai Peninsula Lowlands (Brigino et al., unpublished data) and is consistent with the premise that both hillslope groundwater discharge and aquifer-outcrop groundwater discharge are present in the BCR Watershed. We calculated the average groundwater concentrations of Ca and Mg of this dataset and used these values as two endmembers in the mass balance mixing model (Figure 5).

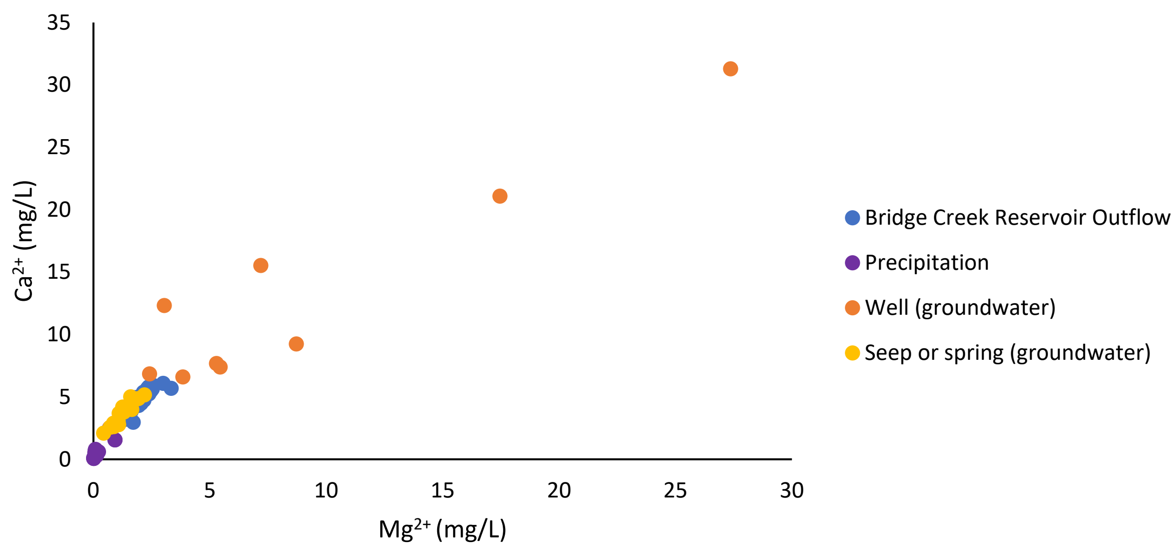

Figure 4. Calcium and magnesium concentrations for the BCR outflow (55 samples), precipitation (14 samples), wells (9 samples), and seeps or springs (15 samples).

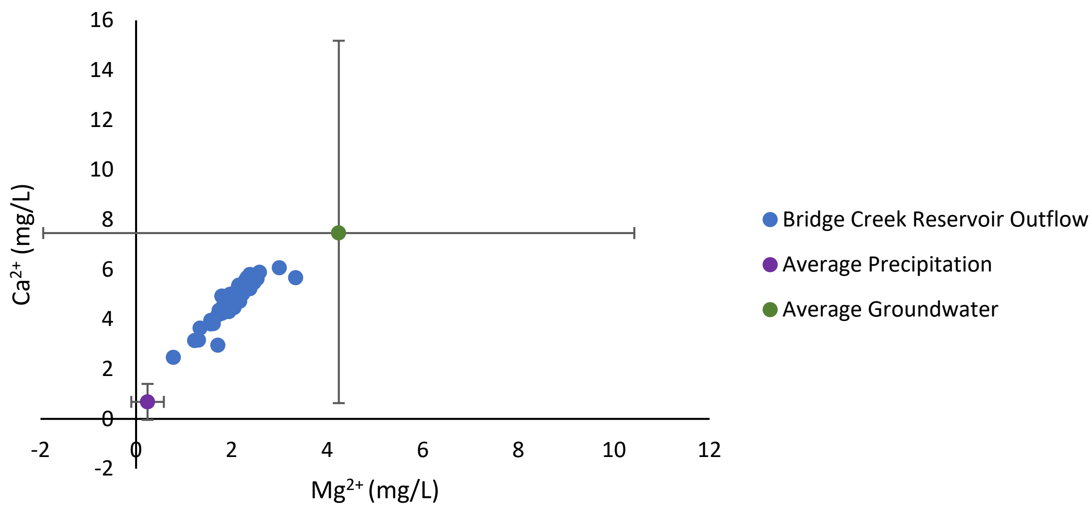

Figure 5. Two endmember mass balance mixing model for the BCR.

The relative contribution of groundwater to the BCR varies temporally, ranging from ~30-80% at any one moment in time but averaging 50-60% throughout the course the year (Figure 6). Groundwater contribution to the reservoir is expected to vary seasonally, as precipitation in the BCR watershed also varies seasonally (Figure 7). Groundwater may discharge directly to the BCR, either above or below the reservoir water surface, but also clearly discharges from seeps and springs that feed the tributaries that in turn discharge to the BCR (Figure 8).

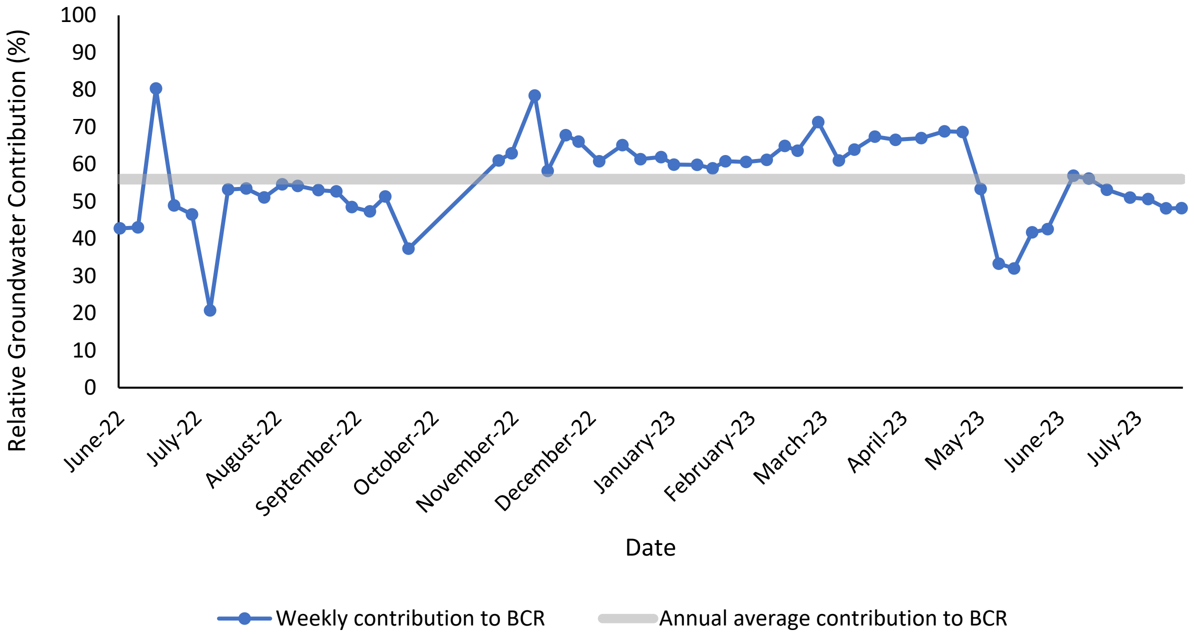

Figure 6. The relative contribution of groundwater to the Bridge Creek Reservoir from June 2022-July 2023. Each dot corresponds to a separate water sample collected at the Bridge Creek Reservoir Outflow.

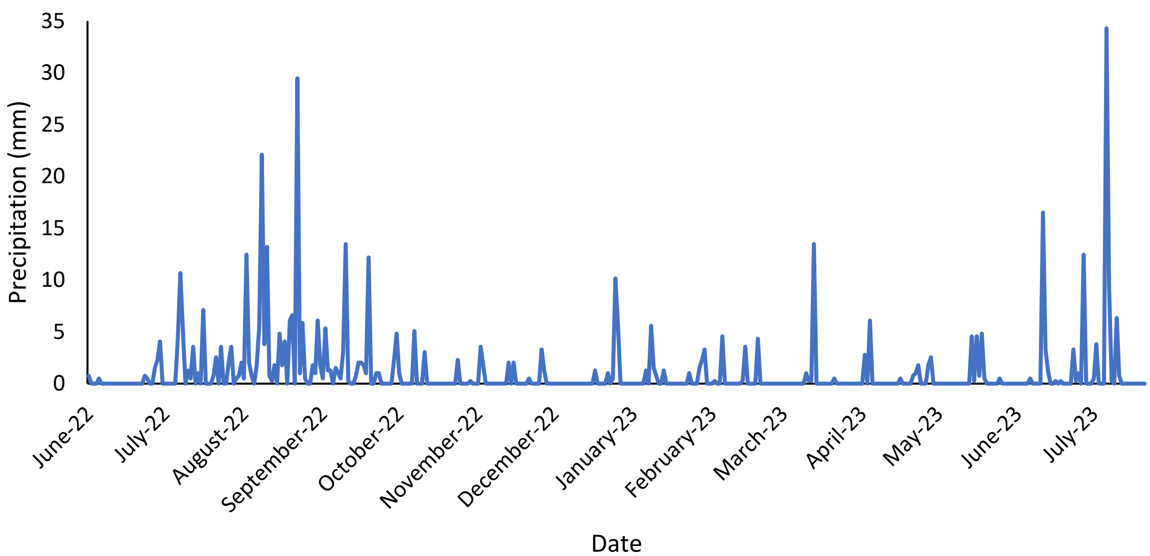

Figure 7. Daily precipitation for the BCR Watershed (T. Cook - City of Homer Water Sewer Superintendent, personal communication, August 16, 2023).

The tributaries entering from the east and south were sampled on July 21, 2022, following a long dry spell (Figure 7). The subsequent analysis indicates that ~40-60% of the tributary streamflow was comprised of groundwater. These tributaries were resampled on September 30, 2022, following a series of rain events (Figure 7). The tributary entering from the north was newly sampled at that time. The subsequent analysis indicates ~30-40% of the tributary streamflow was still comprised of groundwater during the abundant rain that fell during that time. Our results suggest the degree to which the BCR and tributaries to the BCR are comprised of groundwater varies seasonally, increasing as conditions become drier. This timing unfortunately coincides with other demands upon this resource, i.e., increased summer residents and tourism. These results are consistent with what we see in the mainstem of the South Fork Anchor River and in other watersheds of the Kenai Peninsula Lowlands (Callahan et al., 2015; Brigino et al., unpublished data). These results are provisional, as our study of the contributions of groundwater discharge to streamflow throughout the broader Kenai Peninsula Lowlands is ongoing. **We would like to emphasize the tributary results are particularly provisional as we had a very small BCR Watershed dataset, i.e., 1 -2 samples per representative tributary (Figure 8) and did not include the tributary that enters the BCR from the SW.**

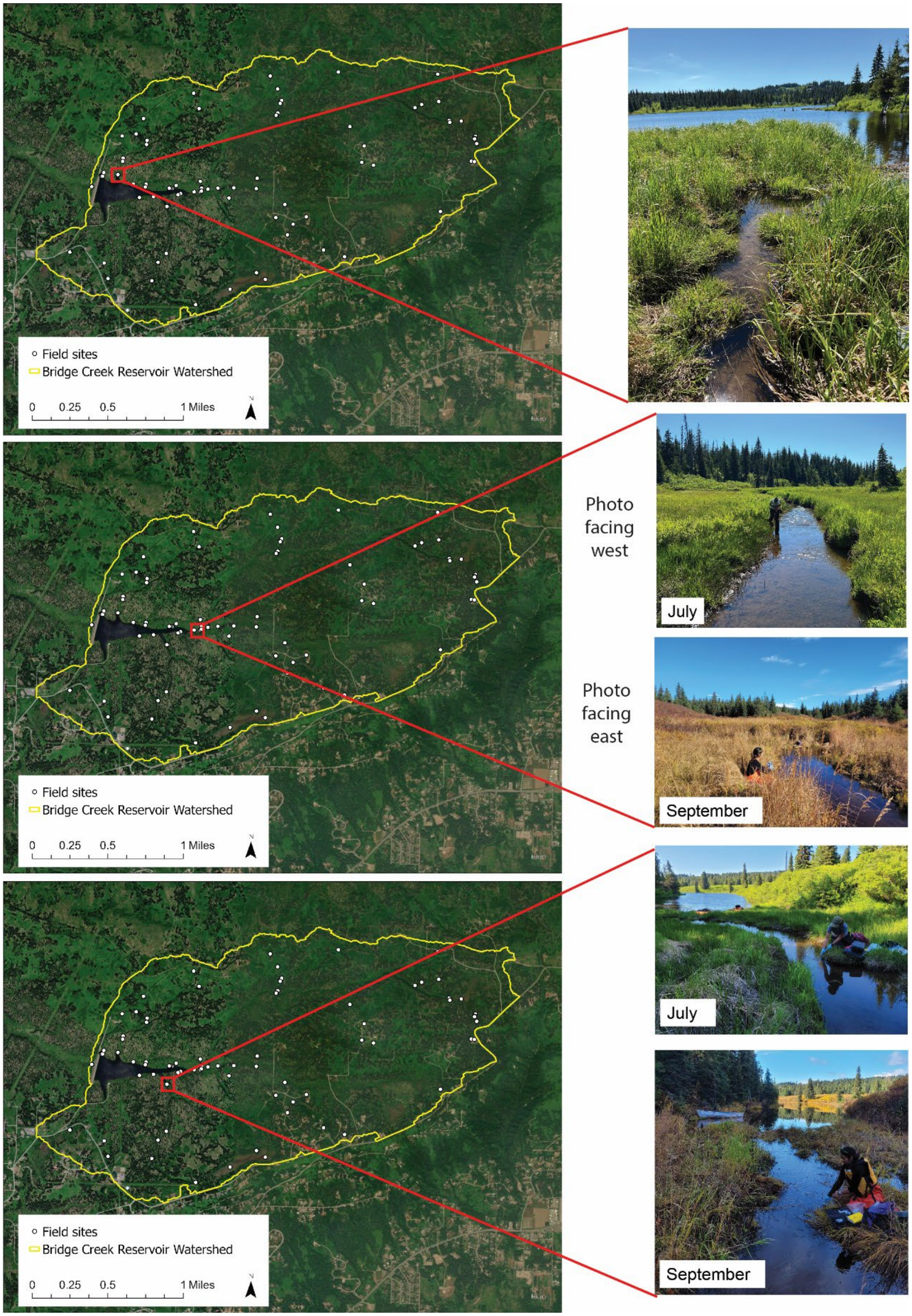

Figure 8. Surface water sampling at the major tributaries to the reservoir. The north (top), east (middle), and south (bottom) were sampled on September 30, 2022, following a series of rain events. Eastern and southern surface waters were additionally sampled earlier on July 21, 2022, following a long dry spell.

Groundwater Discharge and Groundwater Recharge Maps

Groundwater discharge varies throughout the BCR Watershed (Figure 9). Hillslope groundwater discharge occurs where rainfall and snowmelt infiltrate into the shallow subsurface, move laterally downslope through the shallow subsurface, and discharge as diffuse seeps and small springs at groundwater-induced slope failures and valley-bottom toe slopes. Aquifer-outcrop groundwater discharge occurs where rainfall and snowmelt infiltrate into the deep subsurface, move laterally through aquifers, and discharge as larger springs at aquifer outcrops in valleys carved by modern streams (Figure 2). Both typically occur proximal to streams, but especially at the headward extent of stream networks. The model for the entire Kenai Peninsula Lowlands was validated, and the AUC values were 0.95 for training data and 0.91 for testing data, indicating outstanding model performance. Our field validation results similarly support the accuracy of this map in the BCR Watershed (Table 1). The accuracy based on the confusion matrix indicate the accuracy of this map is 91% in the BCR (TN+TP/Total = accuracy, 8+21/32 = 0.91), however, our incidental field observations suggest the accuracy is lower in areas where the ground has been disturbed.

Landscape curvature is an important predictor of groundwater discharge in the Kenai Peninsula Lowlands (Gerlach et al. 2022) and is often high where the hillslope meets a floodplain. The historic shoreline of Bridge Creek has been flooded, artificially raising the elevation to the current shoreline. Our model has predicted abundant seeps and springs on the northeastern and southeastern shorelines which weren't generally supported by our field observations. We traversed the shoreline in small boats on two occasions, landing periodically to look for seeps or springs, but we rarely observed them. Similarly, the false positives and false negatives recorded in the confusion matrix were associated with anthropogenic disturbances such as an excavated hollow and a linear depression carved by powerline activity (Table 1). We suggest using caution when interpreting the Groundwater Discharge map in disturbed areas.

Table 1. Results of field verification of seeps and springheads organized into a confusion matrix. Predicted refers to the predicted locations as per the groundwater discharge map. Actual refers to field observations at those locations.

	Predicted No	**Predicted Yes**	**Total**
Actual No	8	1	9
Actual Yes	2	21	23
Total	10	22	32

In the BCR Watershed, 833.2 ha have a low probability of groundwater discharge occurrence (i.e., <10%) and just 4.73 ha have a high to very high probability of groundwater discharge occurrence (i.e., >70%) (Figure 10). Note that this map does not distinguish between hillslope groundwater discharge and aquifer-outcrop groundwater discharge or between seasonal and perennial groundwater discharge. Further calibration would be needed to distinguish between types of discharge.

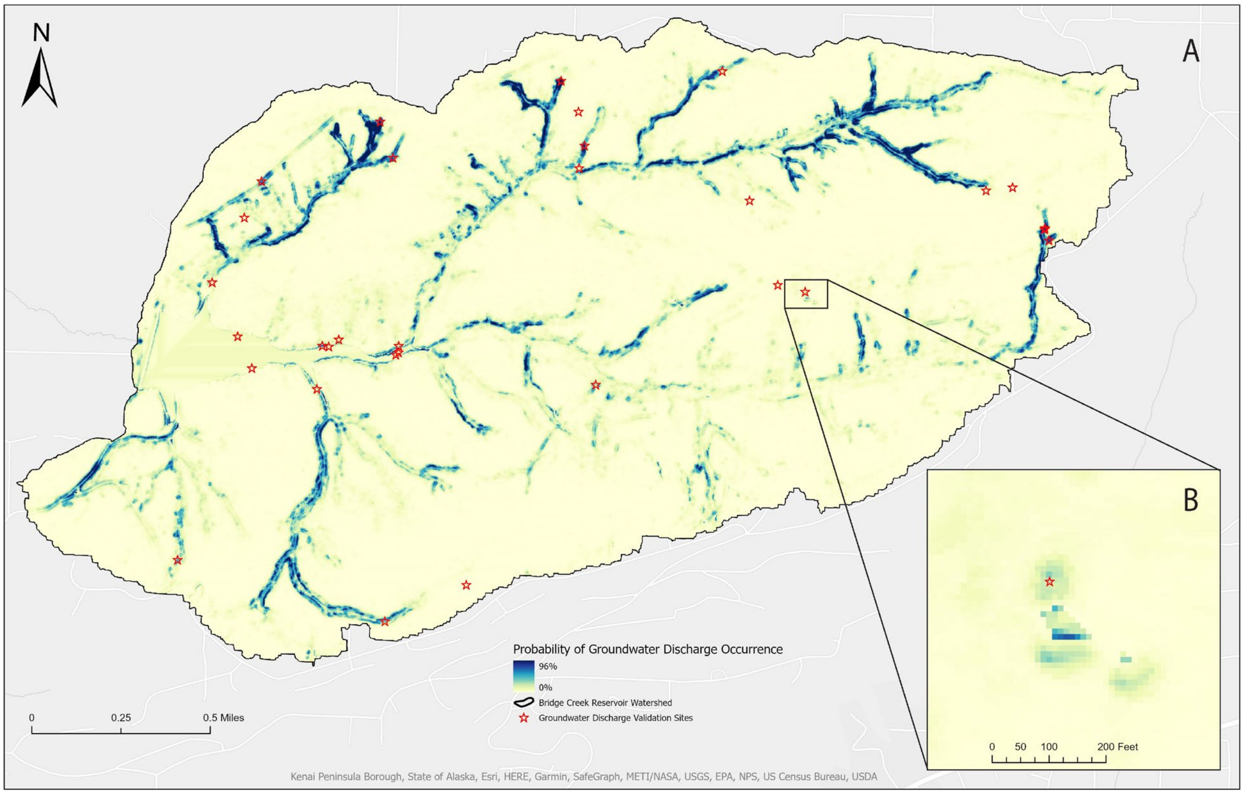

Figure 9. Predicted groundwater discharge occurrence in the BCR Watershed. Seeps and springs are most likely to occur where the probability is high. The red stars show the locations of seeps and springheads that were used to field validate the model. The inset (B) has been added to illustrate there may be localized areas where seeps/springs are predicted that will not be readily apparent from a map unless the user is able to "zoom in".

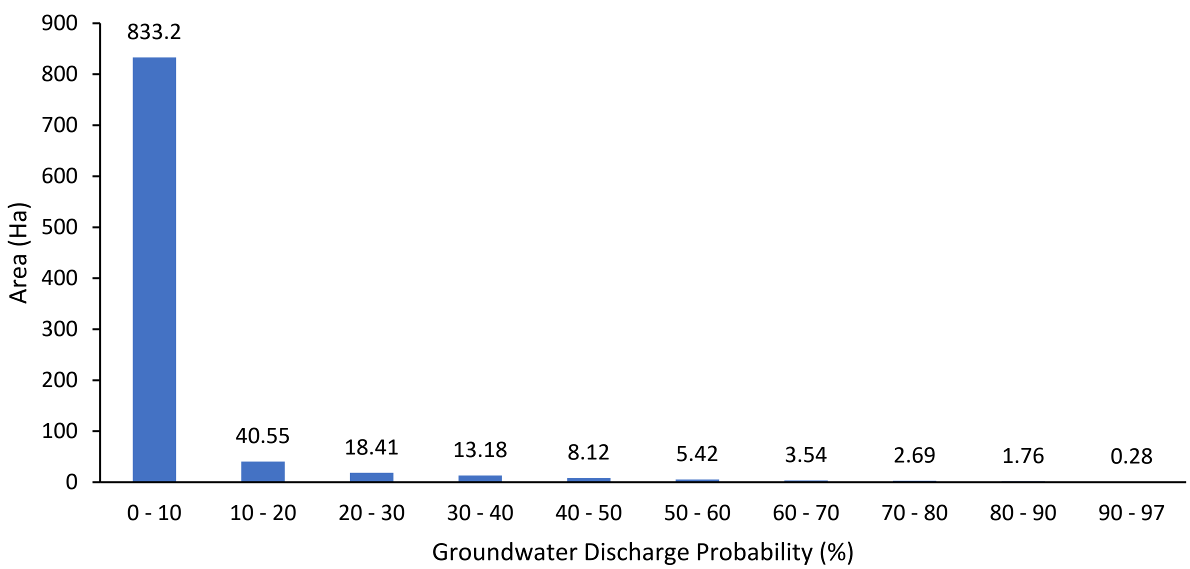

Figure 10. Histogram of the area in hectares and their corresponding probability of groundwater discharge in the BCR Watershed.

GWRP also varies throughout the BCR Watershed. GWRP is highest in areas along streams and floodplains, valley bottoms, and other flat areas with alluvium. Furthermore, GWRP is the highest where precipitation is relatively high, geologic deposits are coarse-grained and unconsolidated, soils are variants of sands and gravels, the terrain is flat, drainage density is low, and land cover is undeveloped (Figure 11) (Guerrón-Orejuela et al., 2023). The model for the entire Anchor River Watershed was validated, and overall accuracy was 87%. Our field validation results similarly support the accuracy of this map in the BCR Watershed.

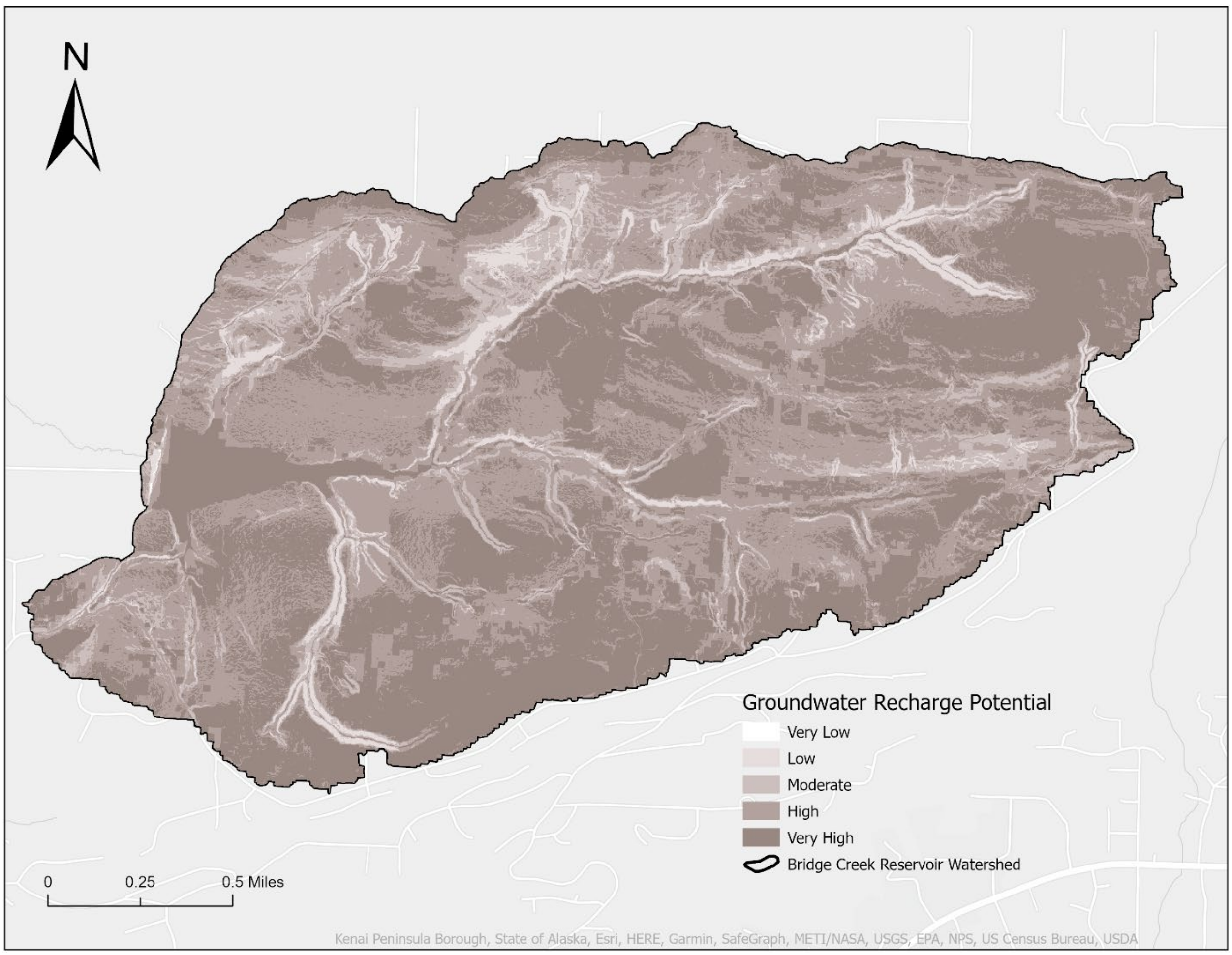

Figure 11. Distribution of GWRP in the BCR Watershed. Groundwater recharge is most likely to occur in areas where the GWRP is High or Very High.

In the BCR Watershed, < 1% of the area has Very Low GWRP, 4% of the area has Low GWRP, 11% of the area has Moderate GWRP, 42% of the area has High GWRP, and 43% of the area has Very High GWRP. Overall, ~85% of the BCR Watershed has High or Very High GWRP (Figure 14).

Preliminary Water Budget

Though not part of the scope of this project, we have been independently studying the water budget for the BCR Watershed, using Equation 2:

$$P - ET - Q - R_D = \Delta S \qquad \text{Equation 2}$$

where P is precipitation across the BCR Watershed, ET is evapotranspiration across the BCR Watershed, Q is surface water flowing out of the BCR Watershed, R_D is deep groundwater recharge flowing out of the BCR Watershed, and ΔS is change in storage across the BCR Watershed. We have been conducting this analysis over yearly timescales, so the ΔS across the BCR Watershed is effectively equal to zero. Furthermore, Q has two components: water being used by the City of Homer and water flowing through the BCR outflow. Therefore, we have simplified the water budget for the BCR Watershed, using Equation 3:

$$P - ET - Q_H - Q_O - R_D = 0 \qquad \text{Equation 3}$$

where Q_H is water being used by the City of Homer, Q_O is the water flowing out of the BCR outflow, and all other terms are as previously defined (Figure 12).

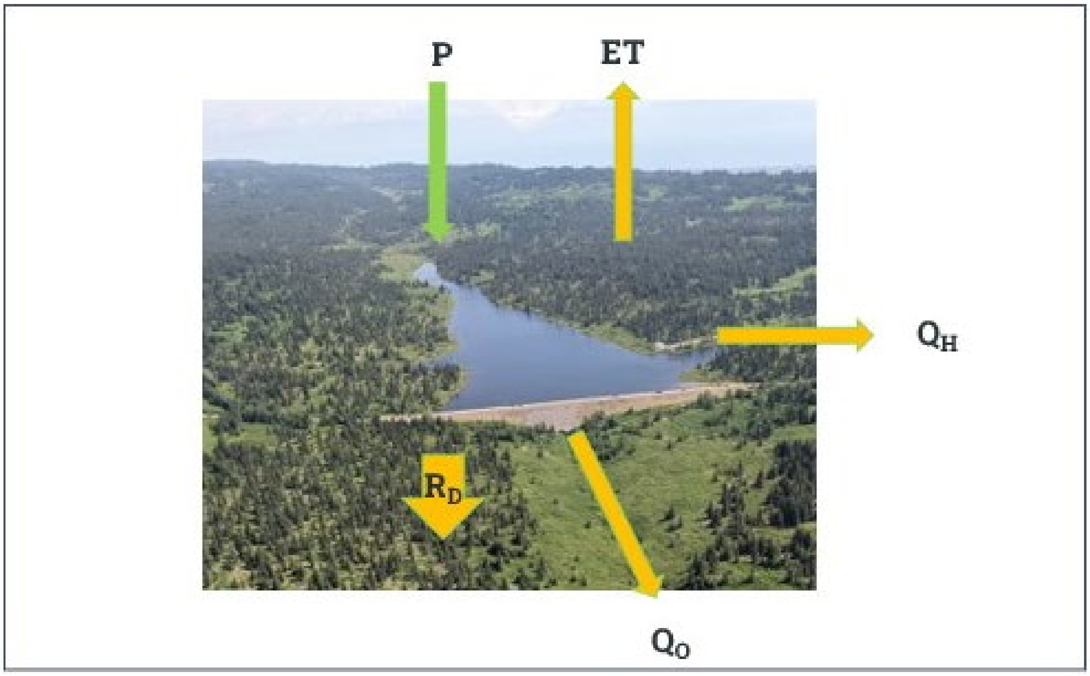

Figure 12. Conceptualization of the water budget for the BCR Watershed. The arrow in green represents water entering the watershed, and the arrows in yellow represent the different ways in which water leaves the watershed. P is precipitation, ET is evapotranspiration, Q_H is water being used by the City of Homer, Q_O is the water flowing out of the reservoir through the outflow, and R_D is deep groundwater recharge

We have used long-term data to calculate averages for precipitation, evapotranspiration, and city water use. We have treated deep groundwater recharge as an error term (i.e., if we measure or calculate all other terms correctly, the remainder must have been lost to deep groundwater recharge). Reservoir outflow has been the most difficult term to calculate because there are no long-term data and even short-term measurement is difficult. As a first order estimate, we had previously estimated average reservoir outflow from the geomorphology of Bridge Creek below the BCR outflow. Those provisional estimates indicated that reservoir outflow was comparable in magnitude to the city water use (Mastrion, 2022). These results are provisional and are reported for internal discussion only and they should not be used for planning purposes.

During the course of this study, but outside the scope, we conducted a feasibility analysis of measuring reservoir outflow by continuously measuring stream stage with a Solinst Levelogger

(Solinst, Georgetown, ON). We placed the Levelogger in the concrete vault of the BCR outflow so we could use the spillway as a weir and calculate outflow from the measured stage. Results were difficult to interpret. There were significant flood flows that damaged the Levelogger which had to be repaired and replaced. Additionally, freezing during winter altered the spillway cross section, which made it difficult to calculate outflow from the measured stage. This remains an important unknown, as the reservoir outflow could represent additional water available for consumptive use yet also supports habitat for salmonids that are found directly below the reservoir outflow, as Bridge Creek is a tributary to the Anchor River (Figure 13).

Figure 13. Jacob Argueta (KBNERR) shows community members salmonids he caught at the outflow of the BCR.

Conclusions

Our results show that over half of the BCR water supply starts its journey underground (Figure 6). However, there are two types of groundwater discharge that may play varying roles throughout the year. Hillslope groundwater discharge is commonly seasonal and aquifer-outcrop groundwater discharge is commonly perennial (Brigino et al., unpublished data). Those aquifers also support household water supply wells within the BCR Watershed. With the potential increased consumptive use of limited groundwater resources and a warming and possible drying trend in the regional climate (e.g., Klein et al., 2005), source water protection within the BCR Watershed is particularly important.

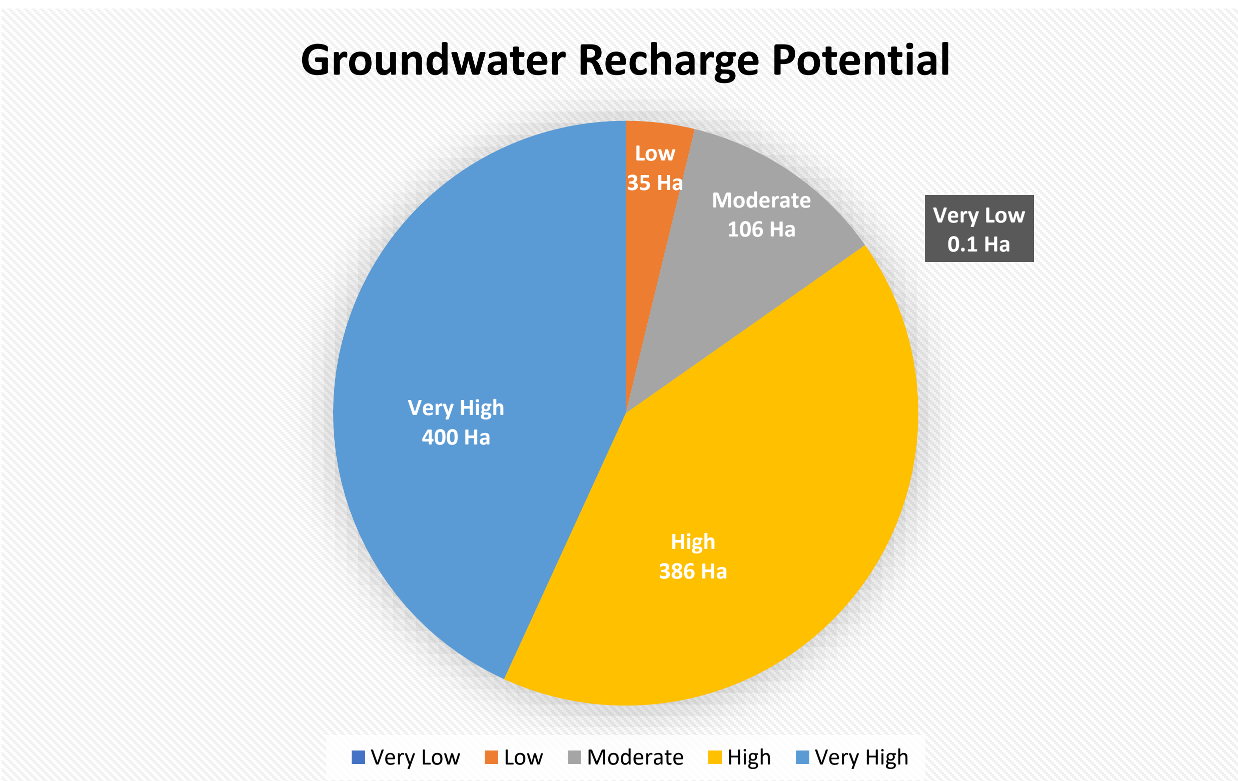

Figure 14. Classification of the GWRP by area in the BCR Watershed, the areas reported in the figure are in Hectares. The GWRP categories Low to Very High are depicted in the figure. The category Very Low was not depicted in the figure; however, its value is reported.

Coupling the modelled areas of groundwater discharge and GWRP can inform management decisions for source water protection, including land acquisition and conservation easements. There are very few areas where the probability of groundwater discharge is high (Figure 9 and Figure 10). Conversely, there are many areas where the GWRP is High or Very High (Figure 11 and Figure 14). Therefore, the most efficient way to use these results for source water protection is to identify those rare areas where the probability of groundwater discharge is high, then delineate the upgradient areas where the likely associated GWRP is High or Very High (Figure 15). These, then, could be areas where one might consider the use of land acquisition and/or conservation easements to protect source water for the BCR Watershed.

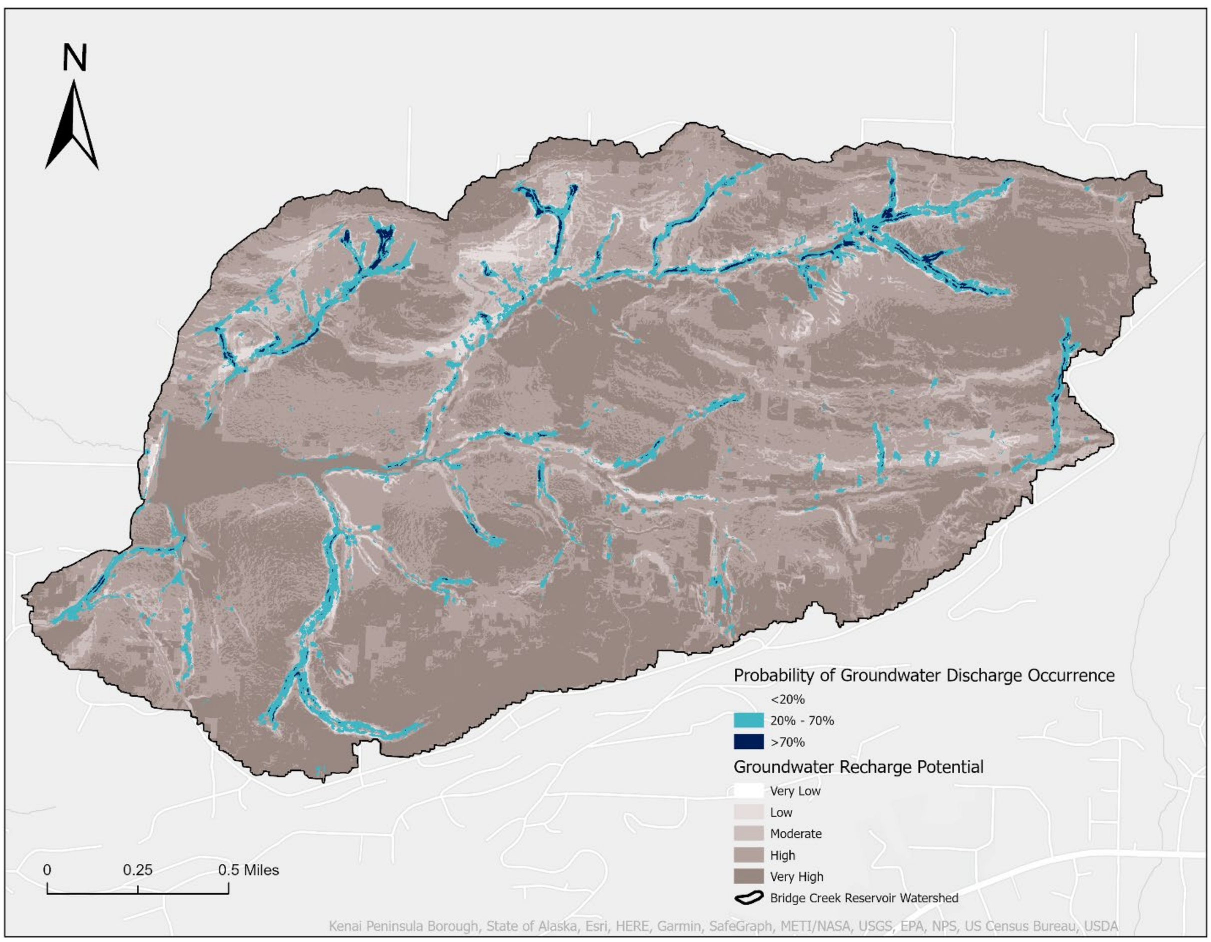

Figure 15. Example analysis to identify critical source water protection areas in the BCR Watershed. For example, it is clear that there are areas in the northeast portion of the BCR Watershed that have both a high probability of groundwater discharge and Very High GWRP.

Acknowledgements

We would like to acknowledge the contributions made by our many collaborators. Coowe Walker has recently retired from KBNERR but was instrumental in every aspect of this study. We would like to thank Jacob Argueta for his persistent water sampling and field insights. We would also like to thank Aviva Intveld, and Pierce Mastrion for field assistance, data analysis, and interpretation. We are particularly grateful to the City of Homer Public Works Department, especially Aaron Yeaton and Todd Cook, for their invaluable logistical support. We also benefitted from the contributions made by many other stakeholders, including the Kachemak Heritage Land Trust, the Center for Alaskan Coastal Studies, the Homer Soil and Water Conservation District, and the many private landowners who provided access to their lands and well water samples. Finally, we would like to acknowledge the other funding entities whose contributions made the out-of-scope portions of this work possible, including funding from the NOAA Margaret A. Davidson Fellowship (E. Guerron-Orejuela), the NOAA Ernest B. Hollings Scholarship (A. Intveld, P. Mastrion), the NSF S-STEM Scholarship from NSF Grant No. 1930451 (T. Brigino), the Southeastern Geological Society Student Research Award (T. Brigino), the USF Richard A. Davis Endowed Fellowship in Geology (T. Brigino), and the USF Ecohydrology Research Group (K. Rains, M. Rains).

References

Arulbalaji, P., Padmalal, D., & Sreelash, K. (2019). GIS and AHP Techniques Based Delineation of Groundwater Potential Zones: A case study from Southern Western Ghats, India. *Scientific Reports*, *9*(1), 2082. https://doi.org/10.1038/s41598-019-38567-x

Baldwin, H. L., & McGuinness, C. L. (1963). *A primer on ground water* (1990 reprint, General Interest Publication, p. 31) [Report]. U.S. Geological Survey; USGS Publications Warehouse. https://doi.org/10.3133/7000056

Broadman, E., Kaufman, D. S., Henderson, A. C. G., Berg, E. E., Anderson, R. S., Leng, M. J., Stahnke, S. A., & Muñoz, S. E. (2020). Multi-proxy evidence for millennial-scale changes in North Pacific Holocene hydroclimate from the Kenai Peninsula lowlands, south-central Alaska. *Quaternary Science Reviews*, *241*, 106420. https://doi.org/10.1016/j.quascirev.2020.106420

Callahan, M. K., Rains, M. C., Bellino, J. C., Walker, C. M., Baird, S. J., Whigham, D. F., & King, R. S. (2015). Controls on Temperature in Salmonid-Bearing Headwater Streams in Two Common Hydrogeologic Settings, Kenai Peninsula, Alaska. *JAWRA Journal of the American Water Resources Association*, *51*(1), 84–98. https://doi.org/10.1111/jawr.12235

Callahan, M. K., Whigham, D. F., Rains, M. C., Rains, K. C., King, R. S., Walker, C. M., Maurer, J. R., & Baird, S. J. (2017). Nitrogen Subsidies from Hillslope Alder Stands to Streamside Wetlands and Headwater Streams, Kenai Peninsula, Alaska. *JAWRA Journal of the American Water Resources Association*, *53*(2), 478–492. https://doi.org/10.1111/1752-1688.12508

de Graaf, I. E. M., Gleeson, T., (Rens) van Beek, L. PH., Sutanudjaja, E. H., & Bierkens, M. F. P. (2019). Environmental flow limits to global groundwater pumping. *Nature*, *574*(7776), 90–94. https://doi.org/10.1038/s41586-019-1594-4

Dekar, M. P., King, R. S., Back, J. A., Whigham, D. F., & Walker, C. M. (2012). Allochthonous inputs from grass-dominated wetlands support juvenile salmonids in headwater streams:

Evidence from stable isotopes of carbon, hydrogen, and nitrogen. *Freshwater Science*, *31*(1), 121–132. https://doi.org/10.1899/11-016.1

Famiglietti, J. S. (2014). The global groundwater crisis. *Nature Climate Change*, *4*(11), 945–948. https://doi.org/10.1038/nclimate2425

Forslund et al. (2009). *Securing water for ecosystems and human well-being the importance of environmental flows.* (Swedish Water House Report 24). Stockholm International Water Institute (SIWI). http://www.siwi.org/documents/Resources/Reports/Report24_E-Flows-low-res.pdf

Gerlach, M. E., Rains, K. C., Guerrón-Orejuela, E. J., Kleindl, W. J., Downs, J., Landry, S. M., & Rains, M. C. (2022). Using Remote Sensing and Machine Learning to Locate Groundwater Discharge to Salmon-Bearing Streams. *Remote Sensing*, *14*(1), 63. https://doi.org/10.3390/rs14010063

Guerrón-Orejuela, E. J., Rains, K. C., Brigino, T. M., Kleindl, W. J., Landry, S. M., Spellman, P., Walker, C. M., & Rains, M. C. (2023). Mapping Groundwater Recharge Potential in High Latitude Landscapes Using Public Data, Remote Sensing, and Analytic Hierarchy Process. *Remote Sensing*, *15*(10), 2630. https://doi.org/10.3390/rs15102630

Intveld, A., Brigino, T., Guerrón-Orejuela, E., Rains, K., Rains, M, Walker, C. (2022). Understanding Hydrochemical Data Through a Geological Context in the Anchor River Watershed, Kenai Peninsula Lowlands, Alaska. AGU Fall meeting 2022, Chicago. https://agu.confex.com/agu/fm22/meetingapp.cgi/Paper/1093186

Karlstrom, T. N. V. (1964). *Quaternary Geology of the Kenai Lowland and Glacial History of the Cook Inlet Region, Alaska* (USGS Numbered Series 443; Professional Paper). U.S. Geological Survey.

Klein, E., Berg, E. E., & Dial, R. (2005). Wetland drying and succession across the Kenai Peninsula Lowlands, south-central Alaska. *Canadian Journal of Forest Research*, *35*(8), 1931–1941. https://doi.org/10.1139/x05-129

Margat, J., & van der Gun, J. (2013). *Groundwater around the World: A Geographic Synopsis*. CRC Press. https://doi.org/10.1201/b13977

Mastrion, P. (2022). Collaborative tool development for promoting resilient groundwater resources in the Kachemak Bay area of Homer, Alaska. Hollings and Educational Partnership Program with Minority Serving Institutions Scholars and the National Estuarine Research Reserves, Virtual Symposium 2022. https://agu.confex.com/agu/fm22/meetingapp.cgi/Paper/1093186

Saaty, T. L. (1990). How to make a decision: The Analytic Hierarchy Process. *Desicion Making by the Analytic Hierarchy Process: Theory and Applications*, *48*(1), 9–26. https://doi.org/10.1016/0377-2217(90)90057-I

Shaftel, R. S., King, R. S., & Back, J. A. (2011). Breakdown rates, nutrient concentrations, and macroinvertebrate colonization of bluejoint grass litter in headwater streams of the Kenai Peninsula, Alaska. *Journal of the North American Benthological Society*, *30*(2), 386–398. https://doi.org/10.1899/10-086.1

Shaftel, R. S., King, R. S., & Back, J. A. (2012). Alder cover drives nitrogen availability in Kenai lowland headwater streams, Alaska. *Biogeochemistry*, *107*(1–3), 135–148. https://doi.org/10.1007/s10533-010-9541-3

United Nations. (2022). *The United Nations World Water Development Report 2022: Groundwater: Making the invisible visible*. UNESCO, Paris.

U.S. Census Bureau. (n.d.). U.S. Department of Commerce. Retrieved August 3, 2023, from https://data.census.gov/

Walker, C. M., King, R. S., Whigham, D. F., & Baird, S. J. (2012). Landscape and Wetland Influences on Headwater Stream Chemistry in the Kenai Lowlands, Alaska. *Wetlands*, *32*(2), 301–310. https://doi.org/10.1007/s13157-011-0260-x

Whigham, D. F., Walker, C. M., Maurer, J., King, R. S., Hauser, W., Baird, S., Keuskamp, J. A., & Neale, P. J. (2017). Watershed influences on the structure and function of riparian wetlands associated with headwater streams – Kenai Peninsula, Alaska. *Science of The Total Environment*, *599–600*, 124–134. https://doi.org/10.1016/j.scitotenv.2017.03.290

Winter, T. C., Harvey, J. W., Franke, O. L., & Alley, W. M. (1998). *Ground water and surface water: A single resource* (Report 1139; Circular). USGS Publications Warehouse. https://doi.org/10.3133/cir1139

Appendices

Appendix 1: Scope of Work, Agreement # 069687242

Public Works
3575 Heath Street
Homer, AK 99603

City of Homer

www.cityofhomer-ak.gov

publicworks@cityofhomer-ak.gov
(p) 907- 235-3170
(f) 907-235-3145

Memorandum 22-071

TO: Rob Dumouchel, City Manager

FROM: Janette Keiser, Director of Public Works

DATE: April 12, 2022

SUBJECT: Contract to National Kachemak Bay Estuarine Research Reserve

Issue: The purpose is to request approval to issue a Contract to the Kachemak Bay National Estuarine Research Reserve ("KBNERR") to do ground water research in the Bridge Creek Reservoir watershed.

Background:

Ordinance 21-16(A) authorized the expenditure of $50,000 from the HAWSP Fund for ground water research in the Bridge Creek Reservoir Watershed. KBNERR has been conducting ground water research in a wide area north of the Bridge Creek Reservoir. KBNERR proposes to extend that work south to the Bridge Creek Watershed for $50,000. To quote KBNERR, where's what they intend to do:

> *We propose to identify priority areas where springs, seeps, and their associated recharge areas are located. The identification of these areas will be a combination of geospatial analysis and field verification. The new geospatial modeling will predict locations of groundwater recharge next to seeps and springs in the Bridge Creek Reservoir watershed, which will be field validated.*
>
> *Field work will be performed June 2022. Edgar Guerron Orejuela from the University of South Florida and a NOAA Ernest F. Hollings scholar, will focus on developing and field validating the layer that predicts the locations of groundwater recharge proximal to known seeps and springs in the Bridge Creek Reservoir watershed. Later, Dr. Mark Rains, Dr. Kai Rains, Tyelyn Brigino of the University of South Florida, and another NOAA Ernest F. Hollings scholar, will further field validate the layer that predicts the locations of additional seeps and springs. Onsite technical and logistical support will be provided by KBNERR staff. We request that the City of Homer facilitate physical access to areas within the project domain.*
>
> *Deliverables will include an updated geospatial database and a virtual workshop focused on the identification of areas where the City of Homer might want to consider practicing source-water protection, to ensure lasting groundwater discharge to the Bridge Creek Reservoir.*

Recommendation:

City Council pass a resolution awarding a Contract to KBNERR in the amount of $50,000 and authorizing the City Manager to negotiate and execute the appropriate documents.

Appendix 2: Gerlach, M. E., Rains, K. C., Guerrón-Orejuela, E. J., Kleindl, W. J., Downs, J., Landry, S. M., & Rains, M. C. (2022). Using Remote Sensing and Machine Learning to Locate Groundwater Discharge to Salmon-Bearing Streams. *Remote Sensing,* 14(1), 63. https://doi.org/10.3390/rs14010063

remote sensing

Article

Using Remote Sensing and Machine Learning to Locate Groundwater Discharge to Salmon-Bearing Streams

Mary E. Gerlach [1], Kai C. Rains [1], Edgar J. Guerrón-Orejuela [1], William J. Kleindl [2], Joni Downs [1], Shawn M. Landry [1] and Mark C. Rains [1,*]

1 School of Geosciences, University of South Florida, Tampa, FL 33620, USA; marygerlach@usf.edu (M.E.G.); krains@usf.edu (K.C.R.); edgarguerron@usf.edu (E.J.G.-O.); downs@usf.edu (J.D.); landry@usf.edu (S.M.L.)
2 Land Resources and Environmental Sciences, Montana State University, Bozeman, MT 59717, USA; william.kleindl@montana.edu
* Correspondence: mrains@usf.edu; Tel.: +1-813-974-3310

Abstract: We hypothesized topographic features alone could be used to locate groundwater discharge, but only where diagnostic topographic signatures could first be identified through the use of limited field observations and geologic data. We built a geodatabase from geologic and topographic data, with the geologic data only covering ~40% of the study area and topographic data derived from airborne LiDAR covering the entire study area. We identified two types of groundwater discharge: shallow hillslope groundwater discharge, commonly manifested as diffuse seeps, and aquifer-outcrop groundwater discharge, commonly manifested as springs. We developed multistep manual procedures that allowed us to accurately predict the locations of both types of groundwater discharge in 93% of cases, though only where geologic data were available. However, field verification suggested that both types of groundwater discharge could be identified by specific combinations of topographic variables alone. We then applied maximum entropy modeling, a machine learning technique, to predict the prevalence of both types of groundwater discharge using six topographic variables: profile curvature range, with a permutation importance of 43.2%, followed by distance to flowlines, elevation, topographic roughness index, flow-weighted slope, and planform curvature, with permutation importance of 20.8%, 18.5%, 15.2%, 1.8%, and 0.5%, respectively. The AUC values for the model were 0.95 for training data and 0.91 for testing data, indicating outstanding model performance.

Keywords: seeps; springs; geology; topography; aquifer outcrops; topographic indices; geospatial modeling; Kenai Peninsula Lowlands; Alaska

Citation: Gerlach, M.E.; Rains, K.C.; Guerrón-Orejuela, E.J.; Kleindl, W.J.; Downs, J.; Landry, S.M.; Rains, M.C. Using Remote Sensing and Machine Learning to Locate Groundwater Discharge to Salmon-Bearing Streams. *Remote Sens.* **2022**, *14*, 63. https://doi.org/10.3390/rs14010063

Academic Editor: Mark S. Lorang

Received: 9 October 2021
Accepted: 23 December 2021
Published: 24 December 2021

1. Introduction

Many ecosystems depend on groundwater discharge, including many wetlands [1,2], lakes [3,4], streams [5,6], and estuaries [7,8]. Groundwater discharge to streams is particularly prevalent and critical, being the sole source of baseflow by definition [9] and commonly a substantive subcomponent of stormflow [10]. Though regionally variable, estimates suggest that groundwater discharge provides 14–90% of all stream flow in the conterminous United States [5]. In addition to subsidizing stream flow, groundwater discharge to streams can also modulate stream temperature [11,12] and deliver nutrients and organic carbon [13,14], thereby playing important roles in structuring habitats from the benthos [15] to the fish [16]. Groundwater is also an important water supply component, with 321,000,000 m^3 of groundwater withdrawals comprising 26% of all water use in the United States in 2015 [17]. Many of these withdrawals are centralized, including withdrawals for thermoelectric power generation (41%), public water supply (12%), and industrial water supply (5%). Others are more dispersed, including irrigation water supply (37%) and domestic water supply (1%). Effective management and protection of groundwater resources is critical, therefore, to a diverse suite of natural and human users [18].

The first step toward protecting groundwater discharge to ecosystems is to determine the types of groundwater discharge (e.g., sourced from local versus regional groundwater flow systems), the locations where groundwater discharge occurs, and their support for downgradient ecosystems (e.g., fluvial ecosystems). Field studies are often essential in identifying types and locations of groundwater discharge, especially in geologically complex regions where there may be more than one type of groundwater discharge from more than one type of geologic unit [19,20]. Field mapping of these types of groundwater discharge is possible in some situations (e.g., [21]) but is impractical over large spatial scales and/or in difficult-to-access regions. In these instances, remote sensing, geospatial modeling, and/or machine learning have been used to map remote locations where groundwater discharge occurs, with some degree of success (e.g., [22,23]). These tools are receiving increased attention for general applications in hydrology as computer processing power increases and remote sensing data become more easily available.

The ways remote sensing, geospatial modeling, and/or machine learning are used in hydrologic studies depends on the question being addressed; the spatial and temporal scale of the question; and the type, amount, and quality of the available data [24–26]. Nevertheless, these tools have been incorporated into strategies to forecast groundwater levels [27–30], groundwater quality [31–33], saltwater intrusion and groundwater salinity [34], and groundwater resource availability [35,36]. Using these approaches to better understand and predict groundwater discharge is particularly challenging (e.g., [22,23]). In many cases, groundwater discharge occurs where erosion or tectonic uplift has exposed aquifers, creating aquifer outcrops. This means that better understanding and predicting groundwater discharge requires an understanding of both topography and geology, with subsurface lithology commonly being poorly known [22,23] yet nevertheless playing a disproportionately important role [30].

The primary controls on groundwater recharge, flow, and discharge are climate, geology, and topography [37]. Climate is typically constant across large study areas, and regional-scale geologic data are difficult to obtain, so studies typically rely upon topography to characterize generalized hydrology [38,39] and locations where groundwater discharge is likely to occur [23,40,41]. However, geologic heterogeneity often plays a controlling role in groundwater recharge, flow, and discharge [42], leading some to suggest that geologic data are more important than topographic data when characterizing hydrological processes (e.g., [30,43]). However, accurate prediction of groundwater discharge is often desired in regions where the geology is heterogeneous and anisotropic, poorly understood, and/or inadequately documented. We therefore hypothesized that topographic features alone could be used to locate groundwater discharge, but only where diagnostic topographic signatures could first be identified through field observations and geologic data covering a characteristic subset of the study area. We based this hypothesis on the understanding that groundwater levels and discharges play important roles in structuring local- and watershed-scale geomorphology, thereby affecting topography [44,45], and that groundwater flow systems are typically attracted to the land surface at concave surfaces, such as hillslope failures and toeslopes [2,46,47]. We tested this hypothesis in south-central Alaska, in a large area that is difficult to access and where geologic data are incompletely available but where remotely sensed LiDAR-based topographic data are widely available.

2. Materials and Methods

2.1. Site Description

The study was conducted on the Kenai Peninsula Lowlands in south-central Alaska (Figure 1). The study area is a 1655 km^2 area comprising five watersheds: Anchor River, Stariski Creek, Happy Creek, Deep Creek, and the Ninilchik River, from south to north respectively. All except Happy Creek are salmon-bearing and therefore support vibrant sport and commercial fisheries that are central to the regional economy [48,49]. Groundwater discharge plays a critical role in controlling the structure and function of these streams, by augmenting stream flow, modulating stream temperatures, and delivering nutrient subsidies [12,14]. Most of the study area is roadless or accessible only by unimproved roads. However, more than 80% of the land is privately owned and has begun seeing steadily increasing development pressure [50], particularly in the western region of the study area and primarily to support single-family homes and farm-to-fork agriculture [51]. Groundwater is the primary source of water for domestic, commercial, and industrial uses [52] and is also threatened by land-use/land-cover change [53], aggregate mining [49], and a drying trend in the climate [54–56].

Figure 1. General location of the five watersheds that comprise the study area on the Kenai Peninsula Lowlands. Base map source [57].

The climate is transitional from maritime to coastal and consists of short summers and long winters (HOMER 8 NW, ALASKA [503672], 1981–2010). The mean annual minimum temperature is −0.8 °C, and the mean annual maximum temperature is 6.1 °C. Total annual precipitation is 748 mm, with approximately one-third falling as snow and approximately half falling during the wet season (i.e., August–November). The study area underwent at least five major Pleistocene glaciations and two minor post-Pleistocene glacial advances, each variously recorded in ice-scoured landforms, drift sheets, moraines, and discordant drainage relations separated by unconformities and weathering profiles [58]. Most of the study region is now covered with younger glacial outwash and valley train; glaciolacustrine;

and other minor terminal, recessional, lateral, medial, and ground moraine deposits [59], some reworked by the recent minor glacial advances. Groundwater is found in both surficial deposits, often in wetlands, and in deeper deposits, commonly in thin, discontinuous, and poorly lithified sandstone aquifers formed in buried channel lag and bar deposits [60]. Overall topographic relief ranges from 0 to 889 m above mean sea level (AMSL). Local topography is also commonly steep, as streams have deeply dissected the landscape during the Quaternary.

2.2. Overall Approach

The study proceeded in three phases. During the first phase, we created a geographic information system (GIS) geodatabase from geologic and topographic data. Geologic data were sourced from publicly available well logs available for ~40% of the study area; topographic data were sourced from airborne LiDAR available for the entire study area. During the second phase, we stayed within the subset of the study area where geological data were available, using the geodatabase and field observations to identify two types of groundwater discharge and locations where they occurred. The geologic data and geodatabase were essential to the initial identification of one of those two types of groundwater discharge and locations where it occurred. However, field observations suggested that these locations could also be identified by specific combinations of topographic variables alone even where geologic data were not available (e.g., numerous narrow gullies and other deeply incised headwater stream channels that abruptly start along the same topographic contour interval on a hillslope). In the final phase, we used a machine learning approach using only topographic data to predict the likelihood that either type of groundwater discharge occurs.

2.3. Geodatabase Development

2.3.1. Geologic Data

Subsurface geologic data were obtained from well logs in the publicly available Well Log Tracking System (WELTS) maintained by the Alaska Department of Natural Resources (https://dnr.alaska.gov/welts/; accessed on 29 May 2019). Records from >800 well logs within and immediately adjacent to the study area were used to quantify the locations, depths, thicknesses, and geologic characteristics of the water-bearing formations, i.e., the aquifers.

Depths and thicknesses of the aquifers were converted to top and bottom elevations of the aquifers. The aquifer materials are unconsolidated to poorly lithified buried channel lag and bar deposits and therefore vary slightly in thickness and slope gently in the original direction of drainage. Therefore, a user-specified 5 m vertical buffer was added to the top and subtracted from the bottom elevations of the aquifers. These vertically buffered aquifers were then projected outward from the well logs in concentric circles of increasing radii using the Inverse-Distance Weighting (IDW) interpolation tool. Areas where the buffered aquifers intersected the ground surface were found by intersecting the aquifer boundaries with a digital elevation model (DEM, see below) using the Raster Calculator tool and were mapped as potential aquifer outcrops. The final step was to determine the horizontal spatial scale over which the aquifer interpolations were valid. We did so using standard geologic mapping techniques. Geologic mapping is an interpretive method in which field observations are commonly recorded as qualitative data, such as sketches and narratives [61]. We made such qualitative observations at increasing radial distances from wells, looking for aquifer outcrops of the same material and at the same approximate elevations as described in the corresponding well log. We initially tested circles of 1000 m radius and then tested circles of 2000 and 3000 m radius as we continued to find aquifer outcrops at the outer edges of the projections, though with decreasing frequency with increasing radial distance. We then tested circles of 5000 m radius, finding no aquifer outcrops of the same material at the same approximate elevations as described in the corresponding well log. We concluded that the horizontal spatial scale over which the aquifer interpolations were valid ended somewhere between 3000 and 5000 m, and we adopted the more-conservative limit of 3000 m. This resulted in >800 overlapping circles of 3000 m radius covering ~40% of the study area, which is sufficiently representative of the entire study area. Many of these overlapping circles intersect the ground surface and therefore indicate locations where groundwater discharge from aquifer outcrops likely occurs.

2.3.2. Topographic Data

Topographic data were derived from airborne LiDAR (2008 Kenai Watershed Forum Topographic LiDAR: Kenai Peninsula, Alaska; https://www.fisheries.noaa.gov/inport/item/49620; accessed on 25 February 2019). The LiDAR-based digital elevation model (DEM) was acquired at 1 × 1 m pixel size but was resampled to a 3 × 3 m pixel size, which both reduced run times and smoothed microtopographic anomalies. The DEM was also modified to remove areas that were below the estimated tide level at the time of data collection (~3 m AMSL). This resampled and modified DEM was used to produce all topographic data using standard tools in ArcGIS 10.5 or ArcGIS Pro 2.7.1 (ESRI, Redlands, CA, USA).

Topographic data directly extracted from the DEM included elevation, slope, profile curvature, profile curvature range, planform curvature, and planform curvature range. Slope records the steepness of the terrain expressed as a percentage. Steep slopes can be indicative of steep hydraulic gradients driving shallow groundwater flow [42], and long steep slopes may be indicative of locations where aquifers might outcrop and therefore where deep groundwater discharge might occur. Profile curvature measures convexity or concavity of the slope parallel to the direction of the slope; planform curvature measures convexity or concavity of the slope perpendicular to the direction of the slope. The range of profile and planform curvatures were calculated within a 3 × 3 cell (9 × 9 m) window to measure changes in curvature over short distances, which can be an indicator of slope failures like those induced by groundwater discharge [46,47], the headward extents of channels formed by groundwater discharge [62,63], and/or locations where water tables might be close to or above the land surface [2,64].

Topographic data derived from the DEM included flowlines, terrain ruggedness index (TRI), flow-weighted slope (FWS), and topographic wetness index (TWI). Flowlines were defined by categorizing flow accumulation values higher than 2000 as streams and converting those into vector format. Flowlines may represent locations where water tables might be close to or above the land surface [6], and the headward extents of flowlines likely correlate with the headward extents of channels formed by groundwater discharge [63]. TRI measures topographic heterogeneity, calculated as the square root of the average squared differences in elevation between a pixel and its eight neighbors, and is defined per pixel as:

$$\mathrm{TRI} = \left[\left(X_{ij} - X_{00} \right)^2 \right]^{\frac{1}{2}}, \tag{1}$$

where X_{ij} is the elevation of all eight pixels neighboring pixel X_{00} [65]. TRI was computed using Arc Hydro in ArcGIS Pro. TRI is an indicator of slope failures like those induced by groundwater discharge, the headward extents of channels formed by groundwater discharge, and narrow gullies and other deeply incised headwater stream channels [66]. FWS indicates the degree to which water is concentrated and then driven downslope by topography, and it is defined per subcatchment as:

$$\mathrm{FWS} = \sum (\beta_i * FAC_i) / \sum FAC_i, \tag{2}$$

where β_i is the slope (in percent) at a particular pixel, FAC_i is flow accumulation for that pixel, and $\sum(FAC_i)$ is the summation of flow accumulation for all pixels within the subcatchment. FWS was calculated using Arc Hydro in ArcMap 10.8. Arc Hydro was first used to calculate flow direction and flow accumulation and define, segment, and link streams. These were then used to delineate catchments using the Arc Hydro catchment grid delineation tool. The catchment grid was then converted into a polygon feature class using the Arc Hydro catchment polygon processing tool. The stream link layer was then converted into a drainage line feature class using the Arc Hydro drainage line processing tool. Finally, the Arc Hydro adjoint catchment processing tool was used to generate the aggregated upstream catchments from the catchment feature class. FWS for each catchment was then calculated from these layers using the raster calculator. FWS has been shown to correlate both with groundwater discharge [12] and stream water chemistry which itself may be a function of groundwater discharge [67]. TWI indicates where water is likely to accumulate, and it is defined per pixel as:

$$\text{TWI} = \ln\left(\frac{A}{\text{Tan}\beta_0}\right), \quad (3)$$

where A is the area that contributes flow to a particular pixel and $\text{Tan}\beta_0$ is the tangent of the slope of the pixel being analyzed [68,69]. TWI was calculated using Arc Hydro and the TWI tool in TauDEM Version 5 (Terrain Analysis Using Digital Elevation Models; https://hydrology.usu.edu/taudem/taudem5/; accessed on 7 May 2019) in ArcMap 10.8. The D-infinity (DINF) tool in Arc Hydro was first used to calculate a slope-sensitive flow direction. The DINF is an iterative process which guarantees that each flat pixel ultimately drains to a lower elevation, eliminating the possibility of inconsistencies such as loops in the flow direction angle [70]. The DINF contributing area tool in Arc Hydro was then used to calculate a grid of pixel-specific catchment areas. TWI for each pixel was then calculated using the TWI tool from the TauDEM. TWI has also been called Wetx and Compound Topographic Index (CTI); all three utilize the same formula to represent likelihood of water flow over landscapes [68,69,71].

2.3.3. Layers Derived from the Geologic and Topographic Data

Multiple geologic and topographic layers were derived from the geologic and topographic data (Figure 2). The geologic data were obtained from >800 well logs associated with domestic, commercial, and/or industrial wells, all located proximal to roads in the more-developed western and southern parts of the study area. The topographic data were derived from a DEM which covered the entire, mostly roadless, 1655 km^2 study area. Therefore, the GIS layers which represent the geologic data are situated predominantly in the western and southern portions of the study area while the layers representing the topographic data cover the full extent of the study area.

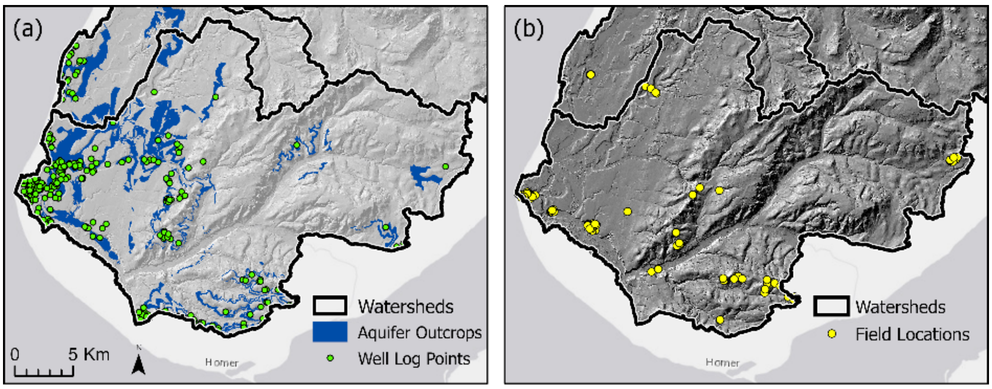

Figure 2. *Cont.*

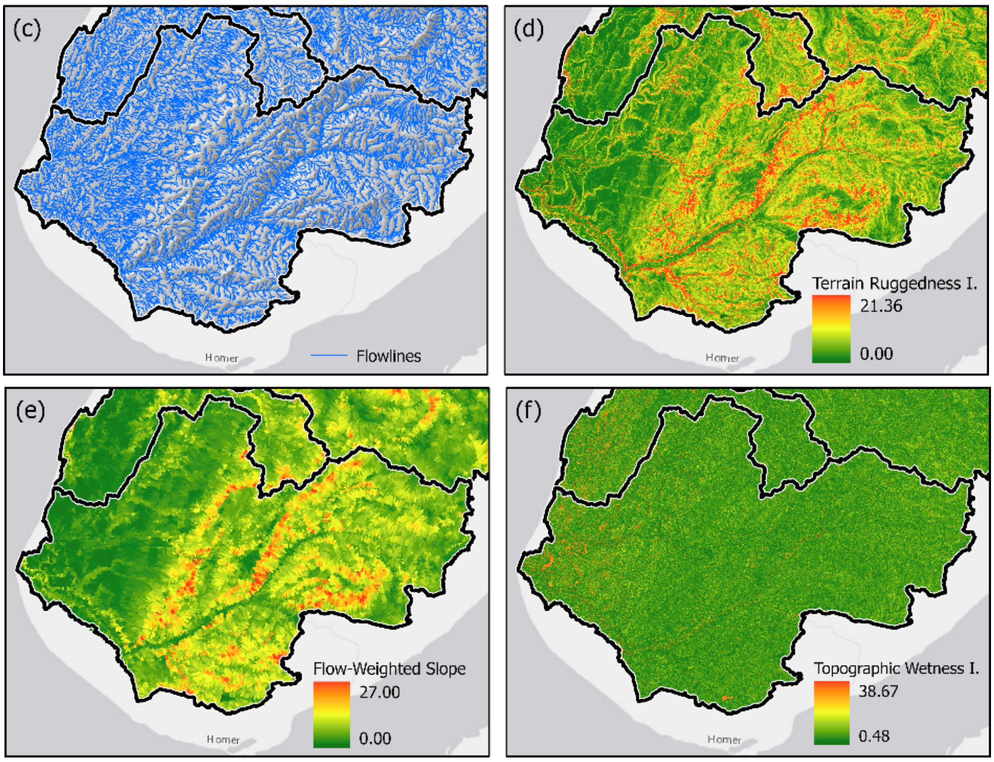

Figure 2. Primary geologic and topographic layers include: (**a**) well log points and modeled aquifer outcrops; (**b**) DEM, represented by a shaded relief to emphasize terrain, with the 67 field points used for training and testing; (**c**) flowlines; (**d**) TRI; (**e**) FWS; and (**f**) TWI. Here, only the Anchor River Watershed, the southernmost of the five watersheds, is shown in full.

2.3.4. Field Work

Field work was conducted during the summers of 2018 and 2019. Initial field work was focused on identifying the types of groundwater discharge that occur and the conditions under which they occur. We then developed and tested procedures for the manual identification of these types of groundwater discharge using the full geologic and topographic portions of the geodatabase (i.e., both the geologic and topographic data). Using these manual procedures, we identified 67 locations in the Anchor River and Stariski Creek watersheds, the southernmost two watersheds in the study area (Figure 2). Our manual procedures predicted that groundwater discharge did occur at 54 of these locations and did not occur at 13 of these locations. We then visited each of these 67 locations, obtaining geographic positioning system (GPS) coordinates at each location with a Garmin Rino 650 handheld GPS unit (Garmin, Olathe, KS, USA) and noting if groundwater discharge actually did or did not occur. Where groundwater discharge did occur, temperature, pH, and specific conductance were measured using a YSI MPS 556 (YSI, Yellow Springs, OH, USA). Specific conductance was particularly important because it is a proxy for water–rock contact time, with precipitation having no water–rock contact time and relatively low specific conductance, shallow soil water having relatively short water–rock contact time and relatively moderate specific conductance, and deep aquifer water having relatively long water–rock contact time and relatively high specific conductance (e.g., [72]). Therefore, it was a useful proxy for distinguishing between younger, shallow hillslope groundwater (e.g., recent precipitation, including snowmelt, moving downslope along the surface and in the shallow subsurface) from older, deep aquifer groundwater (e.g., precipitation, including snowmelt, that had infiltrated and recharged deeper aquifers, then traveled laterally to discharge from an aquifer outcrop). We simultaneously also made observations that indicated we might otherwise identify these types of groundwater discharge using only the topographic portion of the geodatabase (i.e., only the topographic data).

2.3.5. Modeling

The study area is large and difficult to access, and geologic data are only available for ~40% of the study area. Furthermore, field observations indicated that the locations where groundwater discharge occurred could be identified by specific combinations of topographic features alone. Therefore, we applied maximum entropy modeling, a machine learning technique, to predict the likelihood groundwater discharge occurs using only the topographic portion of the geodatabase. We chose a Maxent modeling approach to map the prevalence of seeps and springs across the study area, as it is a robust method that relies on presence-only data. Maxent works by relating occurrence data, in the form of points, to layers of environmental data, which are sometimes called predictors or covariates [73,74]. The method works by using maximum likelihood functions to best distinguish presence points from the landscape. Specifically, the algorithm finds the model that minimizes the relative entropy between the probability density of the presence points and the probability density of background locations, as measured in covariate space. We used Maxent version 3.4 (http://biodiversityinformatics.amnh.org/open_source/maxent; accessed on 1 September 2020) to predict locations of seeps and springs with respect to environmental variables. The 51 seeps and springs identified in the field were used as the presence points, while 10 topographic layers from the geodatabase were used as the predictors: elevation, slope, planform curvature, planform curvature range, profile curvature, profile curvature range, distance to flowlines, TRI, FWS, and TWI.

We modeled the prevalence of seeps and springs using a logistic model with the default parameters, except for specifying a prevalence value of 0.10. The value of 0.10 was selected because we expected seep and spring formation to occur uncommonly, over an estimated 10% of the area. We used a systematic approach to evaluate and reduce the number of environmental layers to obtain a final model. First, the set of candidate variables was reduced by removing highly correlated layers, as collinearity can cause bias and make relationships between individual variables difficult to discern [75,76]. Pairwise correlations were calculated between all candidate layers; a threshold of $r > 0.70$ was used to identify correlated variables. Then, single-variable Maxent models were run for each correlated variable, with the most predictive variable from each pair, as measured using a jackknife test, retained for further analysis. Second, a Maxent model was run on all remaining, uncorrelated variables. The permutation importance of each variable was examined, and any variables with no contribution to the model were removed. Third, a Maxent model consisting only of uncorrelated, contributing variables was run to predict spring prevalence. Finally, a cross-validation procedure was used to test the predictive performance of the final model.

Our manual procedures previously predicted groundwater discharge occurred at 54 locations. Field verification indicated that groundwater discharge actually occurred at 51 of these 54 locations. These 51 presence-only occurrences were used as training and testing data, with 70% (n = 36) used as training data and 30% (n = 15) used as testing data. The performance of the final model was assessed by computing the area under the receiver operating curve (AUC), which measures the probability that a randomly selected presence location will be ranked higher than a randomly selected background location.

3. Results

3.1. Types of Groundwater Discharge

Two types of groundwater discharge were identified in the study area, hillslope groundwater discharge and aquifer-outcrop groundwater discharge (Figure 3). Hillslope groundwater discharge occurs where rainfall and snowmelt infiltrate into the shallow subsurface, move laterally downslope through the shallow subsurface, and discharge as diffuse seeps and small springs at groundwater-induced slope failures and valley-bottom toeslopes. Aquifer-outcrop groundwater discharge occurs where rainfall and snowmelt infiltrate into the deep subsurface, move laterally through aquifers, and discharge as larger springs at aquifer outcrops in valleys carved by modern streams.

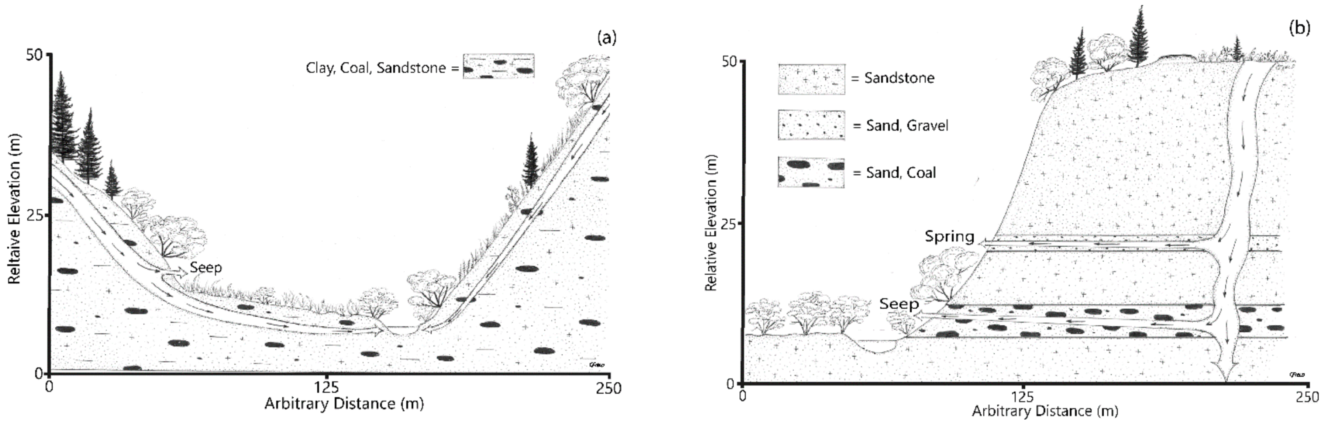

Figure 3. Types of groundwater discharge include (**a**) hillslope groundwater discharge and (**b**) aquifer-outcrop groundwater discharge. Illustrations drawn by Conrad Field from field sketches and notes prepared by Mark Rains.

3.2. Manual Identification of Groundwater Discharge

3.2.1. Hillslope Groundwater Discharge

Hillslope groundwater discharge is likely to occur on large, concave, and steep hillslopes that accumulate, concentrate, and drive shallow groundwater downgradient toward concave midslope and/or toeslope positions. These factors are reflected in FWS, which is a function of the flow accumulation area and slope. FWS is partly a function of slope, so it tends to be highest in the steep terrain characteristic of the eastern section of the study area where high-elevation headwaters are common (Figure 2). Previous work in this study area has demonstrated that hillslopes with relatively moderate–high FWS are commonly associated with groundwater discharge to streams [12]. Flowlines are also a function of flow accumulation area. Therefore, a simple two-step workflow using FWS and flowlines was found to be sufficient for identifying locations where hillslope groundwater discharge was likely to occur, which could then be verified in the field (Figure 4).

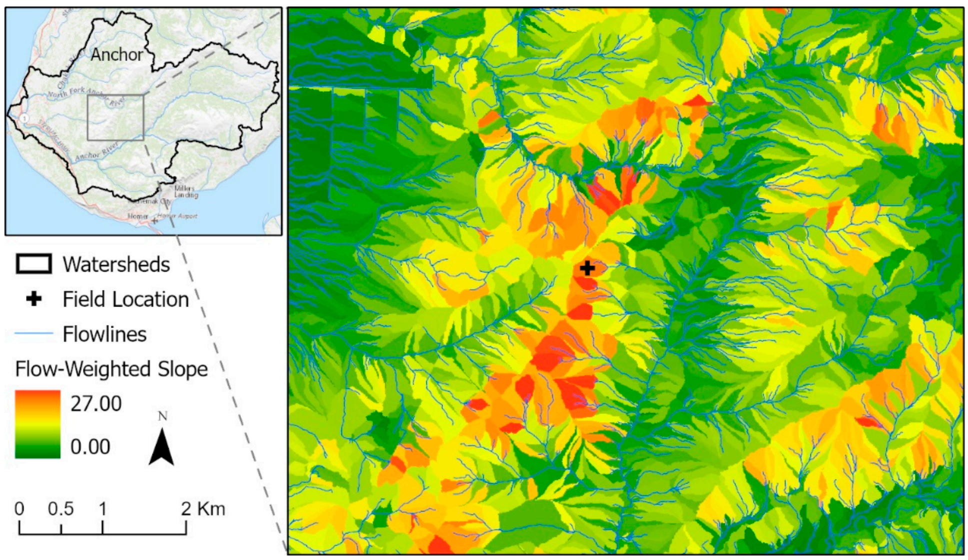

Figure 4. Example of implementing the two-step workflow to locate hillslope groundwater discharge. FWS is first used to identify hillslopes with relatively high FWS. Flowlines are then used to identify specific locations where channels may initiate. Diffuse seeps are commonly found in these settings, including at the field location in this example.

3.2.2. Aquifer-Outcrop Groundwater Discharge

Aquifer-outcrop groundwater discharge is likely to occur where aquifers outcrop and topography indicates the initiation of channelized flow. Aquifer outcrops are reflected in the aquifer outcrop layer, a created layer that covers only the western and southern, i.e., more-developed, settings where well log information was available (Figure 2). These aquifer outcrops commonly support large springs which form the headward extent of prominent channels, typically aligned roughly parallel to one another and abruptly initiating along the same contour interval. The spatially limited aquifer outcrop data product was then used to explore the topographic data that reflected the initiation of channelized flow, including the headward extent of incised topography, the initiation of flowlines, and the sudden concentration of the TWI. Therefore, a simple four-step workflow using the aquifer outcrops overlaid on contour lines, flowlines, and TWI was found to be sufficient for identifying locations where aquifer-outcrop groundwater discharge was likely to occur, which could then be verified in the field (Figure 5).

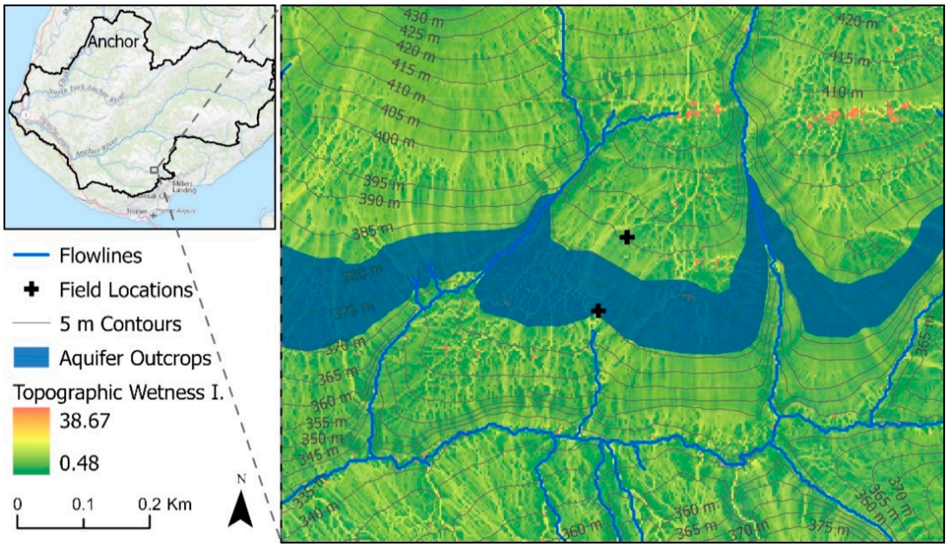

Figure 5. Example of implementing the four-step workflow to locate aquifer-outcrop groundwater discharge. Aquifer outcrops are first used to indicate regions where large volumes of groundwater discharge likely occur. Then each of the three topographic layers, i.e., contour lines, the initiation of flowlines, and sudden increases in TWI, are used to identify locations where channelized flows initiate. Springs are commonly found in these settings. In this case, the lowermost field point was preselected and found in the field to be 13 m from a spring. The uppermost field point was then visited, and the static water level was found to be ~2 m below the ground surface in a hand-dug well.

3.2.3. Field Verification

The procedures for identifying groundwater discharge were field verified by visiting 67 field locations, 54 where groundwater discharge was predicted to occur and 13 where groundwater discharge was predicted not to occur. Groundwater discharge was logged as occurring if a seep or spring was observed within 30 m of the predicted location. Results are tabulated in a confusion matrix (Table 1). The sensitivity (i.e., correctly predicted positives/total actual positives) is 50/51, or 98%, while the precision (i.e., correctly predicted positives/total predicted positives) is 50/54, or 93%. Accuracy, calculated as the percentage of correct predictions, is 62/67, or 93%. That is, overall, the manual procedures accurately predicted the presence or absence of groundwater discharge in 93% of cases. The kappa coefficient (κ), which takes into account the possibility of the agreement occurring by chance, is 0.78, which indicates substantial strength of agreement with the field data [77,78].

Table 1. Confusion matrix of ground-truth points collected to verify the accuracy of the geodatabase predictions.

	Predicted No	Predicted Yes	Total
Actual No	12	4	16
Actual Yes	1	50	51
Total	13	54	67

3.3. Modeled Identification of Groundwater Discharge

The final Maxent model included six topographic variables. Profile curvature range contributed the most information to the model with a permutation importance of 43.2%, followed by distance to flowlines, elevation, TRI, FWS, and planform curvature, with permutation importance of 20.8%, 18.5%, 15.2%, 1.8%, and 0.5%, respectively (Table 2). Predicted prevalence of seeps and springs was highest where profile curvature ranges were large, distances to flowlines were low, elevation was low, TRI was high (i.e., terrain was rugged), FWS was high, and planform curvature values were large (Figure 6). Collectively, the model predicts groundwater discharge where topography changes abruptly over small distances in close proximity to flowlines at lower elevations (Figure 7). The model predicts that seeps and springs are widespread over the study area, with high prevalence locations particularly at the headward extent of and alongside streams and along coastal bluffs. The AUC values for the model were 0.95 for training data and 0.91 for testing data, indicating outstanding performance [79].

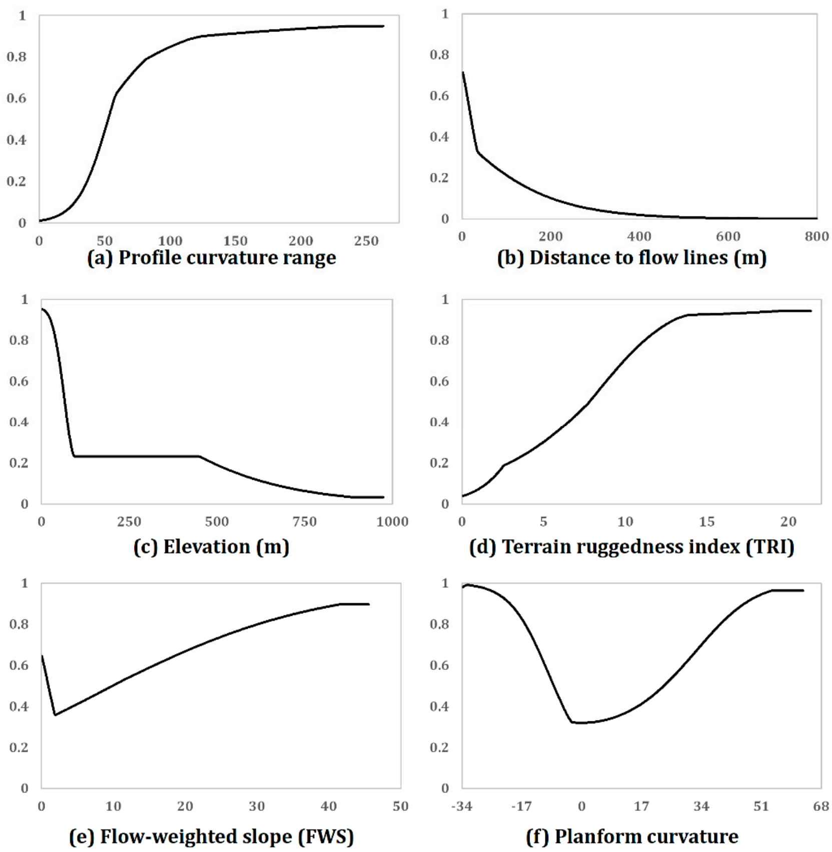

Figure 6. Predicted probability of prevalence (*y*-axis) for six topographic variables used in the final Maxent model to predict seeps and springs: (**a**) profile curvature range, (**b**) distance to flowlines, (**c**) elevation, (**d**) TRI, (**e**) FWS, and (**f**) planform curvature. The curves represent the dependence of predicted prevalence on both the individual topographic variables and the correlations between them.

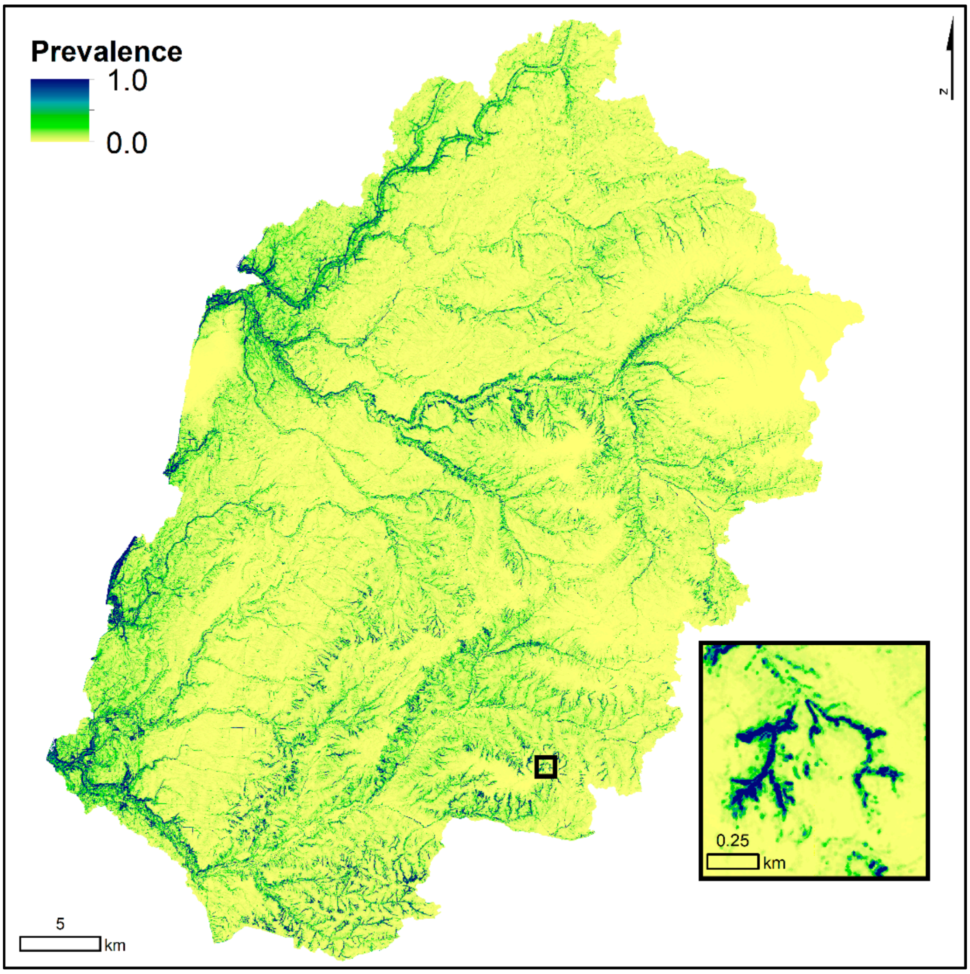

Figure 7. Predicted prevalence of seeps and springs in the entire study area. Seeps and springs are most likely to occur where spring prevalence values are highest. The inset highlights the small box in the southeast of the study area, which is an example area where the probability of the occurrence of seeps and springs is particularly high.

Table 2. Permutation importance for variables used to predict seeps and springs using the Maxent model.

Variable	Permutation Importance (%)
Profile curvature range	43.2
Distance to flowlines	20.8
Elevation	18.5
Terrain ruggedness index	15.2
Flow-weighted slope	1.8
Planform curvature	0.5

4. Discussion

Though the primary controls on groundwater flow and discharge are climate, geology, and topography [37], we demonstrated that the locations where groundwater discharge occurs can be predicted based solely on topography if key diagnostic topographic signatures can be first identified using ancillary field observations and geologic data in a representative subset of the study area. Here, we modeled two types of groundwater discharge: hillslope groundwater discharge and aquifer-outcrop groundwater discharge (Figure 3). We constructed a robust geodatabase comprising field observations and geologic data from >800 well logs covering a representative subset of the study area and topographic data from an airborne LiDAR-derived DEM covering the entire study area (Figure 2). We then developed and refined procedures to manually identify the two types of groundwater discharge in the representative subset of the study area where the field observations, geologic data, and topographic data were available (Table 1; Figures 4 and 5). While doing so, we made observations that indicated we might otherwise identify these two types of groundwater discharge using only the topographic data. We therefore developed and refined procedures to model the two types of groundwater discharge throughout the entire study area from the topographic data alone (Table 2; Figure 7). Devito et al. [43] previously argued that topography was the last control to consider in explaining hydrologic processes, after climate and geology. Rahmati et al. [30] concurred, suggesting that geologic data (e.g., lithology) was a relatively strong predictor of groundwater levels while topographic data (e.g., slope) was a relatively weak predictor of groundwater levels. Here, topography was in fact the only control we considered, but only after topography was contextualized with the field observations and geologic data in the representative subset of the study area.

The modeling benefited greatly from previous field observations by Callahan et al. [12], which in turn benefited greatly from other previous field observations by Walker et al. [66] and King et al. [80]. These studies showed that topography correlates with the structure and function of streams in the Kenai Peninsula Lowlands, including stream flow and stream water temperature [12], stream water chemistry [66], and stream biota [80]. These studies were conducted at 18 shared study sites in the Anchor River, Stariski Creek, Deep Creek, and Ninilchik Creek watersheds, four of the five watersheds included in this study. Callahan et al. [12] made the key insight that motivated our study. Their field observations indicated that a topographic feature, i.e., FWS, could be used to predict the location of hillslope groundwater discharge to streams. We further refined this understanding, noting that, for example, hillslopes with high FWS also had a prevalence of small headwater streams that originated at seeps and small springs. These are evident in the topographic data in a number of ways, including sudden changes in curvature (i.e., profile curvature range), flowlines, and TWI (Figure 2). This then allowed the accurate manual and modeled identification of hillslope groundwater discharge (Figures 4 and 7).

The modeling also benefited greatly from the availability of >800 publicly available well logs (Figure 2). Surficial geology data are available for the entirety of the Kenai Peninsula Lowlands, at the 1:350,000 scale [59]. Such data can be useful in predicting potential groundwater recharge zones (e.g., [81]). However, such coarse data alone cannot be used to map thin confined aquifers and their outcrops, as was necessary for this study. The well logs allowed us to do so. Then subsequent field work further allowed us to refine our understanding of the spatial scale over which the well logs were predictive of aquifer outcrops (Figure 2). This allowed us to find numerous springs, which we then used to explore the topographic data that reflected the initiation of channelized flow, including the headward extent of incised topography, the initiation of flowlines, and the sudden concentration of the TWI. Once these relationships were identified, the topography could in many cases be used as a proxy for the geology, such as in cases where aquifer outcrops were instead indicated by the initiation of multiple, parallel channelized flows along the same contour intervals on the same and/or opposite hillslopes (e.g., Figure 5). This then allowed the accurate manual and modeled identification of aquifer-outcrop groundwater discharge (Table 2; Figures 5 and 7).

The novelty of our modeling approach lies in the integration between field observations, remote-sensing data, and machine learning. Workflows for the manual identification of groundwater discharge were used to locate hillslope and aquifer-outcrop groundwater discharges in the field, with an overall accuracy of 93% (Table 1; Figures 4 and 5). Though labor-intensive, this approach enabled the field identification of a large enough sample of seep and spring locations to develop an "outstanding" predictive model for the entire study area using topographic data alone, with an AUC of 0.95 and 0.91 for training and testing data, respectively (Table 2; Figure 7). Using only topographic data was ideal in our study area because well logs and therefore crucial geologic data (i.e., aquifer-outcrop locations) were only available over ~40% of the study area. Maxent modeling in particular was advantageous because it uses presence-only data and therefore can be used to make widespread predictions over a large study area with limited data over only a subset of the study area (e.g., [82]). Another advantage of the Maxent approach is its ability to quantify the relationships between feature prevalence and the environmental predictors [72,73]. Our model confirms field observations that groundwater discharge is most likely to occur where topography changes abruptly over small distances in close proximity to flowlines, supporting the findings of other studies (e.g., [2,46,47,63]).

Both field observations and modeling results indicate that seeps and springs are commonly located proximal to streams, both the headward extent of streams and along hillslopes adjacent to streams (e.g., Figure 7). Following the five major Pleistocene glaciations and two minor post-Pleistocene glacial advances, the Kenai Peninsula Lowlands comprised mixed ice-scoured landforms, drift sheets, and moraines separated by unconformities and weathering profiles, much covered with younger glacial outwash and valley train, glaciolacustrine, and other minor moraine deposits [58,59]. This heterogeneity was reflected at the surface, where local topographic relief was sufficient to direct surface-water flows into the earliest watersheds, and in the subsurface, where aquifers were commonly thin and discontinuous, often formed in thin glacial outwash and valley train deposits. Subsequent downcutting by the streams shaped and steepened valley hillslopes, thereby creating and enhancing hillslope groundwater discharge, and exposed aquifer outcrops, thereby creating and enhancing aquifer-outcrop groundwater discharge (Figure 3). This enhanced stream flow and therefore stream power, creating a positive feedback which further enhanced downcutting by the streams.

This groundwater discharge is essential for the proper functioning of streams on the Kenai Peninsula Lowlands. Groundwater discharge to these streams augments stream flow, providing approximately half of the summer stream flow and likely all of the winter stream flow [12]. Groundwater discharge to these streams also modulates stream temperatures, providing cold-water refugia in summer and warm-water refugia in winter [12]. Salmonids are cold-water species with life-history stages sensitive to high stream water temperatures, including sublethal temperatures which can affect everything from cellular function to behavior [83,84]. Therefore, cold-water refugia in summer are crucial, and increasingly so in light of climate-induced warming trends in Alaska's salmon-bearing streams [85]. Juvenile salmonids must overwinter in these streams prior to outmigrating the following spring. Therefore, warm-water refugia in winter are also crucial, keeping some reaches unfrozen and available as overwintering habitats [86]. Lastly, much of this groundwater first passes through and interacts with nitrogen-fixing alder patches on adjacent hillslopes, delivering nitrogen-rich groundwater to riparian wetlands and these streams [14], where it enhances primary productivity in the riparian wetlands [14,87] and controls rates of in-stream nitrogen fixation and respiration [15,85]. The nutrient subsidies to these streams are then evident in the juvenile salmonids, who preferentially use abundant allochthonous sources, especially in the headwater settings [88]. Groundwater discharge is therefore thought to at least partly explain the predictable species composition along specific reaches in these streams, especially in headwater settings [66]. This new understanding of the importance of groundwater discharge to proper functioning of streams on the Kenai Peninsula Lowlands has led to groundwater being adopted as a central feature of the conceptual model underlying the management of the salmonid resources that underlie important sport and commercial fisheries [49].

Meanwhile, groundwater is the primary source of water for domestic, commercial, and industrial uses on the Kenai Peninsula Lowlands [52]. Most wells are domestic and are drilled by, maintained, and operated at the sole discretion and expense of the individual landowner. Drilling costs are calculated per unit depth, so there is little incentive to drill beyond the shallowest aquifer that can provide sufficient quantities of water. Well logs indicate that these aquifers are thin and discontinuous and commonly yield ~0.01–0.1 m^3/min (see also [60]). These then are the same aquifers that often outcrop on nearby hillslopes, commonly at the headward extent of streams and along hillslopes adjacent to streams (e.g., Figures 3 and 7). These aquifers are therefore the nexus of a potential conflict over limited groundwater resources between natural and human users. These results have heightened awareness, with recent and ongoing work focused on using this new understanding to explore sources and locations of acute groundwater vulnerability and connecting this new understanding to decision-making by building capacity to support both peer and institutional discussions [49].

Author Contributions: This paper was the result of a broad, collaborative effort by all authors. Conceptualization, M.C.R.; Methodology, M.E.G., K.C.R., E.J.G.-O., J.D. and M.C.R.; Validation, M.E.G., K.C.R., E.J.G.-O., W.J.K., J.D. and M.C.R.; Formal Analysis, M.E.G., E.J.G.-O. and J.D.; Investigation, M.E.G., K.C.R., E.J.G.-O., W.J.K., J.D., S.M.L. and M.C.R.; Data Curation, M.E.G., K.C.R., E.J.G.-O. and S.M.L.; Writing—Original Draft Preparation, M.E.G. and M.C.R.; Writing—Review & Editing, K.C.R., E.J.G.-O., W.J.K., J.D. and S.M.L.; Visualization, S.M.L. and J.D.; Supervision, K.C.R. and M.C.R.; Project Administration, K.C.R. and M.C.R.; Funding Acquisition, M.C.R. All authors have read and agreed to the published version of the manuscript.

Funding: This research was funded primarily by the National Estuarine Research Reserve System Science Collaborative under Grant No. 54584 (https://nerrssciencecollaborative.org/project/Walker17; accessed on 23 December 2021). Additional faculty support was funded by the National Science Foundation under Grant No. 1702029 (https://www.nsf.gov/awardsearch/showAward?AWD_ID=1702029; accessed on 23 December 2021). Additional student scholarships were funded by the National Science Foundation under Grant No. 1930451 (https://nsf.gov/awardsearch/showAward?AWD_ID=1930451; accessed on 23 December 2021).

Institutional Review Board Statement: Not applicable.

Informed Consent Statement: Not applicable.

Data Availability Statement: Publicly available datasets were analyzed in this study. This data can be found here: doi:10.6084/m9.figshare.16586903.

Acknowledgments: This project benefitted immeasurably from in-kind support provided by the Kachemak Bay National Estuarine Research Reserve, which provided lodging, local knowledge, introductions to stakeholders, the coordination of formal stakeholder engagements, and more. Coowe Walker and Syverine Bentz were particularly instrumental. Conrad Field illustrated Figure 3 from field sketches and notes prepared by M Rains. Annalyssa Hernandez assisted in some field work. A special thank you to all of the many stakeholders who provided their time, local knowledge, and access to private properties.

Conflicts of Interest: The authors declare no conflict of interest.

References

1. Rains, M.C.; Fogg, G.E.; Harter, T.; Dahlgren, R.A.; Williamson, R.J. The role of perched aquifers in hydrological connectivity and biogeochemical processes in vernal pool landscapes, Central Valley, California. *Hydrol. Process.* **2006**, *20*, 1157–1175. [CrossRef]
2. Neff, B.P.; Rosenberry, D.O.; Leibowitz, S.G.; Mushet, D.M.; Golden, H.E.; Rains, M.; Brooks, J.R.; Lane, C.R. A Hydrologic Landscapes Perspective on Groundwater Connectivity of Depressional Wetlands. *Water* **2019**, *12*, 50. [CrossRef] [PubMed]
3. Kornelsen, K.; Coulibaly, P. Synthesis review on groundwater discharge to surface water in the Great Lakes Basin. *J. Great Lakes Res.* **2014**, *40*, 247–256. [CrossRef]
4. Solana, M.X.; Londoño, O.M.Q.; Romanelli, A.; Donna, F.; Martínez, D.E.; Weinzettel, P. Connectivity of temperate shallow lakes to groundwater in the Pampean Plain, Argentina: A remote sensing and multi-tracer approach. *Groundw. Sustain. Dev.* **2021**, *13*, 100556. [CrossRef]
5. Winter, T.C.; Harvey, J.W.; Franke, O.L.; Alley, W.M. *Ground Water and Surface Water: A Single Resource*; Circular 1139; US Geological Survey: Reston, VA, USA, 1998. [CrossRef]
6. Winter, T.C. Relation of streams, lakes, and wetlands to groundwater flow systems. *Hydrogeol. J.* **1999**, *7*, 28–45. [CrossRef]
7. Moore, W.S.; Blanton, J.O.; Joye, S. Estimates of flushing times, submarine groundwater discharge, and nutrient fluxes to Okatee Estuary, South Carolina. *J. Geophys. Res. Space Phys.* **2006**, *111*, 111. [CrossRef]
8. Moore, W.S. The Effect of Submarine Groundwater Discharge on the Ocean. *Annu. Rev. Mar. Sci.* **2010**, *2*, 59–88. [CrossRef]

9. Misra, D.; Daanen, R.P.; Thompson, A.M. Base Flow/Groundwater Flow. In *Encyclopedia of Snow, Ice and Glaciers*; Encyclopedia of Earth Sciences Series; Singh, V.P., Singh, P., Haritashya, U.K., Eds.; Springer: Dordrecht, The Netherlands, 2011.
10. Guérin, A.; Devauchelle, O.; Robert, V.; Kitou, T.; Dessert, C.; Quiquerez, A.; Allemand, P.; Lajeunesse, E. Stream-Discharge Surges Generated by Groundwater Flow. *Geophys. Res. Lett.* **2019**, *46*, 7447–7455. [CrossRef]
11. Caissie, D. The thermal regime of rivers: A review. *Freshw. Biol.* **2006**, *51*, 1389–1406. [CrossRef]
12. Callahan, M.K.; Rains, M.; Bellino, J.C.; Walker, C.M.; Baird, S.J.; Whigham, D.F.; King, R.S. Controls on Temperature in Salmonid-Bearing Headwater Streams in Two Common Hydrogeologic Settings, Kenai Peninsula, Alaska. *JAWRA J. Am. Water Resour. Assoc.* **2014**, *51*, 84–98. [CrossRef]
13. Luke, S.H.; Luckai, N.J.; Burke, J.M.; Prepas, E.E. Riparian areas in the Canadian boreal forest and linkages with water quality in streams. *Environ. Rev.* **2007**, *15*, 79–97. [CrossRef]
14. Callahan, M.K.; Whigham, D.F.; Rains, M.; Rains, K.C.; King, R.S.; Walker, C.M.; Maurer, J.R.; Baird, S.J. Nitrogen Subsidies from Hillslope Alder Stands to Streamside Wetlands and Headwater Streams, Kenai Peninsula, Alaska. *JAWRA J. Am. Water Resour. Assoc.* **2017**, *53*, 478–492. [CrossRef]
15. Hiatt, D.L.; Robbins, C.J.; Back, J.A.; Kostka, P.K.; Doyle, R.D.; Walker, C.M.; Rains, M.C.; Whigham, D.F.; King, R.S. Catchment-scale alder cover controls nitrogen fixation in boreal headwater streams. *Freshw. Sci.* **2017**, *36*, 523–532. [CrossRef]
16. Power, G.; Brown, R.S.; Imhof, J.G. Groundwater and Fish—Insights from Northern North America. *Hydrol. Process.* **1999**, *13*, 401–422. [CrossRef]
17. Dieter, C.A.; Maupin, M.A.; Caldwell, R.R.; Harris, M.A.; Ivahnenko, T.I.; Lovelace, J.K.; Barber, N.L.; Linsey, K.S. *Estimated Use of Water in the United States in 2015*; Circular 1441; US Geological Survey: Reston, VA, USA, 2018. [CrossRef]
18. Falkenmark, M.; Rockström, J. *Balancing Water for Humans and Nature: The New Approach in Ecohydrology*; Earthscan: London, UK; Sterling, VA, USA, 2004; ISBN 978-1-85383-927-6.
19. Khalil, M.A.; Bobst, A.; Mosolf, J. Utilizing 2D Electrical Resistivity Tomography and Very Low Frequency Electromagnetics to Investigate the Hydrogeology of Natural Cold Springs Near Virginia City, Southwest Montana. *Pure Appl. Geophys. PAGEOPH* **2018**, *175*, 3525–3538. [CrossRef]
20. Gleason, C.L.; Frisbee, M.D.; Rademacher, L.K.; Sada, D.W.; Meyers, Z.P.; Knott, J.R.; Hedlund, B.P. Hydrogeology of desert springs in the Panamint Range, California, USA: Geologic controls on the geochemical kinetics, flowpaths, and mean residence times of springs. *Hydrol. Process.* **2020**, *34*, 2923–2948. [CrossRef]
21. Mocior, E.; Rzonca, B.; Siwek, J.; Plenzler, J.; Płaczkowska, E.; Dabek, N.; Jaskowiec, B.; Potoniec, P.; Roman, S.; Zdziebko, D. Determinants of the distribution of springs in the upper part of a flysch ridge in the Bieszczady Mountains in southeastern Poland. *Episodes* **2015**, *38*, 21–30. [CrossRef]
22. Howard, J.; Merrifield, M. Mapping Groundwater Dependent Ecosystems in California. *PLoS ONE* **2010**, *5*, e11249. [CrossRef]
23. Pourtaghi, Z.S.; Pourghasemi, H.R. GIS-based groundwater spring potential assessment and mapping in the Birjand Township, southern Khorasan Province, Iran. *Hydrogeol. J.* **2014**, *22*, 643–662. [CrossRef]
24. Lange, H.; Sippel, S. Machine Learning Applications in Hydrology. In *Forest-Water Interactions*; Levia, D.F., Carlyle-Moses, D.E., Iida, S., Michalzik, B., Nanko, K., Tischer, A., Eds.; Ecological Studies; Springer International Publishing: Cham, Switzerland, 2020; Volume 240, pp. 233–257. ISBN 978-3-030-26085-9.
25. Nearing, G.S.; Kratzert, F.; Sampson, A.K.; Pelissier, C.S.; Klotz, D.; Frame, J.M.; Prieto, C.; Gupta, H.V. What Role Does Hydrological Science Play in the Age of Machine Learning? *Water Resour. Res.* **2021**, *57*, e2020WR028091. [CrossRef]
26. Shen, C.; Chen, X.; Laloy, E. Editorial: Broadening the Use of Machine Learning in Hydrology. *Front. Water* **2021**, *3*, 681023. [CrossRef]
27. Sahoo, S.; Russo, T.A.; Elliott, J.; Foster, I. Machine learning algorithms for modeling groundwater level changes in agricultural regions of the U.S. *Water Resour. Res.* **2017**, *53*, 3878–3895. [CrossRef]
28. Rahman, A.S.; Hosono, T.; Quilty, J.M.; Das, J.; Basak, A. Multiscale groundwater level forecasting: Coupling new machine learning approaches with wavelet transforms. *Adv. Water Resour.* **2020**, *141*, 103595. [CrossRef]
29. Afan, H.A.; Osman, A.I.A.; Essam, Y.; Ahmed, A.N.; Huang, Y.F.; Kisi, O.; Sherif, M.; Sefelnasr, A.; Chau, K.-W.; El-Shafie, A. Modeling the fluctuations of groundwater level by employing ensemble deep learning techniques. *Eng. Appl. Comput. Fluid Mech.* **2021**, *15*, 1420–1439. [CrossRef]
30. Rahmati, O.; Pourghasemi, H.R.; Melesse, A.M. Application of GIS-based data driven random forest and maximum entropy models for groundwater potential mapping: A case study at Mehran Region, Iran. *Catena* **2016**, *137*, 360–372. [CrossRef]
31. El Bilali, A.; Taleb, A.; Brouziyne, Y. Groundwater quality forecasting using machine learning algorithms for irrigation purposes. *Agric. Water Manag.* **2021**, *245*, 106625. [CrossRef]
32. Shiri, N.; Shiri, J.; Yaseen, Z.M.; Kim, S.; Chung, I.-M.; Nourani, V.; Zounemat-Kermani, M. Development of artificial intelligence models for well groundwater quality simulation: Different modeling scenarios. *PLoS ONE* **2021**, *16*, e0251510. [CrossRef] [PubMed]
33. Tan, Z.; Yang, Q.; Zheng, Y. Machine Learning Models of Groundwater Arsenic Spatial Distribution in Bangladesh: Influence of Holocene Sediment Depositional History. *Environ. Sci. Technol.* **2020**, *54*, 9454–9463. [CrossRef] [PubMed]
34. Tran, D.A.; Tsujimura, M.; Ha, N.T.; Nguyen, V.T.; Van Binh, D.; Dang, T.D.; Doan, Q.-V.; Bui, D.T.; Ngoc, T.A.; Phu, L.V.; et al. Evaluating the predictive power of different machine learning algorithms for groundwater salinity prediction of multi-layer coastal aquifers in the Mekong Delta, Vietnam. *Ecol. Indic.* **2021**, *127*, 107790. [CrossRef]

35. Hussein, E.A.; Thron, C.; Ghaziasgar, M.; Bagula, A.; Vaccari, M. Groundwater Prediction Using Machine-Learning Tools. *Algorithms* **2020**, *13*, 300. [CrossRef]
36. Jaafarzadeh, M.S.; Tahmasebipour, N.; Haghizadeh, A.; Pourghasemi, H.R.; Rouhani, H. Groundwater recharge potential zonation using an ensemble of machine learning and bivariate statistical models. *Sci. Rep.* **2021**, *11*, 1–18. [CrossRef]
37. Winter, T.C. The concept of hydrologic landscapes. *JAWRA J. Am. Water Resour. Assoc.* **2001**, *37*, 335–349. [CrossRef]
38. Wolock, D.M.; Winter, T.C.; McMahon, G. Delineation and Evaluation of Hydrologic-Landscape Regions in the United States Using Geographic Information System Tools and Multivariate Statistical Analyses. *Environ. Manag.* **2004**, *34*, S71–S88. [CrossRef] [PubMed]
39. Wigington, P.J.; Leibowitz, S.G.; Comeleo, R.L.; Ebersole, J. Oregon Hydrologic Landscapes: A Classification Framework1. *JAWRA J. Am. Water Resour. Assoc.* **2012**, *49*, 163–182. [CrossRef]
40. Brydsten, L. *Modelling Groundwater Discharge Areas Using Only Digital Elevation Models as Input Data*; Swedish Nuclear Fuel and Waste Management: Stockholm, Sweden, 2006; p. 18.
41. Tweed, S.O.; Leblanc, M.; Webb, J.; Lubczynski, M.W. Remote sensing and GIS for mapping groundwater recharge and discharge areas in salinity prone catchments, southeastern Australia. *Hydrogeol. J.* **2006**, *15*, 75–96. [CrossRef]
42. Haitjema, H.M.; Mitchell-Bruker, S. Are Water Tables a Subdued Replica of the Topography? *Ground Water* **2005**, *43*, 781–786. [CrossRef] [PubMed]
43. Devito, K.; Creed, I.; Gan, T.; Mendoza, C.; Petrone, R.; Silins, U.; Smerdon, B. A framework for broad-scale classification of hydrologic response units on the Boreal Plain: Is topography the last thing to consider? *Hydrol. Process.* **2005**, *19*, 1705–1714. [CrossRef]
44. Toth, J. Groundwater discharge: A common generator of diverse geologic and morphologic phenomena. *Int. Assoc. Sci. Hydrol. Bull.* **1971**, *16*, 7–24. [CrossRef]
45. Huang, X.; Niemann, J.D. Modelling the potential impacts of groundwater hydrology on long-term drainage basin evolution. *Earth Surf. Process. Landforms* **2006**, *31*, 1802–1823. [CrossRef]
46. Iverson, R.M.; Reid, M.E. Gravity-driven groundwater flow and slope failure potential: 1. Elastic Effective-Stress Model. *Water Resour. Res.* **1992**, *28*, 925–938. [CrossRef]
47. Reid, M.E.; Iverson, R.M. Gravity-driven groundwater flow and slope failure potential: 2. Effects of slope morphology, material properties, and hydraulic heterogeneity. *Water Resour. Res.* **1992**, *28*, 939–950. [CrossRef]
48. UACED (University of Alaska Center for Economic Development). *Kenai Peninsula 2021–2026 Comprehensive Economic Development Strategy*; Kenai Peninsula Economic Development District: Kenai, AK, USA, 2021; p. 97.
49. Walker, C.M.; Whigham, D.F.; Bentz, I.S.; Argueta, J.M.; King, R.S.; Rains, M.C.; Simenstad, C.A.; Guo, C.; Baird, S.J.; Field, C.J. Linking landscape attributes to salmon and decision-making in the southern Kenai Lowlands, Alaska, USA. *Ecol. Soc.* **2021**, *26*, 1. [CrossRef]
50. ADLWD (Alaska Department of Labor and Workforce Development). *Alaska Population Projections 2019–2045*; Alaska Department of Labor and Workforce Development: Juneau, AK, USA, 2020.
51. HSWCD (Homer Soil and Water Conservation District). *Growing Local Food: A Survey of Commercial Producers on the Southern Kenai Peninsula*; Homer Soil and Water Conservation District: Homer, AK, USA, 2018.
52. Glass, R. *Ground-Water Conditions and Quality in the Western Part of Kenai Peninsula, Southcentral Alaska*; Open-File Rep. 96-446; US Geological Survey: Reston, VA, USA, 1996. [CrossRef]
53. Baughman, C.A.; Loehman, R.A.; Magness, D.R.; Saperstein, L.B.; Sherriff, R.L. Four Decades of Land-Cover Change on the Kenai Peninsula, Alaska: Detecting Disturbance-Influenced Vegetation Shifts Using Landsat Legacy Data. *Land* **2020**, *9*, 382. [CrossRef]
54. Klein, E.; Berg, E.E.; Dial, R. Wetland drying and succession across the Kenai Peninsula Lowlands, south-central Alaska. *Can. J. For. Res.* **2005**, *35*, 1931–1941. [CrossRef]
55. Berg, E.E.; Hillman, K.M.; Dial, R.; DeRuwe, A. Recent woody invasion of wetlands on the Kenai Peninsula Lowlands, south-central Alaska: A major regime shift after 18000 years of wet Sphagnum–sedge peat recruitment. *Can. J. For. Res.* **2009**, *39*, 2033–2046. [CrossRef]
56. Magness, D.R.; Morton, J.M. Using climate envelope models to identify potential ecological trajectories on the Kenai Peninsula, Alaska. *PLoS ONE* **2018**, *13*, e0208883. [CrossRef] [PubMed]
57. USGS (U.S. Geological Survey). *The National Map U.S. Geological Survey's (USGS) National Geospatial Program.*. Available online: https://www.usgs.gov/core-science-systems/national-geospatial-program/national-map (accessed on 30 August 2021).
58. Karlstrom, T.N. *Quaternary Geology of the Kenai Lowland and Glacial History of the Cook Inlet Region, Alaska*; Professional Paper 443; US Geological Survey: Reston, VA, USA, 1964. [CrossRef]
59. Wilson, F.H.; Hults, C.P. *Geology of the Prince William Sound and Kenai Peninsula Region, Alaska*; Scientific Investigations Map 3110; US Geological Survey: Anchorage, AK, USA, 2012. [CrossRef]
60. Nelson, G.; Johnson, P. *Ground-Water Reconnaissance of Part of the Lower Kenai Peninsula, Alaska*; Open-File Rep. 81-905; US Geological Survey: Reston, VA, USA, 1981. [CrossRef]
61. Spencer, E.W. *Geologic Maps: A Practical Guide to Preparation and Interpretation*; Waveland Press: Long Grove, IL, USA, 2017; ISBN 1-4786-3488-X.
62. Heine, R.A.; Lant, C.L.; Sengupta, R.R. Development and Comparison of Approaches for Automated Mapping of Stream Channel Networks. *Ann. Assoc. Am. Geogr.* **2004**, *94*, 477–490. [CrossRef]

63. Jaeger, K.L.; Montgomery, D.R.; Bolton, S.M. Channel and Perennial Flow Initiation in Headwater Streams: Management Implications of Variability in Source-Area Size. *Environ. Manag.* **2007**, *40*, 775–786. [CrossRef]
64. Detty, J.M.; McGuire, K.J. Topographic controls on shallow groundwater dynamics: Implications of hydrologic connectivity between hillslopes and riparian zones in a till mantled catchment. *Hydrol. Process.* **2010**, *24*, 2222–2236. [CrossRef]
65. Riley, S.J.; DeGloria, S.D.; Elliot, R. A Terrain Ruggedness Index That Quantifies Topographic Heterogeneity. *Intermt. J. Sci.* **1999**, *5*, 23–27.
66. Korzeniowska, K.; Pfeifer, N.; Landtwing, S. Mapping gullies, dunes, lava fields, and landslides via surface roughness. *Geomorphology* **2018**, *301*, 53–67. [CrossRef]
67. Walker, C.M.; King, R.S.; Whigham, D.F.; Baird, S.J. Landscape and Wetland Influences on Headwater Stream Chemistry in the Kenai Lowlands, Alaska. *Wetlands* **2012**, *32*, 301–310. [CrossRef]
68. Beven, K.J.; Kirkby, M.J. A physically based, variable contributing area model of basin hydrology/Un modèle à base physique de zone d'appel variable de l'hydrologie du bassin versant. *Hydrol. Sci. Bull.* **1979**, *24*, 43–69. [CrossRef]
69. Sørensen, R.; Zinko, U.; Seibert, J. On the calculation of the topographic wetness index: Evaluation of different methods based on field observations. *Hydrol. Earth Syst. Sci.* **2006**, *10*, 101–112. [CrossRef]
70. Tarboton, D. A new method for the determination of flow directions and upslope areas in grid digital elevation models. *Water Resour. Res.* **1997**, *33*, 309–319. [CrossRef]
71. Horvath, E.K.; Christensen, J.R.; Mehaffey, M.H.; Neale, A.C. Building a potential wetland restoration indicator for the contiguous United States. *Ecol. Indic.* **2017**, *83*, 463–473. [CrossRef]
72. Rains, M.; Mount, J.F. Origin of shallow ground water in an alluvial aquifer as determined by isotopic and chemical procedures. *Ground Water* **2002**, *40*, 552–563. [CrossRef] [PubMed]
73. Phillips, S.J.; Dudík, M. Modeling of species distributions with Maxent: New extensions and a comprehensive evaluation. *Ecography* **2008**, *31*, 161–175. [CrossRef]
74. Elith, J.; Phillips, S.J.; Hastie, T.; Dudík, M.; Chee, Y.E.; Yates, C.J. A statistical explanation of MaxEnt for ecologists. *Divers. Distrib.* **2011**, *17*, 43–57. [CrossRef]
75. Merow, C.; Smith, M.J.; Silander, J.A. A practical guide to MaxEnt for modeling species' distributions: What it does, and why inputs and settings matter. *Ecography* **2013**, *36*, 1058–1069. [CrossRef]
76. Feng, X.; Park, D.S.; Liang, Y.; Pandey, R.; Papeş, M. Collinearity in ecological niche modeling: Confusions and challenges. *Ecol. Evol.* **2019**, *9*, 10365–10376. [CrossRef]
77. Cohen, J. A Coefficient of Agreement for Nominal Scales. *Educ. Psychol. Meas.* **1960**, *20*, 37–46. [CrossRef]
78. Landis, J.R.; Koch, G.G. An Application of Hierarchical Kappa-type Statistics in the Assessment of Majority Agreement among Multiple Observers. *Biometrics* **1977**, *33*, 363. [CrossRef]
79. Mandrekar, J.N. Receiver Operating Characteristic Curve in Diagnostic Test Assessment. *J. Thorac. Oncol.* **2010**, *5*, 1315–1316. [CrossRef]
80. King, R.S.; Walker, C.M.; Whigham, D.F.; Baird, S.J.; Back, J.A. Catchment topography and wetland geomorphology drive macroinvertebrate community structure and juvenile salmonid distributions in south-central Alaska headwater streams. *Freshw. Sci.* **2012**, *31*, 341–364. [CrossRef]
81. Souissi, D.; Msaddek, M.H.; Zouhri, L.; Chenini, I.; El May, M.; Dlala, M. Mapping groundwater recharge potential zones in arid region using GIS and Landsat approaches, southeast Tunisia. *Hydrol. Sci. J.* **2018**, *63*, 251–268. [CrossRef]
82. Rhoden, C.M.; Peterman, W.E.; Taylor, C.A. Maxent-directed field surveys identify new populations of narrowly endemic habitat specialists. *PeerJ* **2017**, *5*, e3632. [CrossRef] [PubMed]
83. Taylor, S.G. Climate warming causes phenological shift in Pink Salmon, Oncorhynchus gorbuscha, behavior at Auke Creek, Alaska. *Glob. Chang. Biol.* **2008**, *14*, 229–235. [CrossRef]
84. Bowen, L.; von Biela, V.R.; McCormick, S.D.; Regish, A.M.; Waters, S.C.; Durbin-Johnson, B.; Britton, M.; Settles, M.L.; Donnelly, D.S.; Laske, S.M.; et al. Transcriptomic response to elevated water temperatures in adult migrating Yukon River Chinook salmon (Oncorhynchus tshawytscha). *Conserv. Physiol.* **2020**, *8*, coaa084. [CrossRef]
85. Shaftel, R.S.; King, R.S.; Back, J.A. Breakdown rates, nutrient concentrations, and macroinvertebrate colonization of bluejoint grass litter in headwater streams of the Kenai Peninsula, Alaska. *J. N. Am. Benthol. Soc.* **2011**, *30*, 386–398. [CrossRef]
86. Gutsch, M.K. *Dentification and Characterization of Juvenile Coho Salmon Overwintering Habitats and Early Spring Outmigration in the Anchor River Watershed, Alaska*; University of Alaska, Fairbanks: Fairbanks, AK, USA, 2011.
87. Whigham, D.; Walker, C.; Maurer, J.; King, R.; Hauser, W.; Baird, S.; Keuskamp, J.; Neale, P. Watershed influences on the structure and function of riparian wetlands associated with headwater streams—Kenai Peninsula, Alaska. *Sci. Total Environ.* **2017**, *599*, 124–134. [CrossRef] [PubMed]
88. Dekar, M.P.; King, R.S.; Back, J.A.; Whigham, D.; Walker, C.M. Allochthonous inputs from grass-dominated wetlands support juvenile salmonids in headwater streams: Evidence from stable isotopes of carbon, hydrogen, and nitrogen. *Freshw. Sci.* **2012**, *31*, 121–132. [CrossRef]

Appendix 3: Guerrón-Orejuela, E. J., Rains, K. C., Brigino, T. M., Kleindl, W. J., Landry, S. M., Spellman, P., Walker, C. M., & Rains, M. C. (2023). Mapping Groundwater Recharge Potential in High Latitude Landscapes Using Public Data, Remote Sensing, and Analytic Hierarchy Process. *Remote Sensing,* 15(10), 2630. https://doi.org/10.3390/rs15102630

remote sensing

Article

Mapping Groundwater Recharge Potential in High Latitude Landscapes Using Public Data, Remote Sensing, and Analytic Hierarchy Process

Edgar J. Guerrón-Orejuela [1,*], Kai C. Rains [1], Tyelyn M. Brigino [1], William J. Kleindl [2], Shawn M. Landry [1], Patricia Spellman [1], Coowe M. Walker [3,4] and Mark C. Rains [1]

1 School of Geosciences, University of South Florida, Tampa, FL 33620, USA; krains@usf.edu (K.C.R.); tyelynb@usf.edu (T.M.B.); landry@usf.edu (S.M.L.); pdspellm@usf.edu (P.S.); mrains@usf.edu (M.C.R.)
2 Land Resources and Environmental Sciences, Montana State University, Bozeman, MT 59717, USA; william.kleindl@montana.edu
3 Kachemak Bay National Estuarine Research Reserve, Homer, AK 99603, USA; cmwalker9@alaska.edu
4 Alaska Center for Conservation Science, University of Alaska, Anchorage, AK 99508, USA
* Correspondence: edgarguerron@usf.edu; Tel.: +1-941-713-2606

Abstract: Understanding where groundwater recharge occurs is essential for managing groundwater resources, especially source-water protection. This can be especially difficult in remote mountainous landscapes where access and data availability are limited. We developed a groundwater recharge potential (GWRP) map across such a landscape based on six readily available datasets selected through the literature review: precipitation, geology, soil texture, slope, drainage density, and land cover. We used field observations, community knowledge, and the Analytical Hierarchy Process to rank and weight the spatial datasets within the GWRP model. We found that GWRP is the highest where precipitation is relatively high, geologic deposits are coarse-grained and unconsolidated, soils are variants of sands and gravels, the terrain is flat, drainage density is low, and land cover is undeveloped. We used GIS to create a map of GWRP, determining that over 83% of this region has a moderate or greater capacity for groundwater recharge. We used two methods to validate this map and assessed it as approximately 87% accurate. This study provides an important tool to support informed groundwater management decisions in this and other similar remote mountainous landscapes.

Keywords: Alaska; Analytic Hierarchy Process (AHP); GIS; groundwater mapping; Kenai lowlands; recharge

check for updates

Citation: Guerrón-Orejuela, E.J.; Rains, K.C.; Brigino, T.M.; Kleindl, W.J.; Landry, S.M.; Spellman, P.; Walker, C.M.; Rains, M.C. Mapping Groundwater Recharge Potential in High Latitude Landscapes Using Public Data, Remote Sensing, and Analytic Hierarchy Process. *Remote Sens.* **2023**, *15*, 2630. https://doi.org/10.3390/rs15102630

Academic Editors: Jiun-Yee Yen and Chuen-Fa Ni

Received: 14 April 2023
Revised: 12 May 2023
Accepted: 16 May 2023
Published: 18 May 2023

1. Introduction

Globally, groundwater is used for agriculture (70.1%), public water supply (21.2%), and industrial activities (8.7%), thus playing a vital role in food security and human health [1–4]. Groundwater also sustains natural ecosystems. For example, it traverses natural flow paths to form and support a variety of aquatic ecosystems, such as wetlands and nearshore marine environments, and can provide a consistent discharge of water to streams and lakes [5–7]. However, over the past 50 years, groundwater extraction has risen dramatically, and as human populations continue to grow, groundwater consumption also increases [8].

Though essential, groundwater is also a limited resource. Its sustained availability depends on maintaining the balance between groundwater discharge and recharge [9,10]. Discharge is the expression of groundwater at the surface, often in the form of springs, some of which have been targeted for regulatory protection [11,12]. Recharge is the downward movement of water to the aquifer system, the rate of which is determined by interactions of climate, geology, topography, and land cover [13]. Recharge areas are often dispersed, less recognizable by the public, and generally lack regulatory protection as such [14]. Understanding where groundwater recharge occurs is an essential first step toward ensuring source-water protection and, therefore, groundwater supply. Multiple studies show that groundwater recharge management not only increases the groundwater supply, but when done correctly, it can raise the awareness of groundwater resources in local communities [15–17].

Historically, groundwater studies have relied upon field hydrogeological and geophysical measurements, geochemical tracers, and hydrologic models, depending on the questions addressed [18,19]. The accuracy of these studies depends on the scale of the analysis and the amount of data available since most methods used are data intensive [18,20,21]. Groundwater recharge studies have been performed using groundwater level data [22–24], sometimes integrated into water-balance models [25,26]. Physical data are often integrated with geochemical and/or isotopic data, providing further evidence to constrain groundwater recharge rates [27–29]. In the last decade, studies of groundwater recharge have increasingly used machine-learning algorithms [30,31]. Groundwater recharge studies that use machine learning algorithms have been successfully conducted in mid- and low-latitude regions using extensive field data and spatial datasets used for model training and testing [32,33]. However, field data collection is time-consuming and expensive, particularly inasmuch as access to field locations can be limited due to climatic extremes, rugged topography, the lack of roads, and/or land ownership. For example, exposure to extended subfreezing temperatures makes deployment and maintenance of instruments challenging in mountainous or high-latitude regions.

Increasingly, scientists have overcome these barriers by using remote sensing data and geospatial analyses to conduct groundwater studies [34,35]. This has greatly reduced the time and cost of groundwater research and enabled groundwater research even in data-poor regions [36,37]. However, many of these still require quantitative field data to define objective functions, which are then used for model training and testing [36]. Furthermore, remote sensing data come with their own challenges, as data availability and resolution (spatial and temporal) vary by region. Thus, a coherent methodology is needed to define the relative importance of remote sensing data to individual studies.

Multicriteria decision analysis (MCDA) is a methodology for organizing and assigning importance to datasets [38]. The Analytic Hierarchy Process (AHP) is the preferred MCDA technique when using geospatial data [39,40]. AHP provides a systematic methodology to classify and prioritize among heterogeneous spatial datasets and ultimately define the dataset hierarchy that best represents fundamental processes [41,42]. The coupling of these methods with GIS has made them a powerful tool for regional hydrogeologic research and decision-making.

GIS-AHP techniques can be used to address complex, multidimensional problems, such as delineating groundwater recharge zones [43,44]. The coupling of GIS and AHP techniques allows for integrating different types of data, such as in situ, remote sensing, quantitative, qualitative, or spatial data from various sources (i.e., local, regional, or global). Thus, datasets may include a range of environmental variables that cover climatic, geologic, topographic, and land cover characteristics. This versatility is critical when data are limited. When data are not readily available, and custom data acquisition is too costly or time-consuming, being able to effectively utilize common publicly available spatial data from global models, satellite imagery, and community engagement is key for knowledge development and resource management [17,21,45].

Many rural and remote areas in developed countries have incomplete or missing datasets. This data deficit has slowed the development of data-driven resource management tools. Nevertheless, many of these communities rely on groundwater for potable water and for local food production (e.g., local farms or fisheries) and require practical tools to manage these resources. In the Anchor River Watershed, south-central Alaska, a lack of comprehensive groundwater data has precluded accurate estimates of groundwater recharge to a critical aquifer system that supports local communities and connected ecosystems. As the regional population grows, consumptive use of groundwater is expected to increase, stressing this limited shared resource. Here, we used GIS, AHP, and limited remote sensing and field-derived datasets to develop and validate a groundwater recharge potential (GWRP) map in this high-latitude remote location.

2. Materials and Methods

2.1. Site Description

The study area was the Anchor River Watershed on the Kenai Peninsula Lowlands in south-central Alaska (Figure 1). The Kenai Peninsula Lowlands (~9400 km^2) is the unglaciated southernmost tip of the Kenai Peninsula, bordered by Kachemak Bay to the south, Cook Inlet to the west, and the Kenai Mountains range to the east. Over 40% of the Kenai Peninsula Lowlands consists of headwater streams, wetlands, and lakes [46]. The Anchor River Watershed (~586 km^2) is the largest and southernmost salmon-bearing watershed on the Kenai Peninsula Lowlands. The Anchor River is a non-glacial river comprised of two main river forks that meet near the town of Anchor Point and continue west to Cook Inlet. Access to most of the watershed is challenging due to the prevalence of wetlands, streams, rugged terrain, and the lack of roads.

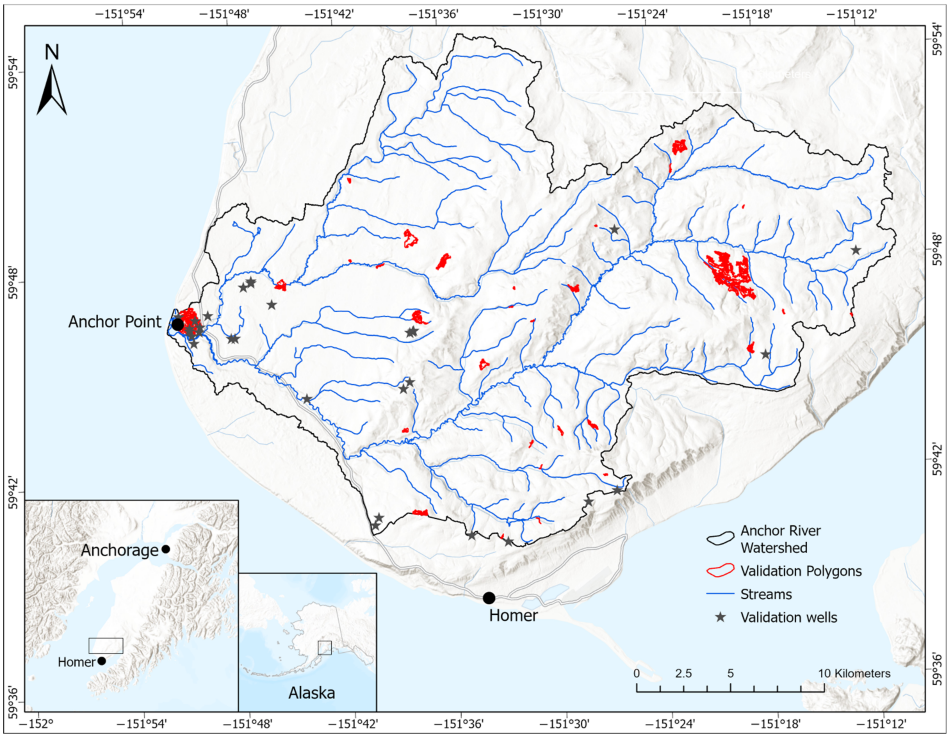

Figure 1. Geographic location of the Anchor River Watershed in the Kenai Peninsula, south of Anchorage, in the State of Alaska, USA. The locations of polygons and wells used to validate the final GWRP map are depicted in this figure. Base map source: Esri, HERE, Garmin, FAO, NOAA, USGS, © OpenStreetMap contributors, and the GIS User Community.

The climate, geology, topography, and land cover of the Anchor River Watershed are typical of the Kenai Peninsula Lowlands. The climate is driven by continental and maritime patterns, from north to south, and consists of short summers and long cold winters. Mean annual temperature and precipitation are 2.9 °C and 755.14 mm, respectively (HOMER 8 NW, AK US USC00503672, 1991–2020). Seasonal precipitation is influenced by the strength and position of the Aleutian Low, with most of the precipitation occurring between November and March [47], with the orographic effects of the bordering mountains creating distinctive climatic zonation [48]. The region has experienced at least five major glaciations and two minor glacial advances over the last 125,000 years [48]. Geologic deposits are a complex mix of Pleistocene glacial deposits overlaying weakly lithified Tertiary bedrock [48–50]. Groundwater can be found in all deposits, most notably in the

Pleistocene glacial deposits, especially in valley train and outwash channel deposits [36,51]. Relief is rugged and steep, with total relief ranging from 0 m to 621 m above mean sea level (AMSL).

The water resources availability and patterns of use in the Anchor River Watershed are also typical of the Kenai Peninsula Lowlands. People rely almost exclusively on groundwater for domestic, commercial, and industrial uses [52], but there are few statewide or local restrictions on groundwater use. Wherever water occurs naturally in Alaska, it is a common property resource, not attached to land ownership unless the landowner applies for a water right [53]. Similarly, ecosystems rely on groundwater, notably salmon-bearing streams. Groundwater augments streamflow [54] and may provide >50% of the streamflow during spring breakup and fall freshets and >80% of the streamflow during late summer and throughout the winter (Brigino, unpublished data). In many cases, aquifers used for water supply are the same aquifers that outcrop on hillslopes and support seeps and springs that discharge to the streams [36,55]. The balance is delicate because the shared aquifer resources are largely glacial channel and floodplain deposits that are multitiered, thin, discontinuous, and prone to drawdown and drying [52].

The largest municipality in the region is the City of Homer, which has a population of ~6000 people and has seen a population increase of 10% since the 2010 census [56]. Although the City of Homer is not entirely located within the Anchor River Watershed, the source of the City's drinking water (Bridge Creek Reservoir) is in the headwaters. Natural tracer studies indicate that >50% of the water in the Bridge Creek Reservoir originates from groundwater discharging from seeps and springs (Brigino, unpublished data). This reservoir not only serves the City of Homer but also provides drinking water to people that live in the region. The only other potable water sources are private or public groundwater wells and naturally flowing springs.

2.2. Overall Approach

Our study included four stages to develop a spatial model to delineate GWRP zones: (1) develop a conceptual model, (2) select and process spatial datasets, (3) rank spatial datasets and their corresponding classes, (4) create and validate a GIS-based map of GWRP. We used ArcGIS Pro 2.9.2 (ESRI, Redlands, CA, USA), QGIS 3.22 Biatowieza (QGIS Development Team (2022)), and the Soil & Water Assessment Tool+ (SWAT+) (USDA-ARS) to process and analyze our spatial datasets.

2.3. Conceptual Model Development

Our conceptual model of groundwater resources in our study area was developed over many field seasons [36,54,55,57], but most specifically during three visits in 2018–2019 and 2021–2022. During these visits, we initially focused on using remote sensing data and machine learning to locate the seeps and springs that discharge groundwater to the salmon-bearing streams [36]. In the Kenai Peninsula Lowlands, groundwater discharge in one location implies groundwater recharge in another, likely nearby and upgradient. Therefore, we simultaneously made field observations about areas that likely supported groundwater recharge, focusing on evidence that could be derived from publicly available data (e.g., climate, geology, soils, topography, and land cover). We simultaneously incorporated community insights, including indigenous tribal knowledge, through surveys and interviews (Guerrón-Orejuela, unpublished data) [55]. We used the conceptual model developed from these field observations and community knowledge to identify and rank the spatial datasets and criteria that drive groundwater recharge.

2.4. Spatial Dataset Selection

We performed a literature review of twenty-three geospatial groundwater potential and groundwater recharge potential studies to crowdsource possible criteria and supporting spatial datasets [21,40,43,58–77]. Detailed results, including spatial datasets organized by reference, are supplied in Supplementary Materials Table S1. These studies used different quantities and types of spatial datasets, ranging from 5 to 13, typically picked from climatic, geologic, topographic, and land cover data sources. Our analysis showed twenty-eight unique spatial datasets used in all the studies. Eleven were only used in one study, and eight were used at least two times more than any other. These eight common spatial datasets are precipitation, geology, lineament density, soils, geomorphology, slope, drainage density, and land use and land cover (Figure 2).

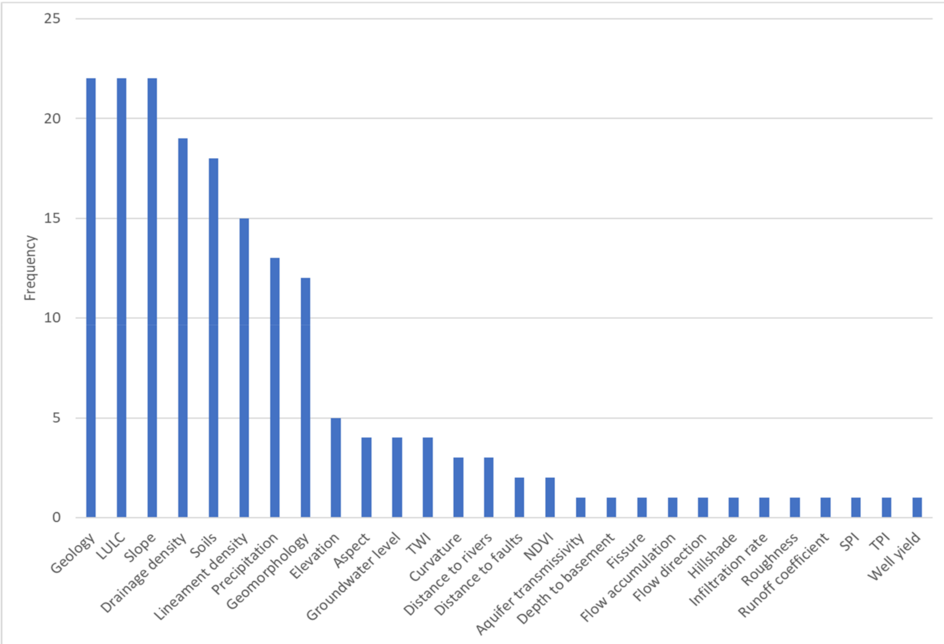

Figure 2. The frequency of spatial datasets utilized in twenty-three published groundwater studies. TWI Topographic Wetness Index, NDVI Normalized Difference Vegetation Index, TPI Topographic Position Index, SPI Stream Power Index. Detailed results, including spatial datasets organized by reference, are supplied in Supplementary Materials Table S1.

We were interested in developing a methodology with a high likelihood of being available and applicable to various regions. Therefore, we chose to work with the spatial datasets our literature review revealed were exceptionally common in groundwater studies. Of the eight spatial datasets presented above, six spatial datasets or the related underlying data that collectively represented climatic, geologic, topographic, and land cover characteristics were available for our study area: precipitation (P), geology (G), soil texture (ST), slope (SL), drainage density (DD), and land cover (LC). The remaining two, lineaments and geomorphology, were unavailable. All layers used in the analysis were standardized to 3×3 m.

We represented climate through spatially distributed precipitation data, some fraction of which would be available for groundwater recharge [78,79]. Precipitation data were limited in our study area, so we generated a spatially distributed dataset based on data from twenty available weather stations in our region using the weather generator in the SWAT + modeling software [80]. This software uses the global weather station network and data derived from satellite products (Climate Forecast System Reanalysis (CFSR), National Center for Environmental Prediction) [81].

We represented geology through spatially distributed lithology and soils, which affect infiltration [82–85]. We derived lithology data from the United States Geological Survey (USGS) Geologic map of Alaska [86], which is a compilation of regional geologic maps developed and published by the USGS National Survey and Analysis Project for Alaska. We used the lithologic coding to query and identify the most specific part of the lithologic assignment available for our study area. The resulting vector file was rasterized. For soils, we used the National Resources Conservation Service's (NRCS) gridded (10 m resolution)

Soil Survey Geographic Database (gSSURGO) for the State of Alaska [87]. From these data, we extracted soil texture, which is proportional to permeability [88].

We represented topography through a digital elevation model (DEM), which represented the likelihood of precipitation runoff [89,90]. Topographic data were derived from airborne LiDAR (2008 Kenai Watershed Forum Topographic LiDAR: Kenai Peninsula, Alaska; https://www.fisheries.noaa.gov/inport/item/49620; accessed on 25 February 2019). The LiDAR-based digital elevation model (DEM) was acquired at 1 × 1 m pixel size but was resampled to a 3 × 3 m pixel size, which reduced run times and microtopographic anomalies [36]. Topographic data directly extracted from the DEM included slope and drainage density [91,92]. Additionally, this DEM was used to delineate the study area using Arc Hydro Pro tools.

We used the most up-to-date land cover data for this region, representing the degree to which development altered the natural landscape, especially by placing impervious surfaces [93,94]. We derived our grid (30 m spatial resolution) from the 2016 National Land Cover Database (NLCD) [95].

2.5. Spatial Dataset Weighting through Analytic Hierarchy Process (AHP)

We used AHP, and Saaty's relative importance scale, to assess and compare the relative contribution to groundwater recharge of the data represented in the six spatial datasets. In Saaty's relative importance scale, 1 indicates equal importance between classes, and 9 shows the extreme importance of one class above another (Table 1).

Table 1. Saaty's relative importance scale [41].

Scale	**1**	**3**	**5**	**7**	**9**
Importance	Equal	Moderate	Strong	Very Strong	Extreme

Even numbers are also possible in the scale and express intermediate importance.

To determine the weights of each spatial dataset, we constructed a 6 × 6 pairwise comparison matrix (1), where each element a_{ij} was evaluated based on our conceptual model. To fill out the matrix, we conducted pairwise comparisons of each of the six spatial datasets, assigning high relative importance values to spatial datasets that greatly influence groundwater recharge and low relative importance values to those with a small impact on groundwater recharge [41,43,76]. Only comparisons above the matrix diagonal (1) are required.

$$A = \begin{pmatrix} 1 & a_{12} & \dots & a_{1n} \\ a_{21} & 1 & \dots & a_{2n} \\ \dots & \dots & \dots & \dots \\ a_{n1} & a_{n2} & \dots & 1 \end{pmatrix} \quad (1)$$

Elements below the diagonal were assigned reciprocal values of the corresponding above-diagonal values [41], as represented in Equation (2).

$$a_{ij} = \frac{1}{a_{ji}} \quad (2)$$

According to the AHP methodology, the principal eigenvector, $\vec{p}$, is the desired priorities vector. We approximated $\vec{p}$ by normalizing the elements in each column of the comparison matrix and then averaging over each row [41]. We estimated λmax by adding the columns of A and multiplying the resulting vector by $\vec{p}$. The difference between λmax and the number of spatial datasets (n) is a measure of the inconsistency of the comparison matrix. We calculated the consistency index (CI) as per Equation (3) [41], where CI is the consistency index, n is the number of spatial datasets, and λmax is the largest eigenvalue.

$$CI = \frac{\lambda max - n}{n - 1} \quad (3)$$

We also used the random consistency index (RI), a table-based value dependent on the number of variables used, to calculate the consistency of the comparison matrix, which is a measure of how far the comparison matrix is from total consistency [42,96]. For our analysis $n = 6$, which corresponds to RI = 1.24 (Table 2).

Table 2. Random consistency index based on the number of datasets used [41].

N	1	2	3	4	5	6	7	8
RI	0	0	0.58	0.9	1.12	1.24	1.32	1.41

n number of thematic layers, RI random consistency index.

Finally, we calculated the consistency ratio (4), which measures the consistency of the judgment used during the pairwise comparison based on transitive property.

$$CR = \frac{CI}{RI}. \tag{4}$$

Each spatial dataset contains information in classes. The information contained in these classes can be quantitative or qualitative. For this study, we used spatial datasets with classes determined by both. For example, in our study area, the land cover dataset consists of 15 land cover classes, and the slope dataset has slope values ranging from 0% to >60%. We used the natural breaks classification method (Arc Pro v 2.9.2, ESRI) to rank the classes within the quantitative spatial datasets (precipitation, slope, and drainage density) [43], thus maximizing differences between classes. We used our conceptual model to assign ranks for classes within qualitative spatial datasets (geology, soil texture, and land cover). The final class ranking values were based on Saaty's relative importance scale (see Table 1).

2.6. GWRP Model Development and Validation

We used the weighted overlay tool (Arc Pro v 2.9.2, ESRI) to combine the six spatial datasets into a single map. Then, we assigned the corresponding normalized principal eigenvector value to each spatial dataset and reclassified the results using natural breaks classification. The GWRP zones were classified into five categories: Very Low, Low, Moderate, High, and Very High.

We used two methods to validate the GWRP model. In the first validation, two experts with local knowledge conducted an independent assessment of 30 randomly chosen GWRP polygons that the model had scored as GWRP = high or GWRP = low. The experts did not have access to the scores assigned by the model but did have access to the unprocessed layers used in the model (as downloaded from the web). They also had access to ancillary information not used directly in the model, such as well-logs, aquifer outcrops, topographic wetness index (TWI), flow-weighted slope (FWS), terrain ruggedness index (TRI), and planform and profile curvature [36]. In the second validation, we determined whether wells in areas with higher GWRP scores were more likely to have higher well yields than wells in areas with lower GWRP. We obtained well yield information from well logs publicly available in the Well Log Tracking System (WELTS) (https://dnr.alaska.gov/welts/; accessed on 2 December 2022). From over 200 wells, we randomly selected 30 wells located in areas that the model had scored as GWRP = high or GWRP = low. Then, we performed a Mann–Whitney U test on the well yield data from these 30 wells to determine if well yields reported in the two populations were significantly different. We used the receiver operating characteristic curve (ROC) and the area under the curve (AUC) to determine the accuracy of the model using this second validation method [97,98].

3. Results

3.1. Relative Ranking of Individual Spatial Datasets

The spatial dataset weighting procedures resulted in a normalized reciprocal matrix with principal eigenvectors and the largest eigenvalues for each spatial dataset (Table 3). The value of the principal eigenvector reflects the relative influence of each spatial dataset on the GWRP model. Slope has the greatest influence on GWRP, with a weight of 33%. Land cover, soil texture, precipitation, and geology have the subsequent greatest influence on GWRP, with weights of 22%, 17%, 12%, and 11%, respectively. Drainage density has the least influence on GWRP, with a weight of just 4% (Table 3, principal eigenvector). The consistency ratio for the reciprocal matrix is 0.04. Consistency ratios of 0.10 or less have been deemed acceptable [41].

Table 3. Analytical Hierarchy Process results: normalized reciprocal matrix, principal eigenvectors, and largest eigenvalue.

Spatial Dataset	P	G	ST	SL	DD	LC	$\vec{p}$	λ_{max}
P	0.12	0.11	0.07	0.17	0.14	0.11	0.12	6.22
G	0.12	0.11	0.07	0.12	0.14	0.11	0.11	6.22
ST	0.24	0.21	0.14	0.12	0.23	0.11	0.17	6.22
SL	0.24	0.32	0.42	0.35	0.23	0.43	0.33	6.22
DD	0.04	0.04	0.03	0.07	0.05	0.04	0.04	6.22
LC	0.24	0.21	0.28	0.17	0.23	0.21	0.22	6.22

P Precipitation, G Geology, ST Soil Texture, SL Slope, DD Drainage Density, LC Land Cover, $\vec{p}$ principal eigenvector (reflecting the relative importance of each dataset to the model), λ_{max} largest eigenvalue.

3.2. Relative Ranking of Data Classes within Spatial Datasets

The spatial dataset selection procedures resulted in six spatial datasets, with data reclassified in terms of their relative contribution to GWRP (Table 4; Figure 3; Supplementary Materials Tables S2–S7). GWRP is highest where precipitation is relatively high, coarse-grained, unconsolidated deposits are present, soils are variants of sands and gravels, the terrain is flat, the drainage density is low, and there is no development. Conversely, GWRP is lowest where precipitation is relatively low, tertiary sedimentary rock is present, soils have very high organic matter content, the terrain is steep, the drainage density is high, and there is high-density development.

Table 4. Conceptual ranking of data classes within six spatial datasets.

Spatial Datasets	High Ranks	Low Ranks	Selected Citations
Precipitation	Relatively high	Relatively low	[78,79]
Geology	Coarse-grained, unconsolidated deposits	Tertiary sedimentary rock	[82,83]
Soil Texture	Variants of sand and gravel	Very high organic matter content	[84,99]
Slope	Flat	Steep	[89,90]
Drainage Density	Low	High	[91,92]
Land Cover	Open water and wetlands	Densely developed	[93,94]

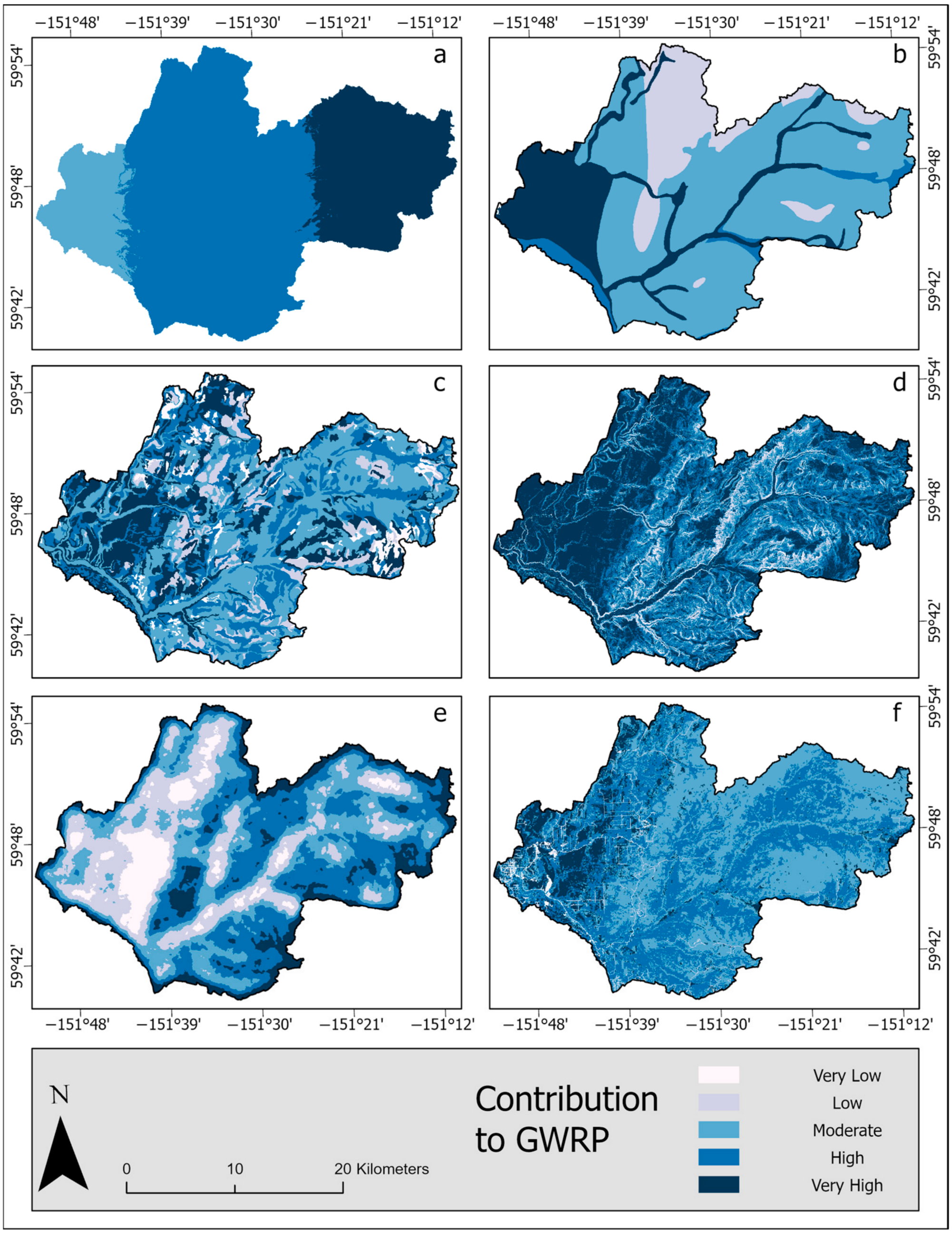

Figure 3. Distribution of classes within spatial datasets and their relative contribution to GWRP in the Anchor River Watershed. The spatial datasets used in our study are (**a**) precipitation, (**b**) geology, (**c**) soil texture, (**d**) slope, (**e**) drainage density, and (**f**) land cover.

3.3. GWRP Model and Validation

The GWRP model reveals that groundwater recharge potential is not uniformly distributed across the landscape, dividing the watershed into five GWRP zones: Very Low, Low, Moderate, High, and Very High (Figure 4). From the total area of our study area, 3% has Very Low GWRP, 14% has Low GWRP, 39% has Moderate GWRP, 36% has High GWRP, and 8% has Very High GWRP. Overall, 83% of the watershed is at least moderately suitable for groundwater recharge.

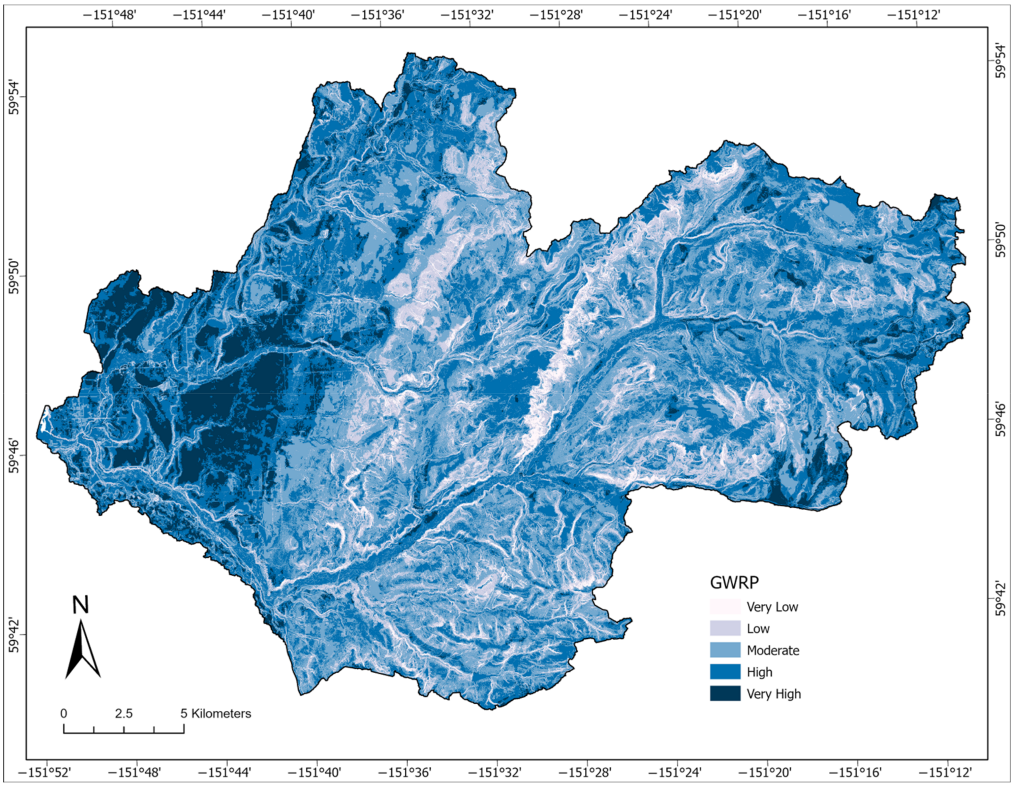

Figure 4. Distribution of Groundwater recharge potential for the Anchor River Watershed.

We built a confusion matrix to summarize and evaluate our expert-based validation results (Table 5). Our expert-based model validation showed a high concurrency between the GWRP model and expert assignments, with an overall accuracy, sensitivity, and precision of 87%.

Table 5. GWRP model verification confusion matrix results.

	Model Predicted High	Model Predicted Low	Total
Expert Scored High	13	2	15
Expert Scored Low	2	13	15
Total	15	15	30

In addition to the expert-based model validation, we compared well yields from 30 wells, equally divided between locations where GWRP values are Low and High. Median well yields for areas where GWRP values are Low and High were 18.9 L per minute and 37.9 L per minute, respectively. The well yields reported in each group were not normally distributed, so we conducted a Mann–Whitney U test and determined the accuracy of the model by calculating the receiver operating characteristic curve (ROC) and the area under the curve (AUC) (Figure 5).

The results indicate that the well yields in locations with low GWRP values were significantly lower than those in areas with high GWRP values (Mann–Whitney $U = 41$, $n_1 = n_2 = 15$, $p < 0.05$ two-tailed). The findings of the ROC analysis indicate that the AUC was 0.8, and the model is, therefore, 80% accurate.

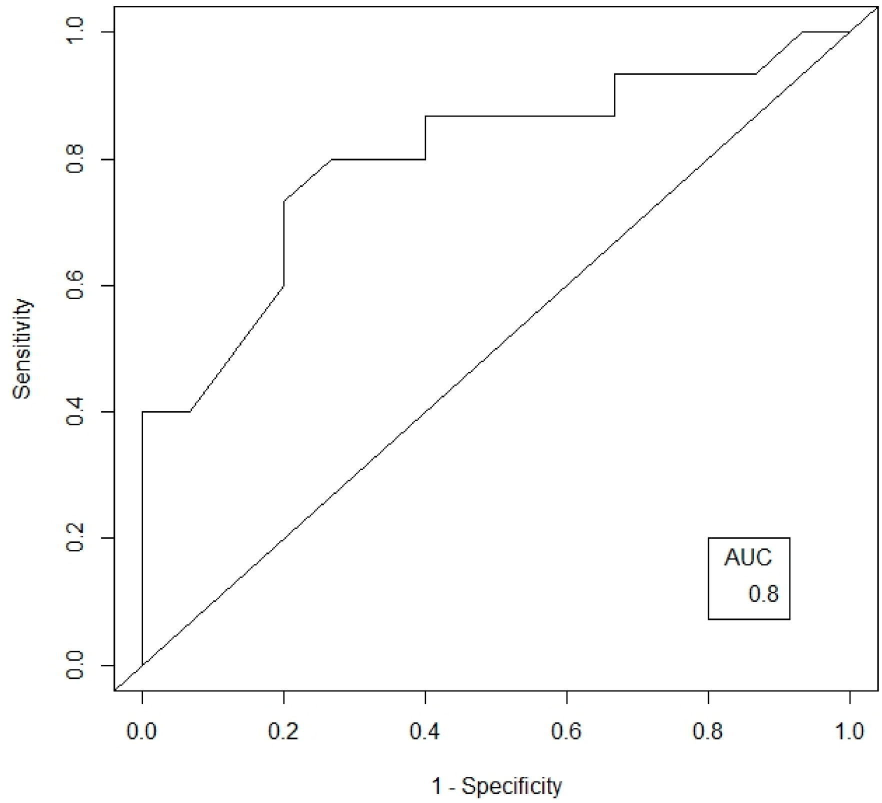

Figure 5. ROC and AUC of the GWRP model in the Anchor River watershed.

4. Discussion

This GWRP model reveals that groundwater recharge potential in the study area is driven primarily by slope, then by land cover, soil texture, precipitation, geology, and drainage density, in that order. Each of these plays a crucial role, so the overall variability in GWRP is a function of variables with both high spatial variability (e.g., slope, soil texture) and low spatial variability (e.g., precipitation, land cover) (Figure 3). Specifically, areas where GWRP values are highest are relatively low gradients and have relatively high-permeable surficial deposits and relatively high precipitation, and largely natural land cover. These areas are not distributed uniformly throughout our study area (Figure 4). The model shows that groundwater recharges mainly in proglacial lake bottom sediments underlying terraced and channeled surfaces between major morainal belts in lowland and mountain valleys, as well as in flood plains and associated higher terraces along major streams and abandoned drainage lines.

The distribution of GWRP zones concurs with other studies conducted in mountainous regions. Areas with steep slopes and shallow bedrock typically have GWRP values of Very Low and Low [73,76,77]. Conversely, areas along streams and floodplains, valley bottoms, and other flat areas with alluvium commonly have GWRP values of High and Very High [62,64,73]. Similarly, field groundwater studies have indicated that groundwater recharge in mountainous areas is spatially variable [79]. Areas with high recharge often are characterized by high precipitation [78], undeveloped landscape [93], and flat alluvial fans as the main geologic feature [83,89].

Our results demonstrate that a large percentage of this landscape is engaged in groundwater recharge at moderate or higher levels, cumulatively contributing to groundwater supply. Independent measurements of total groundwater recharge are unavailable in the study area. However, total groundwater recharge nearby and in similar terrain was approximately 0.19 cm/d in June–September, mostly through closed-basin depressions [26]. An independent estimate of net annual groundwater recharge in the study area suggests volumes of approximately 1% of annual precipitation (M. Rains, unpublished data). Net groundwater recharge is expected to be much lower than total recharge in this area as most of this groundwater recharge is subsequently either extracted by wells [52] or discharged from the numerous seeps and springs (M. Rains, unpublished data) [36]. The maintenance of the total groundwater recharge is crucial because it supports both these communities and these water-dependent ecosystems.

Groundwater is the region's primary source of domestic, commercial, and industrial water supply [52]. People source their domestic drinking water from private and public wells, springs, or the Bridge Creek Reservoir operated by the City of Homer. Although the Bridge Creek Reservoir is a surface-water reservoir, >50% of this water originates from nearby seeps and springs (Brigino, unpublished data). Meanwhile, groundwater discharge from seeps and springs also supports streamflow (Brigino, unpublished data) [54], modulates stream temperatures, providing cool-water refugia in summer and warm-water refugia in winter [54], and delivers nutrient subsidies to the streamside wetlands and streams, mainly from hillslopes covered with N-fixing alders [57,100]. Overall, these groundwater subsidies are crucial to the proper functioning of streams, including the streamside wetlands [57,101], the benthos [102], and the salmonids [103]. Groundwater is the central link between all these processes, with the salmonids being notable beneficiaries.

GWRP maps are important tools for increasing awareness and enabling effective management of groundwater resources, especially source-water protection. To our knowledge, most previous studies that couple GIS and AHP to delineate GWRP have been conducted in low and middle-latitude regions, often in dry climatic regions and in less economically developed nations [59,61,68]. However, many communities in high latitudes, including in wetter regions and in more economically developed nations, are similarly dependent on groundwater and similarly limited by data. Here, we used GIS and AHP to construct a GWRP map in a remote, high-latitude region based on remote sensing data and on a conceptual model developed from a combination of field observations and community engagement.

Our model incorporated high-quality data and insights provided by field experience, as available. Acquiring such data is often a challenge, especially in high-latitude regions. We overcame this by performing a literature review and crowdsourcing eight possible criteria and supporting spatial datasets [21,40,43,58–77], then eliminating two criteria and datasets that were unavailable for our study area (Figure 2). This ensured we only considered widely available criteria and datasets, which are likely to also be available elsewhere. We benefitted from the availability of a LiDAR-derived DEM with a resolution of 1×1 m, which we resampled to a resolution of 3×3 m. The resolution of this DEM is likely higher than will be available in many other remote regions, which might only have DEMs with a much lower resolution (e.g., Landsat Collection 2 Digital Elevation Model, https://www.usgs.gov/landsat-missions/landsat-collection-2-digital-elevation-model, accessed on 10 May 2023). We chose to use our higher resolution DEM because it better represented the rugged topography which played such a crucial role in our study area (see Slope in Figure 3). Though many other high-latitude regions may not have similar higher-resolution DEMs, we note that higher-resolution DEMs are rapidly becoming more widely available (e.g., 1 m Digital Elevation Models (DEMs)—USGS National Map 3DEP Downloadable Data Collection, https://data.usgs.gov/datacatalog/, accessed on 10 May 2023).

Combining AHP with powerful spatial and statistical analysis within a GIS environment creates a valuable tool for water resources management. This method allows qualitative and quantitative criteria to be considered in decision-making. AHP's biggest weakness is the potential for evaluator bias when establishing criteria and developing the pairwise comparison matrix. We overcame this weakness by combining community engagement and fieldwork expertise. Past community engagement [55] and recent surveys and interviews (Guerrón-Orejuela, unpublished data) identified community interest in geospatial information regarding groundwater recharge and assessed community understanding of regional hydrological patterns and processes. Fieldwork provided an improved understanding of the drivers of regional hydrological patterns and processes, especially as they relate to groundwater discharge to streams [54,57] and the structure of regional aquifers that support both water supply and springs [36]. This effectively crowdsourced the spatial datasets and weights.

For the past three decades, scientists and resource managers in the Kenai Peninsula Lowlands have become increasingly aware of the need to understand ecological processes to sustain a healthy and resilient community, especially in this low-regulatory setting that is facing an increasing population, changes in climactic conditions, and potential reduction of vital resources. It has become clear that scientists need to create tools to effectively communicate science to stakeholders, thus facilitating communication and allowing for better and informed local decision-making [55]. This GWRP map can serve in that capacity, guiding land and resource management decisions by identifying recharge areas. Furthermore, given the community's reliance on groundwater as their primary source of potable water, this model provides important information regarding source-water protection. This tool joins an ever-growing list of tools that empower local communities to have an informed dialog about how to manage the landscape best to reduce the risk of groundwater depletion. Finally, our study refines techniques, extends them to a new region, and provides insights critical for management regarding where groundwater recharge occurs in this and other similar landscapes.

Supplementary Materials: The following supporting information can be downloaded at: https://www.mdpi.com/article/10.3390/rs15102630/s1, Table S1: Literature review of possible criteria and supporting spatial datasets; Table S2: Precipitation classes contribution to Groundwater Recharge Potential (GWRP); Table S3: Geology classes contribution to Groundwater Recharge Potential (GWRP), Table S4: Soil Texture classes contribution to Groundwater Recharge Potential (GWRP); Table S5: Slope classes contribution to Groundwater Recharge Potential (GWRP); Table S6: Drainage Density classes contribution to Groundwater Recharge Potential (GWRP); Table S7: Land Cover classes contribution to Groundwater Recharge Potential (GWRP).

Author Contributions: This manuscript is the result of a broad, collaborative effort by all authors. Conceptualization, M.C.R., C.M.W. and E.J.G.-O.; methodology, E.J.G.-O., K.C.R. and M.C.R.; validation, E.J.G.-O., K.C.R. and M.C.R.; formal analysis, E.J.G.-O.; investigation, E.J.G.-O., K.CR., T.M.B., C.M.W. and M.C.R.; data curation, E.J.G.-O.; writing—original draft preparation, E.J.G.-O., K.C.R. and M.C.R.; writing—review and editing, E.J.G.-O., K.C.R., T.M.B., W.J.K., S.M.L., P.S., C.M.W. and M.C.R.; visualization, E.J.G.-O.; supervision, K.C.R. and M.C.R.; project administration, E.J.G.-O., K.C.R., C.M.W. and M.C.R.; funding acquisition, E.J.G.-O., K.C.R., C.M.W. and M.C.R. All authors have read and agreed to the published version of the manuscript.

Funding: This research was funded primarily by the NOAA Office of Coastal Management Margaret A. Davidson Graduate Fellowship, Federal Award Number NA20NOS4200143, and the National Estuarine Research Reserve System Science Collaborative under Grant No. 54584 (https://nerrssciencecollaborative.org/project/Walker17, accessed on 10 May 2023). Additional funding was provided by the University of South Florida School of Geosciences' Fred L. and Helen M. Tharp Endowed Scholarship. The APC was funded by the Ecohydrology Lab at the University of South Florida.

Data Availability Statement: Publicly available datasets were analyzed in this study. This data can be found here:, https://doi.org/10.6084/m9.figshare.22589185.v1, accessed on 15 May 2023.

Acknowledgments: This project benefitted immeasurably from in-kind support provided by the Kachemak Bay National Estuarine Research Reserve, which provided lodging, local knowledge, introductions to stakeholders, the coordination of formal stakeholder engagements, and more. Syverine Bentz was particularly instrumental. A special thank you to all the many stakeholders who provided their time and local knowledge. We would also like to acknowledge the anonymous reviewers for their constructive comments.

Conflicts of Interest: The authors declare no conflict of interest. The funders had no role in the design of the study; in the collection, analyses, or interpretation of data; in the writing of the manuscript; or in the decision to publish the results.

References

1. de Graaf, I.E.M.; Gleeson, T.; van Beek, L.P.H.R.; Sutanudjaja, E.H.; Bierkens, M.F.P. Environmental Flow Limits to Global Groundwater Pumping. *Nature* **2019**, *574*, 90–94. [CrossRef] [PubMed]
2. Forslund, A.; Renöfält, B.M.; Barchiesi, S.; Cross, K.; Davidson, S.; Farrel, T.; Korsgaard, L.; Krchnak, K.; McClain, M.; Meijer, K.; et al. *Securing Water for Ecosystems and Human Well-Being the Importance of Environmental Flows*; Stockholm International Water Institute (SIWI): Stockholm, Sweden, 2009.
3. Margat, J.; van der Gun, J. *Groundwater around the World: A Geographic Synopsis*; CRC Press: Boca Raton, FL, USA, 2013; ISBN 978-1-138-00034-6.
4. United Nations. *The United Nations World Water Development Report 2022: Groundwater: Making the Invisible Visible*; UNESCO: Paris, France, 2022; ISBN 978-92-3-100507-7.
5. Winter, T.C. Relation of Streams, Lakes, and Wetlands to Groundwater Flow Systems. *Hydrogeol. J.* **1999**, *7*, 28–45. [CrossRef]
6. Hood, J.L.; Roy, J.W.; Hayashi, M. Importance of Groundwater in the Water Balance of an Alpine Headwater Lake. *Geophys. Res. Lett.* **2006**, *33*, L13405. [CrossRef]
7. Callegary, J.B.; Kikuchi, C.P.; Koch, J.C.; Lilly, M.R.; Leake, S.A. Review: Groundwater in Alaska (USA). *Hydrogeol. J.* **2013**, *21*, 25–39. [CrossRef]
8. Boretti, A.; Rosa, L. Reassessing the Projections of the World Water Development Report. *NPJ Clean Water* **2019**, *2*, 15. [CrossRef]
9. Baldwin, H.L.; McGuinness, C.L. *A Primer on Ground Water*; General Interest Publication; 1990 reprint; U.S. Geological Survey: Washington, DC, USA, 1963; p. 31.
10. Famiglietti, J.S. The Global Groundwater Crisis. *Nat. Clim. Chang.* **2014**, *4*, 945–948. [CrossRef]
11. Alfaro, C.; Wallace, M. Origin and Classification of Springs and Historical Review with Current Applications. *Environ. Geol.* **1994**, *24*, 112–124. [CrossRef]
12. Gannon, C. Legal Protection for Groundwater-Dependent Ecosystems. *MJEAL* **2014**, *4*, 183. [CrossRef]
13. de Vries, J.J.; Simmers, I. Groundwater Recharge: An Overview of Processes and Challenges. *Hydrogeol. J.* **2002**, *10*, 5–17. [CrossRef]
14. Owen, D. Law, Land Use, and Groundwater Recharge. *Stanf. Law Rev.* **2021**, *73*, 1173. [CrossRef]
15. Cruz-Ayala, M.B.; Megdal, S.B. An Overview of Managed Aquifer Recharge in Mexico and Its Legal Framework. *Water* **2020**, *12*, 474. [CrossRef]
16. Dillon, P. Future Management of Aquifer Recharge. *Hydrogeol. J.* **2005**, *13*, 313–316. [CrossRef]
17. Jadeja, Y.; Maheshwari, B.; Packham, R.; Bohra, H.; Purohit, R.; Thaker, B.; Dillon, P.; Oza, S.; Dave, S.; Soni, P.; et al. Managing Aquifer Recharge and Sustaining Groundwater Use: Developing a Capacity Building Program for Creating Local Groundwater Champions. *Sustain. Water Resour. Manag.* **2018**, *4*, 317–329. [CrossRef]
18. Scanlon, B.R.; Healy, R.W.; Cook, P.G. Choosing Appropriate Techniques for Quantifying Groundwater Recharge. *Hydrogeol. J.* **2002**, *10*, 18–39. [CrossRef]
19. Tóth, J. A Theoretical Analysis of Groundwater Flow in Small Drainage Basins. *J. Geophys. Res.* **1963**, *68*, 4795–4812. [CrossRef]
20. Huet, M.; Chesnaux, R.; Boucher, M.-A.; Poirier, C. Comparing Various Approaches for Assessing Groundwater Recharge at a Regional Scale in the Canadian Shield. *Hydrol. Sci. J.* **2016**, *61*, 2267–2283. [CrossRef]
21. Jaafarzadeh, M.S.; Tahmasebipour, N.; Haghizadeh, A.; Pourghasemi, H.R.; Rouhani, H. Groundwater Recharge Potential Zonation Using an Ensemble of Machine Learning and Bivariate Statistical Models. *Sci. Rep.* **2021**, *11*, 5587. [CrossRef]
22. Meyboom, P. Unsteady Groundwater Flow near a Willow Ring in Hummocky Moraine. *J. Hydrol.* **1966**, *4*, 38–62. [CrossRef]
23. Johansson, P.-O. Estimation of Groundwater Recharge in Sandy till with Two Different Methods Using Groundwater Level Fluctuations. *J. Hydrol.* **1987**, *90*, 183–198. [CrossRef]
24. van der Kamp, G.; Hayashi, M. The Groundwater Recharge Function of Small Wetlands in the Semi-Arid Northern Prairies. *Great Plains Res. J. Nat. Soc. Sci.* **1998**, *8*, 39–56.
25. Todd, A.K.; Buttle, J.M.; Taylor, C.H. Hydrologic Dynamics and Linkages in a Wetland-Dominated Basin. *J. Hydrol.* **2006**, *319*, 15–35. [CrossRef]
26. Rains, M.C. Water Sources and Hydrodynamics of Closed-Basin Depressions, Cook Inlet Region, Alaska. *Wetlands* **2011**, *31*, 377–387. [CrossRef]
27. Labadia, C.F.; Buttle, J.M. Road Salt Accumulation in Highway Snow Banks and Transport through the Unsaturated Zone of the Oak Ridges Moraine, Southern Ontario. *Hydrol. Process.* **1996**, *10*, 1575–1589. [CrossRef]
28. Logan, W.S.; Rudolph, D.L. Microdepression-Focused Recharge in a Coastal Wetland, La Plata, Argentina. *J. Hydrol.* **1997**, *194*, 221–238. [CrossRef]
29. Dempster, A.; Ellis, P.; Wright, B.; Stone, M.; Price, J. Hydrogeological Evaluation of a Southern Ontario Kettle-Hole Peatland and Its Linkage to a Regional Aquifer. *Wetlands* **2006**, *26*, 49–56. [CrossRef]
30. Afrifa, S.; Zhang, T.; Appiahene, P.; Varadarajan, V. Mathematical and Machine Learning Models for Groundwater Level Changes: A Systematic Review and Bibliographic Analysis. *Future Internet* **2022**, *14*, 259. [CrossRef]
31. Osman, A.I.A.; Ahmed, A.N.; Huang, Y.F.; Kumar, P.; Birima, A.H.; Sherif, M.; Sefelnasr, A.; Ebraheemand, A.A.; El-Shafie, A. Past, Present and Perspective Methodology for Groundwater Modeling-Based Machine Learning Approaches. *Arch. Comput. Methods Eng.* **2022**, *29*, 3843–3859. [CrossRef]

32. Pourghasemi, H.R.; Sadhasivam, N.; Yousefi, S.; Tavangar, S.; Ghaffari Nazarlou, H.; Santosh, M. Using Machine Learning Algorithms to Map the Groundwater Recharge Potential Zones. *J. Environ. Manag.* **2020**, *265*, 110525. [CrossRef]
33. Huang, X.; Gao, L.; Crosbie, R.S.; Zhang, N.; Fu, G.; Doble, R. Groundwater Recharge Prediction Using Linear Regression, Multi-Layer Perception Network, and Deep Learning. *Water* **2019**, *11*, 1879. [CrossRef]
34. Jha, M.K.; Chowdhury, A.; Chowdary, V.M.; Peiffer, S. Groundwater Management and Development by Integrated Remote Sensing and Geographic Information Systems: Prospects and Constraints. *Water Resour. Manag.* **2007**, *21*, 427–467. [CrossRef]
35. Waters, P.; Greenbaum, D.; Smart, P.L.; Osmaston, H. Applications of Remote Sensing to Groundwater Hydrology. *Remote Sens. Rev.* **1990**, *4*, 223–264. [CrossRef]
36. Gerlach, M.E.; Rains, K.C.; Guerrón-Orejuela, E.J.; Kleindl, W.J.; Downs, J.; Landry, S.M.; Rains, M.C. Using Remote Sensing and Machine Learning to Locate Groundwater Discharge to Salmon-Bearing Streams. *Remote Sens.* **2022**, *14*, 63. [CrossRef]
37. McDonnell, R.A. Including the Spatial Dimension: Using Geographical Information Systems in Hydrology. *Prog. Phys. Geogr. Earth Environ.* **1996**, *20*, 159–177. [CrossRef]
38. Malczewski, J. GIS-based Multicriteria Decision Analysis: A Survey of the Literature. *Int. J. Geogr. Inf. Sci.* **2006**, *20*, 703–726. [CrossRef]
39. Huang, I.B.; Keisler, J.; Linkov, I. Multi-Criteria Decision Analysis in Environmental Sciences: Ten Years of Applications and Trends. *Sci. Total Environ.* **2011**, *409*, 3578–3594. [CrossRef]
40. Singh, L.K.; Jha, M.K.; Chowdary, V.M. Assessing the Accuracy of GIS-Based Multi-Criteria Decision Analysis Approaches for Mapping Groundwater Potential. *Ecol. Indic.* **2018**, *91*, 24–37. [CrossRef]
41. Saaty, R.W. The Analytic Hierarchy Process—What It Is and How It Is Used. *Math. Model.* **1987**, *9*, 161–176. [CrossRef]
42. Saaty, T.L. How to Make a Decision: The Analytic Hierarchy Process. *Eur. J. Oper. Res.* **1990**, *48*, 9–26. [CrossRef]
43. Arulbalaji, P.; Padmalal, D.; Sreelash, K. GIS and AHP Techniques Based Delineation of Groundwater Potential Zones: A Case Study from Southern Western Ghats, India. *Sci. Rep.* **2019**, *9*, 2082. [CrossRef]
44. Mengistu, T.D.; Chang, S.W.; Kim, I.-H.; Kim, M.-G.; Chung, I.-M. Determination of Potential Aquifer Recharge Zones Using Geospatial Techniques for Proxy Data of Gilgel Gibe Catchment, Ethiopia. *Water* **2022**, *14*, 1362. [CrossRef]
45. Ma, K.; Feng, D.; Lawson, K.; Tsai, W.-P.; Liang, C.; Huang, X.; Sharma, A.; Shen, C. Transferring Hydrologic Data Across Continents—Leveraging Data-Rich Regions to Improve Hydrologic Prediction in Data-Sparse Regions. *Water Resour. Res.* **2021**, *57*, e2020WR028600. [CrossRef]
46. Walker, C.; Baird, S.; Highway, S.; King, R.; Whigham, D. *Wetland Geomorphic Linkages to Juvenile Salmonids and Macroinvertebrate Communities in Headwater Streams of the Kenai Lowlands, Alaska*; Smithsonian Environmental Research Center: Edgewater, MD, USA, 2007.
47. Broadman, E.; Kaufman, D.S.; Henderson, A.C.G.; Berg, E.E.; Anderson, R.S.; Leng, M.J.; Stahnke, S.A.; Muñoz, S.E. Multi-Proxy Evidence for Millennial-Scale Changes in North Pacific Holocene Hydroclimate from the Kenai Peninsula Lowlands, South-Central Alaska. *Quat. Sci. Rev.* **2020**, *241*, 106420. [CrossRef]
48. Karlstrom, T.N.V. *Quaternary Geology of the Kenai Lowland and Glacial History of the Cook Inlet Region, Alaska*; Professional Paper; U.S. Geological Survey: Reston, VA, USA, 1964.
49. Barnes, F.F.; Cobb, E.H. *Geology and Coal Resources of the Homer District, Kenai Coal Field, Alaska*; Bulletin; U.S. Geological Survey: Reston, VA, USA, 1959.
50. Wilson, F.H.; Hults, C.P. *Geology of the Prince William Sound and Kenai Peninsula Region, Alaska: Including the Kenai, Seldovia, Blying Sound, Cordova, and Middleton Island 1:250,000—Scale Quadrangles*; Scientific Investigations Map; U.S. Geological Survey: Reston, VA, USA, 2012.
51. Nelson, G.; Johnson, P. *Ground-Water Reconnaissance of Part of the Lower Kenai Peninsula, Alaska*; Open-File Report; U.S. Geological Survey: Reston, VA, USA, 1981.
52. Glass, R.L. *Glass Ground-Water Conditions and Quality in the Western Part of Kenai Peninsula, Southcentral Alaska*; Open-File Report; U.S. Geological Survey: Reston, VA, USA, 1996.
53. *Alaska Water Use Act AS 46.15*; State of Alaska: Juneau, AK, USA, 2014; Volume 46.15.
54. Callahan, M.K.; Rains, M.C.; Bellino, J.C.; Walker, C.M.; Baird, S.J.; Whigham, D.F.; King, R.S. Controls on Temperature in Salmonid-Bearing Headwater Streams in Two Common Hydrogeologic Settings, Kenai Peninsula, Alaska. *J. Am. Water Resour. Assoc.* **2015**, *51*, 84–98. [CrossRef]
55. Walker, C.M.; Whigham, D.F.; Bentz, I.S.; Argueta, J.M.; King, R.S.; Rains, M.C.; Simenstad, C.A.; Guo, C.; Baird, S.J.; Field, C.J. Linking Landscape Attributes to Salmon and Decision-Making in the Southern Kenai Lowlands, Alaska, USA. *Ecol. Soc.* **2021**, *26*, art1. [CrossRef]
56. ADLW (Alaska Department of Labor and Workforce). *Alaska Populations Estimates 2010 & 2020*; Alaska Department of Labor and Workforce: Juneau, AK, USA, 2022.
57. Callahan, M.K.; Whigham, D.F.; Rains, M.C.; Rains, K.C.; King, R.S.; Walker, C.M.; Maurer, J.R.; Baird, S.J. Nitrogen Subsidies from Hillslope Alder Stands to Streamside Wetlands and Headwater Streams, Kenai Peninsula, Alaska. *J. Am. Water Resour. Assoc.* **2017**, *53*, 478–492. [CrossRef]
58. Achu, A.L.; Thomas, J.; Reghunath, R. Multi-Criteria Decision Analysis for Delineation of Groundwater Potential Zones in a Tropical River Basin Using Remote Sensing, GIS and Analytical Hierarchy Process (AHP). *Groundw. Sustain. Dev.* **2020**, *10*, 100365. [CrossRef]

59. Al-Djazouli, M.O.; Elmorabiti, K.; Rahimi, A.; Amellah, O.; Fadil, O.A.M. Delineating of Groundwater Potential Zones Based on Remote Sensing, GIS and Analytical Hierarchical Process: A Case of Waddai, Eastern Chad. *GeoJournal* **2021**, *86*, 1881–1894. [CrossRef]
60. Chatterjee, R.S.; Pranjal, P.; Jally, S.; Kumar, B.; Dadhwal, V.K.; Srivastav, S.K.; Kumar, D. Potential Groundwater Recharge in North-Western India vs Spaceborne GRACE Gravity Anomaly Based Monsoonal Groundwater Storage Change for Evaluation of Groundwater Potential and Sustainability. *Groundw. Sustain. Dev.* **2020**, *10*, 100307. [CrossRef]
61. Derdour, A.; Benkaddour, Y.; Bendahou, B. Application of Remote Sensing and GIS to Assess Groundwater Potential in the Transboundary Watershed of the Chott-El-Gharbi (Algerian–Moroccan Border). *Appl. Water Sci.* **2022**, *12*, 136. [CrossRef]
62. Fauzia; Surinaidu, L.; Rahman, A.; Ahmed, S. Distributed Groundwater Recharge Potentials Assessment Based on GIS Model and Its Dynamics in the Crystalline Rocks of South India. *Sci. Rep.* **2021**, *11*, 11772. [CrossRef]
63. Gupta, D.S.; Biswas, A.; Ghosh, P.; Rawat, U.; Tripathi, S. Delineation of Groundwater Potential Zones, Groundwater Estimation and Recharge Potentials from Mahoba District of Uttar Pradesh, India. *Int. J. Environ. Sci. Technol.* **2021**, *19*, 12145–12168. [CrossRef]
64. Hasan, M.T.; Jahan, C.S.; Rahaman, M.F.; Mazumder, Q.H. Delineation of Zones and Sites for Artificial Recharge of Groundwater in Dry Land Barind Tract, Bangladesh Using MCDM Technique in GIS Environment. *Sustain. Water Resour. Manag.* **2022**, *8*, 147. [CrossRef]
65. Jesiya, N.P.; Gopinath, G. A Fuzzy Based MCDM–GIS Framework to Evaluate Groundwater Potential Index for Sustainable Groundwater Management—A Case Study in an Urban-Periurban Ensemble, Southern India. *Groundw. Sustain. Dev.* **2020**, *11*, 100466. [CrossRef]
66. Kumar, P.; Bansod, B.K.S.; Debnath, S.K.; Thakur, P.K.; Ghanshyam, C. Index-Based Groundwater Vulnerability Mapping Models Using Hydrogeological Settings: A Critical Evaluation. *Environ. Impact Assess. Rev.* **2015**, *51*, 38–49. [CrossRef]
67. Mitra, R.; Roy, D. Delineation of Groundwater Potential Zones through the Integration of Remote Sensing, Geographic Information System, and Multi-Criteria Decision-Making Technique in the Sub-Himalayan Foothills Region, India. *Int. J. Energy Water Res.* **2022**, 1–21. [CrossRef]
68. Mukherjee, P.; Singh, C.K.; Mukherjee, S. Delineation of Groundwater Potential Zones in Arid Region of India—A Remote Sensing and GIS Approach. *Water Resour. Manag.* **2012**, *26*, 2643–2672. [CrossRef]
69. Nasir, M.J.; Khan, S.; Zahid, H.; Khan, A. Delineation of Groundwater Potential Zones Using GIS and Multi Influence Factor (MIF) Techniques: A Study of District Swat, Khyber Pakhtunkhwa, Pakistan. *Environ. Earth Sci.* **2018**, *77*, 367. [CrossRef]
70. Panahi, M.R.; Mousavi, S.M.; Rahimzadegan, M. Delineation of Groundwater Potential Zones Using Remote Sensing, GIS, and AHP Technique in Tehran–Karaj Plain, Iran. *Environ. Earth Sci.* **2017**, *76*, 792. [CrossRef]
71. Pande, C.B.; Moharir, K.N.; Panneerselvam, B.; Singh, S.K.; Elbeltagi, A.; Pham, Q.B.; Varade, A.M.; Rajesh, J. Delineation of Groundwater Potential Zones for Sustainable Development and Planning Using Analytical Hierarchy Process (AHP), and MIF Techniques. *Appl. Water Sci.* **2021**, *11*, 186. [CrossRef]
72. Phong, T.V.; Pham, B.T.; Trinh, P.T.; Ly, H.-B.; Vu, Q.H.; Ho, L.S.; Le, H.V.; Phong, L.H.; Avand, M.; Prakash, I. Groundwater Potential Mapping Using GIS-Based Hybrid Artificial Intelligence Methods. *Ground Water* **2021**, *59*, 745–760. [CrossRef]
73. Rani, M.; Pande, A.; Kumar, K.; Joshi, H.; Rawat, D.S.; Kumar, D. Investigation of Groundwater Recharge Prospect and Hydrological Response of Groundwater Augmentation Measures in Upper Kosi Watershed, Kumaun Himalaya, India. *Groundw. Sustain. Dev.* **2022**, *16*, 100720. [CrossRef]
74. Saranya, T.; Saravanan, S. Groundwater Potential Zone Mapping Using Analytical Hierarchy Process (AHP) and GIS for Kancheepuram District, Tamilnadu, India. *Model. Earth Syst. Environ.* **2020**, *6*, 1105–1122. [CrossRef]
75. Selvam, S.; Magesh, N.S.; Chidambaram, S.; Rajamanickam, M.; Sashikkumar, M.C. A GIS Based Identification of Groundwater Recharge Potential Zones Using RS and IF Technique: A Case Study in Ottapidaram Taluk, Tuticorin District, Tamil Nadu. *Env. Earth Sci.* **2015**, *73*, 3785–3799. [CrossRef]
76. Singh, S.K.; Zeddies, M.; Shankar, U.; Griffiths, G.A. Potential Groundwater Recharge Zones within New Zealand. *Geosci. Front.* **2019**, *10*, 1065–1072. [CrossRef]
77. Yeh, H.-F.; Lin, H.-I.; Lee, S.-T.; Chang, M.-H.; Hsu, K.-C.; Lee, C.-H. GIS and SBF for Estimating Groundwater Recharge of a Mountainous Basin in the Wu River Watershed, Taiwan. *J. Earth Syst. Sci.* **2014**, *123*, 503–516. [CrossRef]
78. Clilverd, H.M.; White, D.M.; Tidwell, A.C.; Rawlins, M.A. The Sensitivity of Northern Groundwater Recharge to Climate Change: A Case Study in Northwest Alaska1: The Sensitivity of Northern Groundwater Recharge to Climate Change: A Case Study in Northwest Alaska. *JAWRA J. Am. Water Resour. Assoc.* **2011**, *47*, 1228–1240. [CrossRef]
79. Somers, L.D.; McKenzie, J.M. A Review of Groundwater in High Mountain Environments. *WIREs Water* **2020**, *7*, e1475. [CrossRef]
80. Arnold, J.G.; Srinivasan, R.; Muttiah, R.S.; Williams, J.R. Large Area Hydrologic Modeling and Assessment Part I: Model Development. *J. Am. Water Resour. Assoc.* **1998**, *34*, 73–89. [CrossRef]
81. Saha, S.; Moorthi, S.; Pan, H.-L.; Wu, X.; Wang, J.; Nadiga, S.; Tripp, P.; Kistler, R.; Woollen, J.; Behringer, D.; et al. The NCEP Climate Forecast System Reanalysis. *Bull. Amer. Meteor. Soc.* **2010**, *91*, 1015–1058. [CrossRef]
82. Hayashi, M. Alpine Hydrogeology: The Critical Role of Groundwater in Sourcing the Headwaters of the World. *Groundwater* **2020**, *58*, 498–510. [CrossRef]
83. Smerdon, B.D.; Allen, D.M.; Grasby, S.E.; Berg, M.A. An Approach for Predicting Groundwater Recharge in Mountainous Watersheds. *J. Hydrol.* **2009**, *365*, 156–172. [CrossRef]

84. Wang, T.; Franz, T.E.; Zlotnik, V.A. Controls of Soil Hydraulic Characteristics on Modeling Groundwater Recharge under Different Climatic Conditions. *J. Hydrol.* **2015**, *521*, 470–481. [CrossRef]
85. Zomlot, Z.; Verbeiren, B.; Huysmans, M.; Batelaan, O. Spatial Distribution of Groundwater Recharge and Base Flow: Assessment of Controlling Factors. *J. Hydrol. Reg. Stud.* **2015**, *4*, 349–368. [CrossRef]
86. Wilson, F.H.; Hults, C.P.; Mull, C.G.; Karl, S.M. *Geologic Map of Alaska*; Scientific Investigations Map; U.S. Geological Survey: Reston, VA, USA, 2015.
87. Soil Survey Staff. *Gridded Soil Survey Geographic (GSSURGO) Database for Alaska*; United States Department of Agriculture; Natural Resources Conservation Service: Washington, DC, USA, 2022.
88. Singh, V.K.; Kumar, D.; Kashyap, P.S.; Singh, P.K.; Kumar, A.; Singh, S.K. Modelling of Soil Permeability Using Different Data Driven Algorithms Based on Physical Properties of Soil. *J. Hydrol.* **2020**, *580*, 124223. [CrossRef]
89. Naves, A.; Samper, J.; Pisani, B.; Mon, A.; Dafonte, J.; Montenegro, L.; García-Tomillo, A. Hydrogeology and Groundwater Management in a Coastal Granitic Area with Steep Slopes in Galicia (Spain). *Hydrogeol. J.* **2021**, *29*, 2655–2669. [CrossRef]
90. Somers, L.D.; McKenzie, J.M.; Zipper, S.C.; Mark, B.G.; Lagos, P.; Baraer, M. Does Hillslope Trenching Enhance Groundwater Recharge and Baseflow in the Peruvian Andes? *Hydrol. Process.* **2018**, *32*, 318–331. [CrossRef]
91. Carlston, C.W. *Drainage Density and Streamflow*; Professional Paper; U.S. Geological Survey: Reston, VA, USA, 1963.
92. Day, D.G. Drainage Density Variability and Drainage Basin Outputs. *J. Hydrol.* **1983**, *22*, 3–17.
93. Owuor, S.O.; Butterbach-Bahl, K.; Guzha, A.C.; Rufino, M.C.; Pelster, D.E.; Díaz-Pinés, E.; Breuer, L. Groundwater Recharge Rates and Surface Runoff Response to Land Use and Land Cover Changes in Semi-Arid Environments. *Ecol. Process* **2016**, *5*, 16. [CrossRef]
94. Siddik, M.S.; Tulip, S.S.; Rahman, A.; Islam, M.N.; Haghighi, A.T.; Mustafa, S.M.T. The Impact of Land Use and Land Cover Change on Groundwater Recharge in Northwestern Bangladesh. *J. Environ. Manag.* **2022**, *315*, 115130. [CrossRef]
95. Dewitz, J. *National Land Cover Database (NLCD) 2016 Products (Ver. 2.0, July 2020): U.S. Geological Survey Data Release*; U.S. Geological Survey: Reston, VA, USA, 2019.
96. Saaty, T.L. Decision-Making with the AHP: Why Is the Principal Eigenvector Necessary. *Eur. J. Oper. Res.* **2003**, *145*, 85–91. [CrossRef]
97. Abijith, D.; Saravanan, S.; Singh, L.; Jennifer, J.J.; Saranya, T.; Parthasarathy, K.S.S. GIS-Based Multi-Criteria Analysis for Identification of Potential Groundwater Recharge Zones—A Case Study from Ponnaniyaru Watershed, Tamil Nadu, India. *HydroResearch* **2020**, *3*, 1–14. [CrossRef]
98. Jhariya, D.C.; Khan, R.; Mondal, K.C.; Kumar, T.; K., I.; Singh, V.K. Assessment of Groundwater Potential Zone Using GIS-Based Multi-Inflfluencing Factor (MIF), Multi-Criteria Decision Analysis (MCDA) and Electrical Resistivity Survey Techniques in Raipur City, Chhattisgarh, India. *J. Water Supply Res. Technol.-Aqua* **2021**, *70*, 375–400. [CrossRef]
99. Tao, Z.; Li, H.; Neil, E.; Si, B. Groundwater Recharge in Hillslopes on the Chinese Loess Plateau. *J. Hydrol. Reg. Stud.* **2021**, *36*, 100840. [CrossRef]
100. Shaftel, R.S.; King, R.S.; Back, J.A. Alder Cover Drives Nitrogen Availability in Kenai Lowland Headwater Streams, Alaska. *Biogeochemistry* **2012**, *107*, 135–148. [CrossRef]
101. Whigham, D.F.; Walker, C.M.; Maurer, J.; King, R.S.; Hauser, W.; Baird, S.; Keuskamp, J.A.; Neale, P.J. Watershed Influences on the Structure and Function of Riparian Wetlands Associated with Headwater Streams—Kenai Peninsula, Alaska. *Sci. Total Environ.* **2017**, *599–600*, 124–134. [CrossRef]
102. Hiatt, D.L.; Robbins, C.J.; Back, J.A.; Kostka, P.K.; Doyle, R.D.; Walker, C.M.; Rains, M.C.; Whigham, D.F.; King, R.S. Catchment-Scale Alder Cover Controls Nitrogen Fixation in Boreal Headwater Streams. *Freshw. Sci.* **2017**, *36*, 523–532. [CrossRef]
103. Dekar, M.P.; King, R.S.; Back, J.A.; Whigham, D.F.; Walker, C.M. Allochthonous Inputs from Grass-Dominated Wetlands Support Juvenile Salmonids in Headwater Streams: Evidence from Stable Isotopes of Carbon, Hydrogen, and Nitrogen. *Freshw. Sci.* **2012**, *31*, 121–132. [CrossRef]

Appendix 4: City of Homer Reservoir Project Groundwater Study Geodatabase and Metadata